UNIVERSITA' DEGLI STUDI DI MILANO

Facoltà di Scienze Matematiche Fisiche e Naturali

PhD School in Biomolecular Sciences

Scuola di Dottorato in Scienze Biologiche e Molecolari

Dottorato di Ricerca in Biologia vegetale

XXIII ciclo

Viral ion channels production for structural studies.

Tutor: Prof.ssa Anna Moroni

Tesi di Dottorato di:

Giuseppina Ferrara

Matr. N° R07694

Anno Accademico 2009-2010

Table of contents:

Abstract

Crystallization of ion channel proteins is a difficult task for several reasons related to the hydrophobic nature of these proteins, and still is a matter of trials and errors.

In this work I will present an experimental approach to the crystallization of a group of small potassium channels: the viral Kcv channels.

The first part deals with the expression of MA-1D Kcv in the heterologous system *Pichia pastoris* and its purification by detergent solubilization. Attempts to increase the yield of the protein by modification of the construct at the DNA level are discussed.

In parallel the production of Fab fragments from monoclonal antibodies that recognized the tetrameric form of the protein has been established in order to make protein-antibody complexes that can promote an ordered crystallization process by increasing the polar contacts within the crystals.

In the second part of this thesis, the planar lipid bilayer technique is applied to study the functional properties of several Kcv channels at the single channel level. In particular I have analyzed the block by barium of the wt PBCV-1 Kcv and of its mutants in the 4^{th} site of the selectivity filter, residue Threonine 63. This mutation affects protein sensitivity to barium, but also alters the open probability and the number of subconductance levels. The mutation of an adjacent aminoacid, Serine 62, recovers the wt functions. The T63 mutation was then moved also to another Kcv channel, MA-1D Kcv, to check if the behavior related to the mutation is conserved.

The third part deals with Kesv, a Kcv-like channel founding a related class of viruses, ESV that, differently to Kcv, shows a mitochondrial localization when expressed in heterologous systems. Due to the difficulties encountered in measuring from mitochondria of transfected cells, we have not been able to record currents from this channel in the past. It was therefore decided to produce and purify recombinant protein for functional studies in artificial lipid bilayer. Since all attempts to express it in *Pichia pastoris* failed, it was decided to express it in a cell-free system in collaboration with the lab of Dr. Bernhard, at the University of Frankfurt. Functional studies on the reconstituted protein channel have revealed that the protein forms a functional, selective K^+ channel with overall features of the Kcv-like channels.

Introduction

X-ray crystallography

X–ray crystallography it's a technique that allows the determination of the three dimensional structure of a molecule. To perform protein crystallography, a high amount of protein must be available, of a high quality, homogeneous, and soluble. This is the first limiting step because the right expression system has to be found, and different purification conditions have to be test before getting the protein in such high quantity and quality [Drenth, 1999].

The principle of crystallization consists in inducing the protein that is in a high concentration solution, to get out of it and if the process happens under the correct condition (i.e. not too fast) the crystals grow. The process can take days, weeks or even months. The determination of the crystal growth conditions (kind and concentration of the precipitant, pH, protein concentration, buffer, temperature) is also a limiting step, and at the beginning it is a matter of trials and errors [Drenth, 1999].

Once grown the crystals are exposed to a x-ray beam generated by a synchrotron, that produces an extremely intense x-ray beam with high quality optics, which allows much shorter exposure times and a higher signal to noise ratio of the diffraction image. The data are collected and analyzed with software that transforms the mathematical diffraction data in an electron density map that is further refined using molecular models.

X-ray crystallography of membrane proteins

Thousand of 3-D structures have been determined with x-ray crystallography until now, but the amount of membrane proteins crystallized is still not comparable to that of soluble proteins [Ostermeier & Michel, 1997]. Membrane proteins are really represented in nature: the analysis of the genomes of eubacterial, archaean and eukaryotic organisms predicted that the 20-30% of the ORF encode for integral membrane proteins [Wallin & von Heijne, 1998]. The problem is that they are difficult to handle.

First of all membrane proteins are present in the organism at low concentration that usually prevents direct purification form a natural source. The first step consists therefore in selecting the most suitable recombinant expression system, from which to produce and purify high amounts of protein. If the protein is eukaryotic, post-translational modifications have to be considered in the choice of the heterologous organism.

A second problem is directly correlated with the protein nature. Membrane proteins, in fact, posses an amphipathic surface: hydrophobic where they are in contact with the alkyl chains of the lipids of the cell membrane and polar where they facing the aqueous phases at both side of the membrane. In order to use these proteins for crystallization, they have to be extracted from the membranes and solubilized with high detergent concentration that forms, above the CMC (critical micellar concentration), micelles that take up the membrane proteins and cover the hydrophobic surface of the membrane protein with their alkyl chains in a belt-like manner [Garavito & Ferguson-Miller, 1997; Zulauf, 1991]. Protein-detergent complexes form three-dimensional crystals making contacts between polar surfaces that protrude from the micelle [Michel, 1983]. Although detergent micelles stabilized the proteins, the interactions do not led to rigid crystal contacts, so, sometimes, especially if the protein has small hydrophobic domains, increase the polar surface for protein-protein interactions is needed.

A strategy developed for this purpose is the use of binding antibody fragments [Ostermeier et al., 1995] that are obtained by proteolysis of the whole monoclonal antibody that recognized the protein to crystallize. The native antibody is not suitable due to its flexible linker regions connecting the variable and the constant domain so digestion with papain to generate Fab is necessary.

Monoclonal antibodies are obtained from hybridoma cell lines, spleen cells of immunized mice, fused with myeloma cells. The monoclonal antibodies purified by hybridoma cells are then digested with papain to get the Fabs. Once selected the Fabs more suitable for crystallization, that recognize

the native form of the protein to crystallize, they can also be produce as recombinant peptide, cloning the gene in expression vector for *E. coli* [Phickthun, 1991; Kleyman et al., 1995] or with phage display libraries or ribosome display [Kleyman et al., 1995; Burmester & Pluckthun, 2001]. This technique has recently led to the crystallization of many membrane proteins like the cytochrome c oxidase [Ostermeier et al., 1995] and the KcsA potassium channel [Zhou et al., 2001].

An alternative technique also used for membrane protein crystallization is the lipidic cubic phase. This is a system that consists in using lipids, water and the protein in an appropriate concentration that allow to form a structured three-dimensional lipidic array with a system of aqueous channel. This matrix provides nucleation site and support for crystals growth. The proteins in this system keep their activity and native conformation, and the whole complex is really stable and not influenced by high salts or precipitants. With this technique bacteriorhodopsin has been successfully crystallized [Landau & Rosennbusch, 1996].

Potassium channels

Among membrane proteins, ion channels are really interesting to be studied especially from a medical point of view. They are responsible for the ion diffusion through the cell membranes because they create in the phospholipid bilayer, that has the function to isolate the cell from the external solution, an hydrophilic passage for the charged ions.

Ion channels are ubiquitous in all the organisms, prokaryotic and eukaryotic, and they control essential living processes like the signal transduction, the uptake of nutrients, the osmotic regulation and the release of hormones and transmitters [Hille, 1992]. In animals they are also responsible of excitability of neuronal and muscular cells, while in plants they regulate the uptake of ions, the opening and closure of the stomata, the movement of ions into the xylem [Schroeder et al., 1994; Latorre et al., 2003].

The study of ion channels is of high interest because, in human, mutations that affect their functionality, generate a number of diseases termed "channelopathies" like myotonia (mutation of Cl^- channel of muscles), paramyotonia (mutation of Na^+ channel of muscles), cystic fibrosis (mutations of Cl^- channel CFTR), short QT syndrome (cardiopathic diseases by mutation of K^+ KCNQ1, KCNH2, KCNE1, KCNE2 channels and Na^+ SCN5A channel), hemiplegia of childhood (alterations of KCNQ2 and KCNQ3) and diabetes type 2 (mutations of Kir6.2) [Ashcroft, 2000].

Potassium channels are members of the superfamily of ion channels. The first potassium channel discovered was the Shaker channel, whose gene was isolated in the 1987 from the *Drosophila melanogaster* genome [Kamb et al. 1987]. After the expression of Shaker in *Xenopus* oocytes and physiological studies, it was possible to confirm that the protein was really a K^+ channel [Iverson et al. 1988; Papazian et al. 1988]. Using the shaker cDNA as a probe, it was possible to identify a K^+ channel from rat brain, RCK1 [Baumann et al. 1988] and RBK1 [Christie et al. 1989], and some inward rectifying channels [Kubo et al. 1993]. Subsequently, the RCK1 sequence was used to probe cDNA libraries and led to the isolation of several more neuronal voltage-dependent K^+ channel clones [Stuhmer et al. 1988]. At the same time, 3 more voltage-dependent K^+ channels (Shab, Shal and Shaw) were identified in *Drosophila* by cross-hybridization with the shaker sequence [Covarrubias et al., 1991]. As for shaker, equivalents of these channels were also found in mammalian cDNA libraries. A confirmation that these channels are ubiquitous came from the identification of potassium channel also in bacteria [Schrempf et al., 1995; Durrell & Guy, 2001] and in viruses [Plugge et al., 2000; Kang et al., 2004].

Potassium channels are formed by four identical α-helical subunits that generate a pore in the membrane and a loop between them [Hille, 2001]. Every subunit can be formed by 2, 4 or 6 transmembrane domains (TM) and two cytoplasmatic domains N- and C- terminus (fig. 1). The pore region (P), between two TM, controls selectivity and gating and is highly conserved across the channel family [Jan & Jan 1990; Heghinbotham et al, 1992]. Small changes in the amino acid residues of pore domain usually result in functional diversity. Molecular cloning and mutagenesis experiment have revealed that all potassium channels share the signature sequence TXXTXGYG between the two most carboxy-terminal transmembrane helices. The only exceptions are Kir6.2, HERG/HEAG and Kcv, which have GFG instead of GYG. Whenever one of these amino acids is mutated, the channel changes selectivity and acquires new gating properties [Doyle et al. 1998].

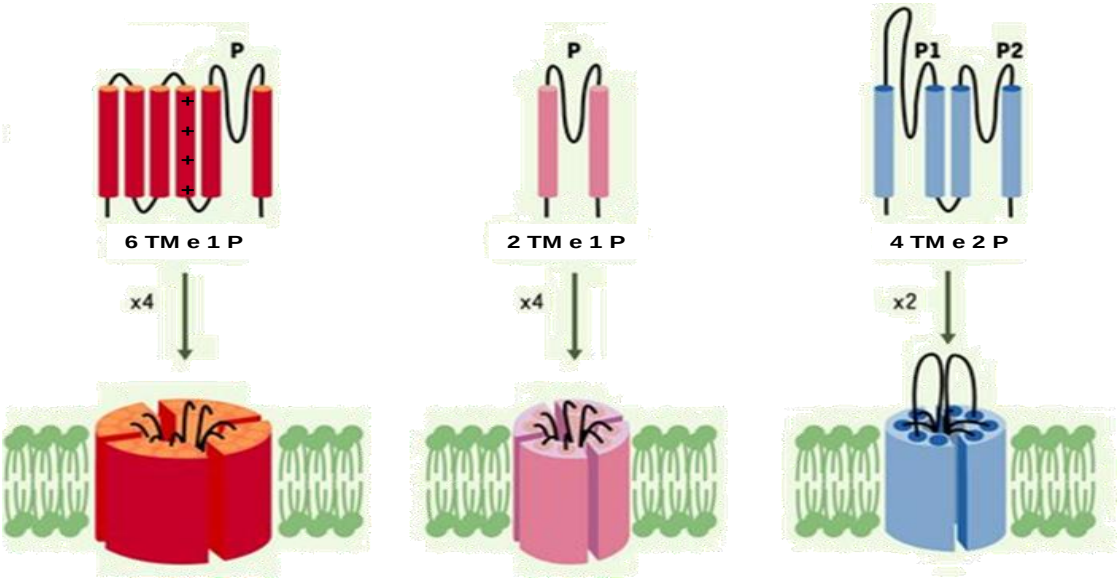

Fig. 1. Structural model of K^+ channels at 6TM, 4TM and 2TM that form a pore into the membranes.

According to their structure the potassium channels are divided into three groups (fig. 2).

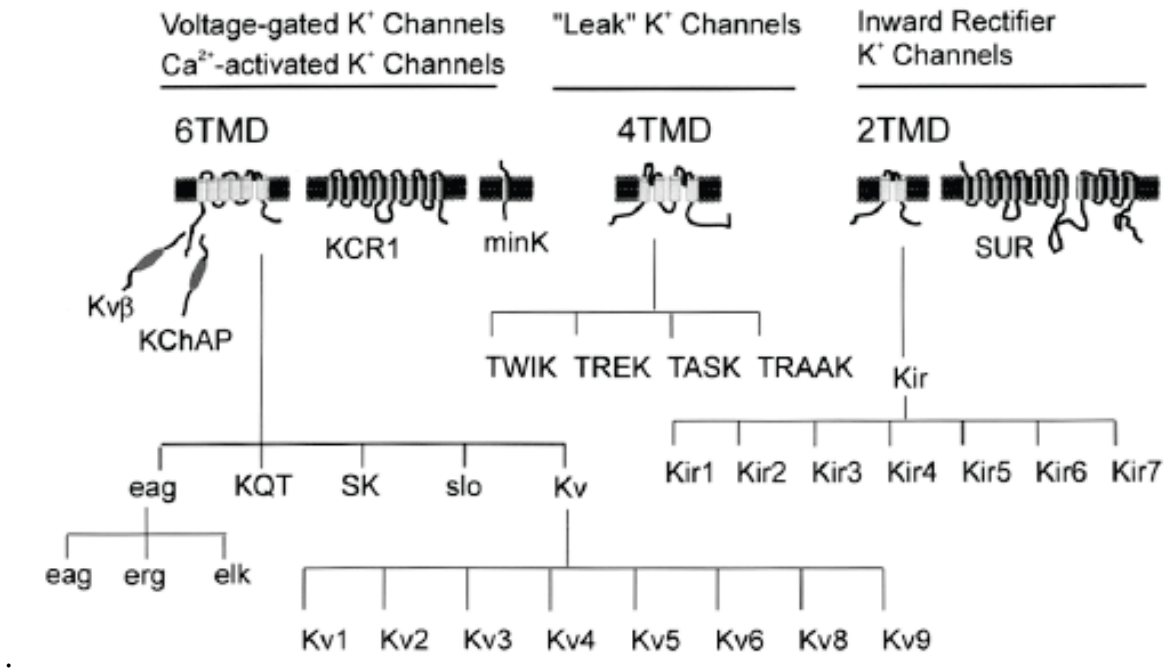

Fig. 2. Classification of K^+ channel families. The three classes are based on the structure of the α subunits [Coetzee et al., 1999].

The 6TM channels form the largest class of K^+ channels that is divided into two subclasses, the Ca^+-activated (BKCa, IKCa and SKCa) and the voltage-gated channels (Kv channels). The channels are formed by homo or hetero tetramers of 6TM α subunits that contain one pore domain each [Jenkinson, 2006]. Changes in voltage or intracellular calcium cause these channels to open and conduct an outward flow of potassium, down its concentration gradient. Each subunit presents the voltage sensor constituted by positively charge amino acids in TM4 [Gambale & Uozumi, 2006]. The pore region is between TM5 and TM6.

The 4TM channels, also called tandem pore domain channels, are an unusual class of potassium channels since each α subunit contains two pore-forming sequences (P1 and P2) [Kim, 2005] and only P1 conserved the GY(F)G sequence while P2 the sequence GIG or GLG is present. The 4TM subunits are thought to dimerize, thus the channel has a pore similar to channels in other classes. These channels are termed leak or background channels, they are voltage-independent and can contribute to setting the resting membrane potential and regulating cellular excitability [Patel & Honorè, 2001; Cohen et al., 2009].

The 2TM channels are the smallest and they are supposed to be the phylogentically oldest potassium channels [Hille, 2001]. The structure of the 2TM channels represents the basic arrangement of more complex potassium channels in fact each subunit is composed of only two TM domains containing the pore region. Four individual subunits form a single potassium ion pore [Yang et al., 1995]. The 2TM channel group includes the Kir channels, initially termed "anomalous" rectifiers, that conduct an inward potassium current at membrane voltages negative to the K^+ equilibrium potential and conduct little, if any, outward current during depolarization [Katz, 1949; Lu, 2004].

X-Ray crystallographic structure of KcsA and KirBac1.1, two bacterial potassium channels

Important enhancements in the comprehension of potassium channels structural feature have been obtained with the resolution of the fist crystallized potassium channels: the bacterial KcsA (*Streptomyces lividans*) and KirBac1.1 (*Burkholderia mallei*). As introduced before, although all the difficulties to crystallize ion channels, the X-ray structures of two prokaryotic potassium channels have been obtained [Doyle et al., 1998; Kuo et al., 2003]. Comparing electrophysiological data and the x-ray crystal structure, the properties of selectivity and gating have been elucidated.

The structure of KcsA (3.2 Å) revealed for the first time the tetrameric structure of the potassium channel and identified the selectivity filter within the pore as the structure responsible for the ion selectivity.

The KcsA and KirBac structures (fig. 3) revealed that the channels are formed by four identical subunits, each constituted by two α-helices (TM1 and TM2) bond by the pore region (P) that is formed by a turret, a pore helix and the selectivity filter. The TM2 (the inner helix) of the four subunit are bended of 25° and making contact one to each other form an inverted cone that confers the channel a closed conformation. The pore loop, located between the TM1 and TM2 helices, contains the descending pore helix and the ascending K^+ channel signature sequence. Both structures suggest that the bundle crossing formed by the inner pore helices constitute the intracellular channel gate. The KirBac1.1 structure includes an additional helix, the ‘slide helix’, which runs parallel to the cytoplasmatic face of the membrane.

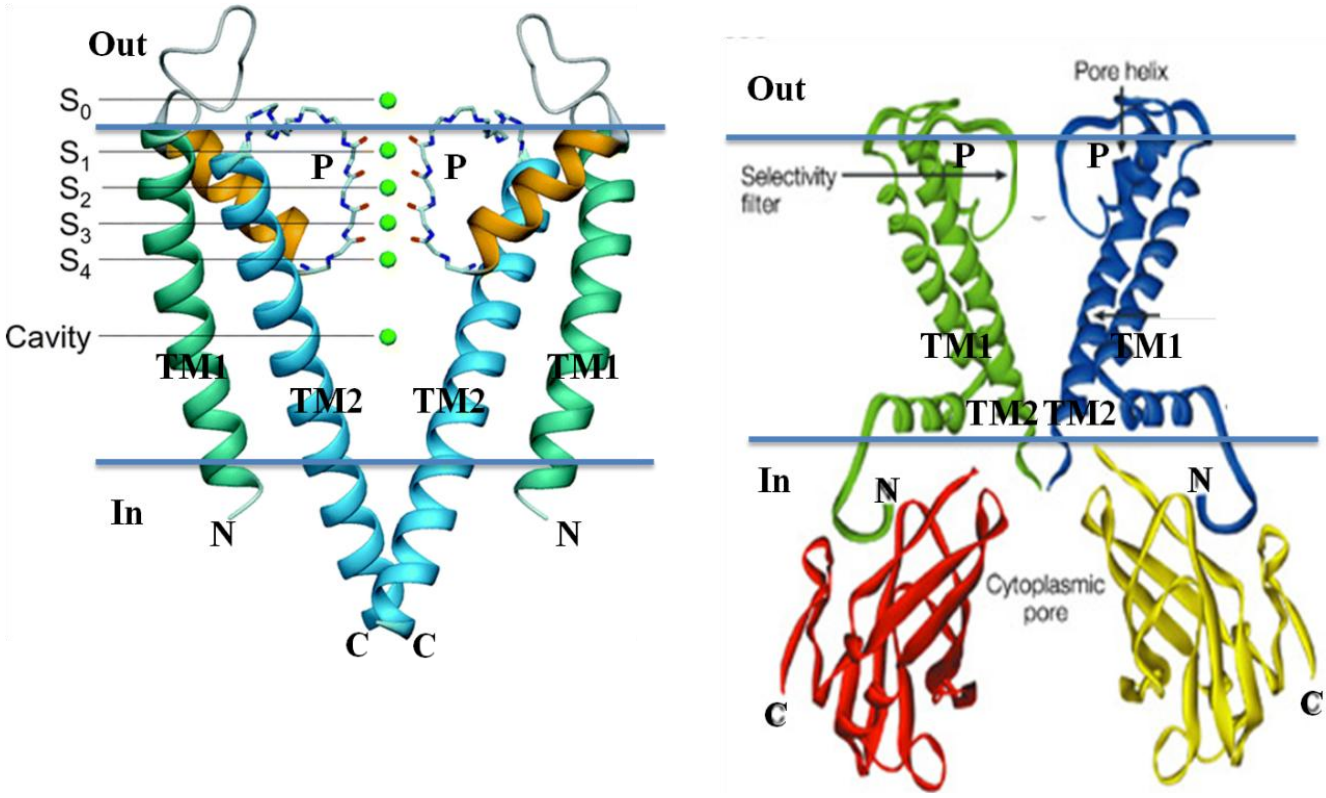

Fig. 3. Crystal structures of Kcsa and KirBac1.1. View of two of the four subunits of the channels. Green dots represent the position that the K^+ ions can occupy.

The selectivity, which is the property of the channel to discriminate between ions, i.e. sodium and potassium, is conferred by the conserved signature sequence TXGY(F)G in the pore helix. The carbonyl oxygens of this sequence form the binding site for K^+ ions, in fact, point mutations in this sequence, abolish the selectivity to potassium [Heginbotham et al., 1994].

The structure of the KcsA channel at 2 Å obtained with the co-crystallization of the channel and Fab fragments of the monoclonal antibody that recognize the tetramer, allowed to get more details about the mechanism of selectivity [Zhou et al., 2001]. The hydrated K^+ ions are attracted by the negative charge of the glutamic acid at the channel entryway and then go into the selectivity filter discarding the water molecules and interacting with the 4 carbonyl-oxygen atoms of the pore and the oxidril-oxygen of the threonine at the end of the filter. Since the radius of the pore is 2.8 Å and the K^+ ion hydrated with 8 water molecules is 4.2 Å, the ion has to leave its hydration shell and interacts with the oxygens of the carbonyl amino acids of the pore (fig. 4) that recreate the hydration of the ion.

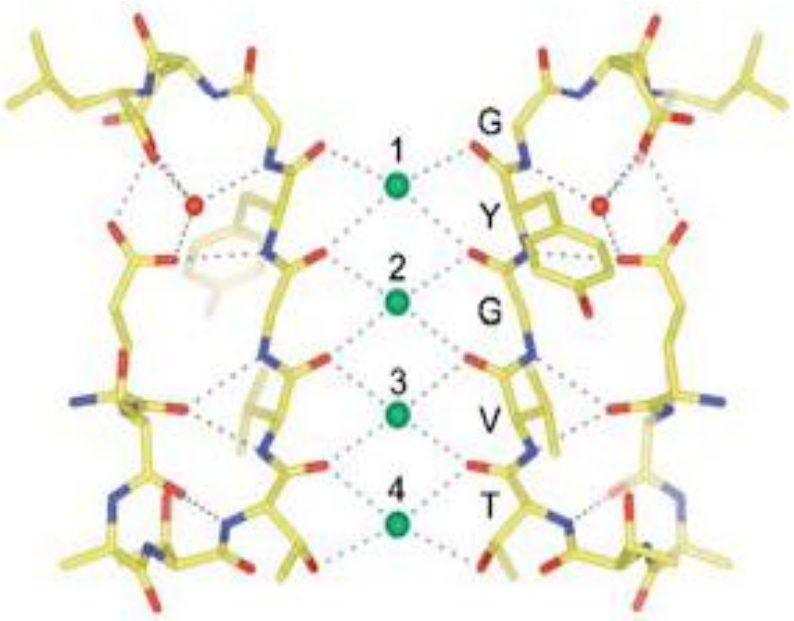

Fig. 4. Structure of the selectivity filter of KcsA. In green the 4 binding sites for potassium.

Although sodium is smaller of potassium it cannot interact with the carbonyls and cannot pass through the pore. The selectivity is given by this interaction, although not due to size effect.

Inside the filter two K^+ ions are present at the same time and they present two configurations, with alternate occupancy of the site by the ion or by a water molecule.

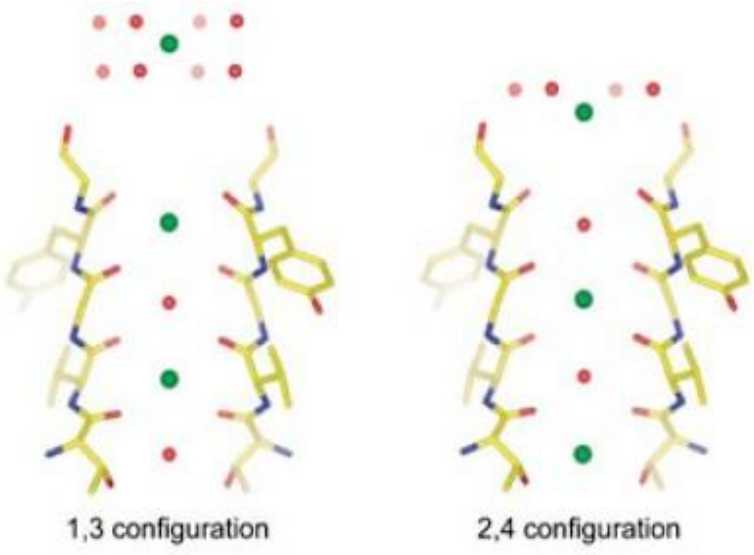

Fig. 5. Structure of Kesv filter in 1,3 and 2,4 configurations. In green the K^+ ion, in red the water molecules. The K^+ ion is hydrated by 8 water molecules and when enter the pore is dehydrate.

The entrance of one ion is associated with the exit of another ion in the opposite direction and generates a change of configuration. The entrance of another ion induces a conformational change that makes the interaction of the ion less stable and favors the flux of ions [Zhou et al., 2001, MacKinnon, 2003].

The crystallization of the KcsA in low (3 mM) and high (200 mM) K^+ concentration has also explained the involvement of the filter in the gating mechanism. Bundle crossing is not the only responsible of gating. Mutational studies in the selectivity filter [Lu et al, 2001] or changes in the permeant ions [Swenson & Armstrong, 1981] combined with electrophysiological data reveal that the selectivity filter too is responsible of a second gating mechanism. The indication that the filter is not a rigid structure is consistent with this hypothesis.

Since the K^+ channel signature sequence is conserved among all K^+ channels, and the KcsA pore can substitute for the pore of other K^+ channels [Lu Z et al., 2001] maintaining its properties, it can be concluded that the mechanism of ion selectivity and permeation at the level selectivity filter is similar in all K^+ channels.

Viral potassium channels: PBCV-1 Kcv

As mentioned before, at the end of ’90, potassium channels have been discovered also in viruses. Viruses in which potassium channels have been identified are members of the family of Phycodnaviridae, big icosahedral viruses, with double-strand DNA, that infect algae [Van Etten & Meints, 1999]. The viral potassium channels are 2TM channels and they are so small that are reduced to the pore of more complex proteins.

The fist potassium channel discovered was PBCV-1 Kcv (*Paramecium bursaria* Chlorella virus). It was found in the genome of the PBCV-1 virus, a large icosahedral virus (genome 330 Kb), prototype of the Phycodnavirus family, that has about 50 members, that infect and replicates in single-channel alga *Chlorella* NC64A (fig. 6) [Van Etten & Meints, 1999]. The *Chlorella* alga lives in symbiosis with the *Paramecium bursaria*, but it is interesting that the virus infects only the cells that have lost the symbiosis [Kang et al. 2003].

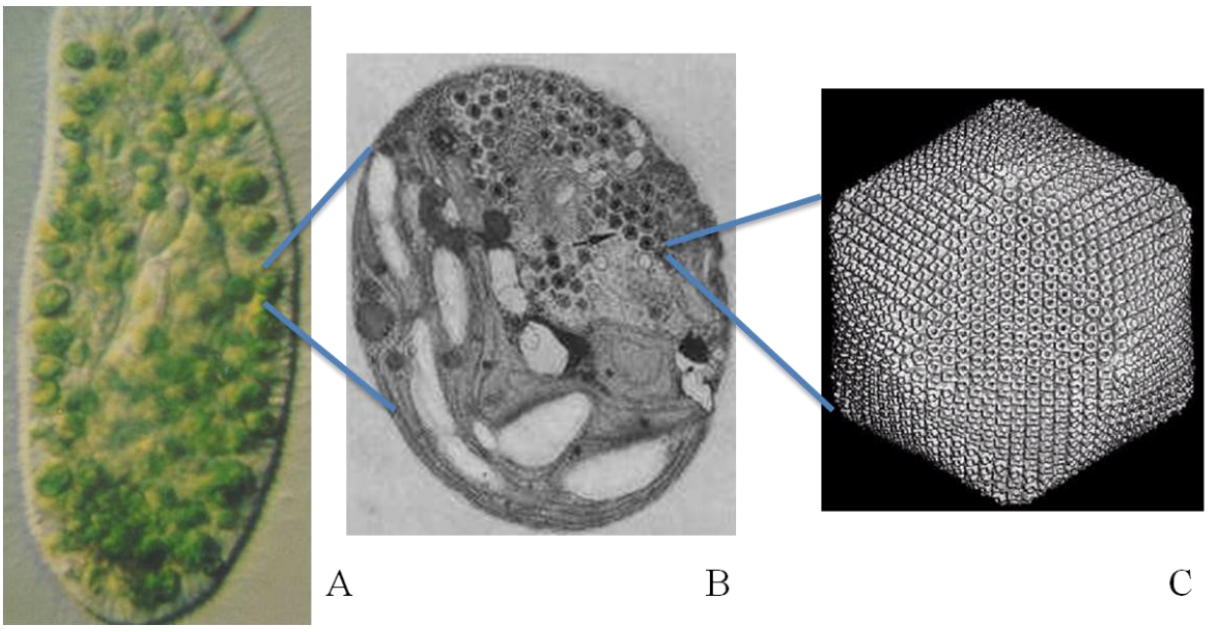

Fig. 6. Relation between *Paramecium bursaria*, *Chlorella* NC64A and the PBCV-1 virus. A) *Paramecium* cell in symbiosis with *Chlorella* cells at the optic microscopy; B) Electron Microscopy image of *Chlorella* NC64A infected by the virus; C) PBCV-1 image obtained with electron microscopy (100 nm).

Sequencing the DNA of the virus [Lu et al., 1996] an ORF (A250R) coding for a 94 amino acids peptide was found. The sequence of Kcv has two TM domains separated by a stretch of 44 amino acids that contains the K^+ channel signature sequence THSTVGFG. The 26 amino acids

surrounding this motif display show, on average, 61% similarity and 38% identity with the pore domains of many K^+ channel proteins [Plugge et al., 2000]. The main difference with the other 2TM channels is in the cytoplasmic domains. The N- terminus is in fact only 12 amino acids long and the C-terminus is not cytoplasmic and it is part of the TM2 domain (fig. 7).

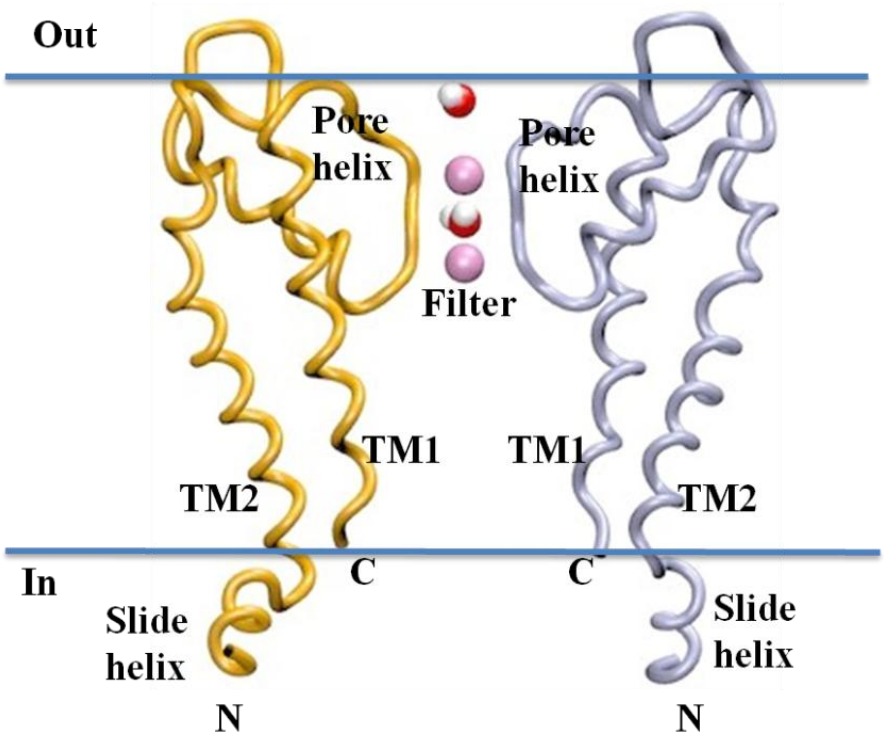

Fig. 7. Structural model of Kcv channel obtained by homology with KirBac1.1 crystal. Only two of the four subunits are showed.

As showed by the structure of Kcv obtained by homology with the structure of KirBac1.1 the TM2 seems to be too short to generate the bundle crossing and seems not to be involved into gating mechanism, although recent analysis of molecular dynamics revealed that the four TM2 of the channel can get closer and obstruct the passage of the ion through the pore [Tayafeh et al., 2007]. This structure can suggest that the channel is always open, but the hypothesis contrasts the experimental data.

PBCV-1 Kcv has been expressed in heterologous systems as *Xenopus* oocytes [Plugge et al., 2000], yeast and mammalian cells HEK 293 [Moroni et al., 2002] and in these systems it forms K^+ selective ion channel characterized by voltage clamp analysis [Gazzarrini et al., 2003].

Kcv was first expressed in oocyte of the *Xenopus laevis* heterologous system. The expression revealed that the protein forms a channel that conducts inward and outward currents. Kcv current is composed by an instantaneous component and a time-dependant component. The I/V curve (current/voltage) it's linear over a broad range and decreases at extreme voltages suggesting the Kcv is a slightly sensitive K^+ channel (fig. 8).

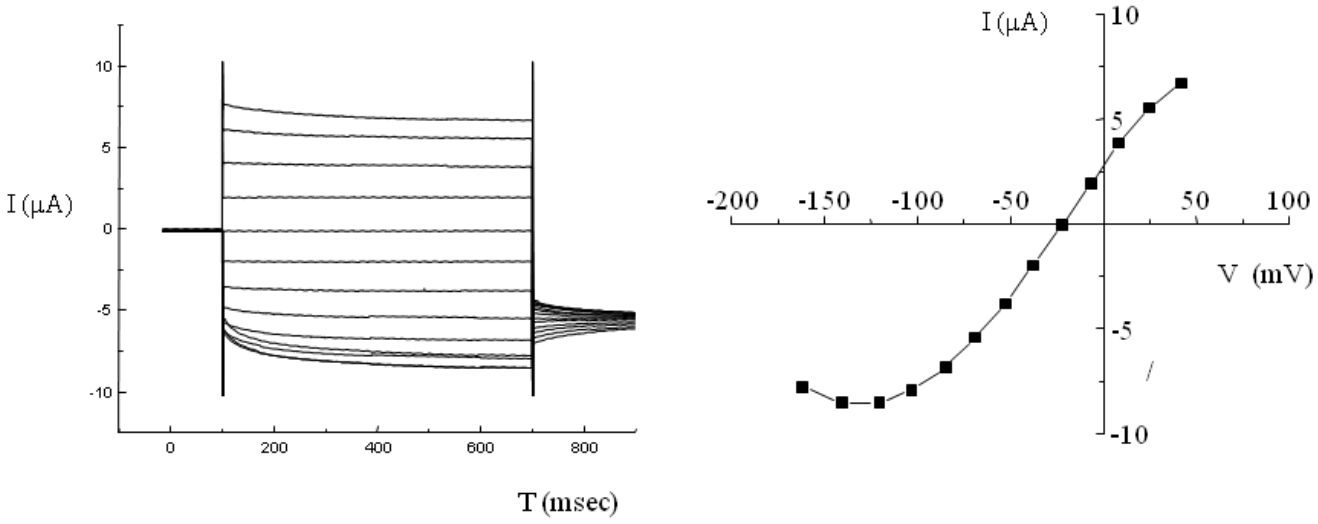

Fig. 8. Exemplary currents recorded from –180 mV to +80 mV and relative current-relation of Kcv expressing in *Xenopus* oocytes (external solution contained 50 mM KCl).

Kcv is a K^+ selective channel and the permeability ration PK^+/PNa^+ is about 10 [Plugge et al., 2000; Moroni et al., 2002].

Since it was known that the expression of recombinant proteins in *Xenopus* oocytes can produce artifacts because the overproduction of the protein induces the oocytes to upregulate endogenous channels [Coady et al., 1998; Barhanin et al., 1996] several experiments have been done to establish if the conductances recorded in oocytes after injection of Kcv cRNA were due to Kcv or to endogenous currents. A mutant of Kcv was created in which the Phe 66, in the selectivity filter, was exchanged for an Ala. K^+ channels with this amino acidic substitution were expressed by the heterologous cell but they were unable to conduct [Heginbotham et al., 1994]. Also in Kcv, this mutation was completely removing the current specifically induced by wt Kcv in control oocytes.

Similar results were also obtained in other heterologous systems, the mammalian HEK 293 cell and in the CHO (Chinese Hamster Ovary) cells. The only differences were in the kinetic properties and

in the voltage-dependence of the channel. Expression system are known to affects the properties of other channel [Peterson et al., 1990], but the reasons for these differences are unknown.

From these studies also emerged that the currents are blocked in presence of barium and amantadine an antiviral drug. Both amantadine and Ba^{2+} also block at the same concentration the infection of *Chlorella* alga [Mehmel et al., 2003]. This evidence suggests that the channel is involved in viral replication.

The physiological roles of the viral channel proteins are largely unknown except for the M2 protein from influenza virus. The M2 channel allows hydrogen atoms to enter the virion, which results in a pH dependent fusion of endosomal and viral membranes [Ciampor et al., 1995; Martin et al., 1991]. For other viral channels current hypothesis suggest a role in the infection, physiological modifications of the host, or release of progeny viruses [Carrasco et al., 1995].

There are evidences [Mehmel et al., 2003] that Kcv channel plays an essential role in virus replication because both PBCV-1 plaque formation and Kcv channel activity in Xenopus oocytes have a similar sensibility to the inhibitors. Recordings of membrane voltage in the host cells *Chlorella* NC64A reveal a membrane depolarization with release of a flux of K^+ ions within the first few minutes of infection. The loss of potassium is related with a water flux from the host that reduces the turgor pressure of the cell and may allow the ejection of viral DNA into the *Chlorella* [Neupärtl et al., 2008].

This model assumes that Kcv is located in the internal membrane of the virus [Yan et al., 2000]. The proposed model of the infection (fig. 9) predicts that PBCV-1 virus attacks *Chlorella* by attaching rapidly to the external surface of the cell wall. Attachment always occurs at a virus vertex and is followed by degradation of the cell wall at the attachment point. The attachment allows the virus membrane to come in contact with and fuse with the host membrane. This fusion event, presumably aided by a virus packaged fusion protein, releases virus DNA and probably some DNA-associated proteins into interior of the host cell. The depolarization of the host plasma membrane could also explain the exclusion phenomenon associated with the chlorella viruses, that means that the infection by one chlorella virus, like many bacteriophages, results in poor infection by a second virus [Chase et al., 1989; Greiner et al., 2009].

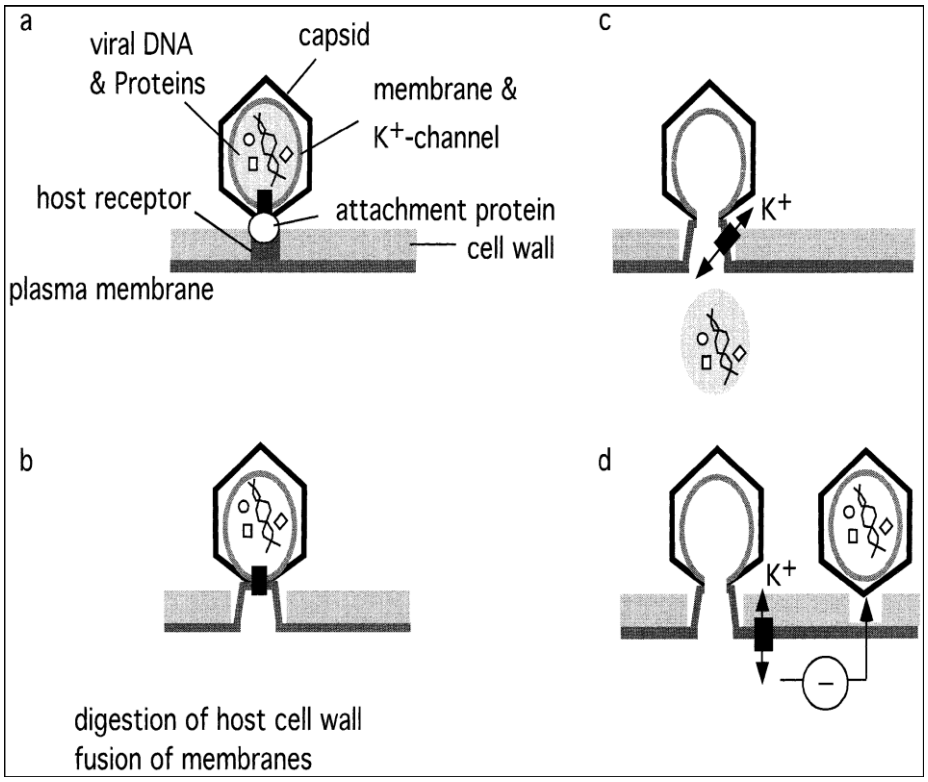

Fig. 9. Model for early events and role of the K^+ channel in PBCV-1 infection of *Chlorella* NC64A cells. a) Sketch of PBCV-1 architecture including capsid, internal membrane and Kcv and schematic view of virus attachment to *Chlorella* cells. b) Digestion of cell wall and fusion of membranes may lead to incorporation of Kcv into host cell membrane. c) Elevated K^+ conductance would result in depolarization, loss of K^+ and consequent decrease in host cell turgor pressure. Altogether this may make easier for the virus to insert large genome and proteins into the host cell. d) Membrane depolarization may be a signal, which avoids multiple infections.

Viral potassium channels: Kcv-like channels

Considering the essential role of the PBCV-1 Kcv channel in the virus, it was expected that Kcv channels could be present also in other Chlorella infecting viruses. Using PBCV-1 Kcv as probe genes encoding "Kcv-like" proteins were isolated from 40 additional Chlorella viruses. Differences in 16 of the 94 amino acids of the protein were discovered, producing six Kcv-like proteins (CA-4B, AL-2A, MA-1D, NY-2B, AN-69C Kcv) with amino acid substitutions occurring in most of the functional domains of the protein (N-terminus, TM1 and TM2, pore helix and selectivity filter) [Kang, 2003].

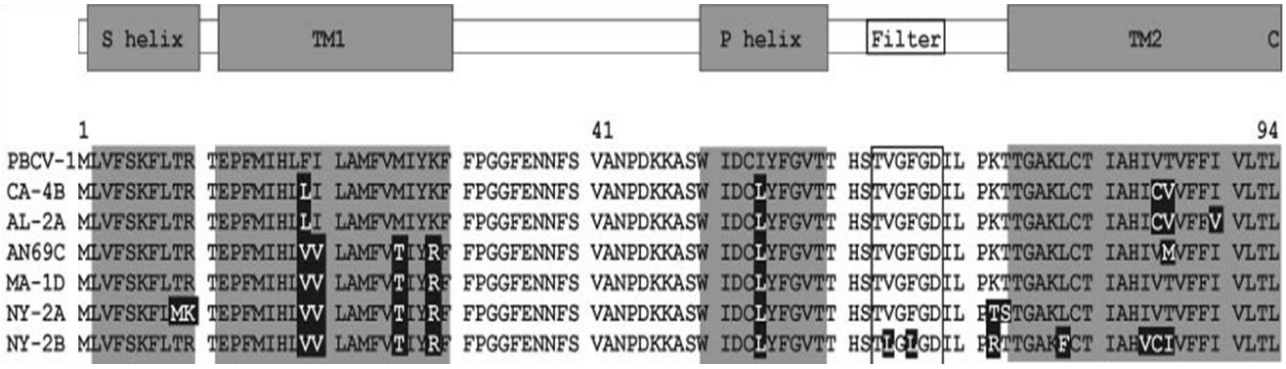

Fig. 10. Alignment of Kcv proteins. Each protein is named after a virus (PBCV-1, CA-4B, AL-2A, AN69C, MA-1D, NY-2A, NY-2B) representative of each group. Amino acid substitutions, compared with PBCV-1 Kcv, are highlighted in black. The assignment of putative structural domains is based on the alignment between PBCV-1 Kcv and KirBac1.1.

Expression of these six Kcv-like proteins in *Xenopus laevis* oocytes showed that they all form K^+ selective channels and that the properties of the six new K^+channels, or subgroups among them, differ from those of the reference channel PBCV-1 Kcv [Kang, 2003; Gazzarrini et al., 2004]. These differences include the inactivation of inward current in K^+ solutions (all channels), the absence of inactivation of inward current in Rb^+ solutions (all except NY-2B Kcv) and the full block of inward current by external Cs^+ (MA-1D, NY-2A, and NY-2B Kcv channels).

The six Kcv-like channels differ from PBCV-1 Kcv by a minimum of four amino acids (CA-4B) to a maximum of 12 amino acids (NY-2B). Amino acid substitutions exist in slide helix, TM1, TM2, pore helix, and also in the selectivity filter sequence "GFG," highly conserved among K^+ channels (Hille, 2001). Positions of key residues of PBCV-1 Kcv are shown in a putative structural model (fig. 11).

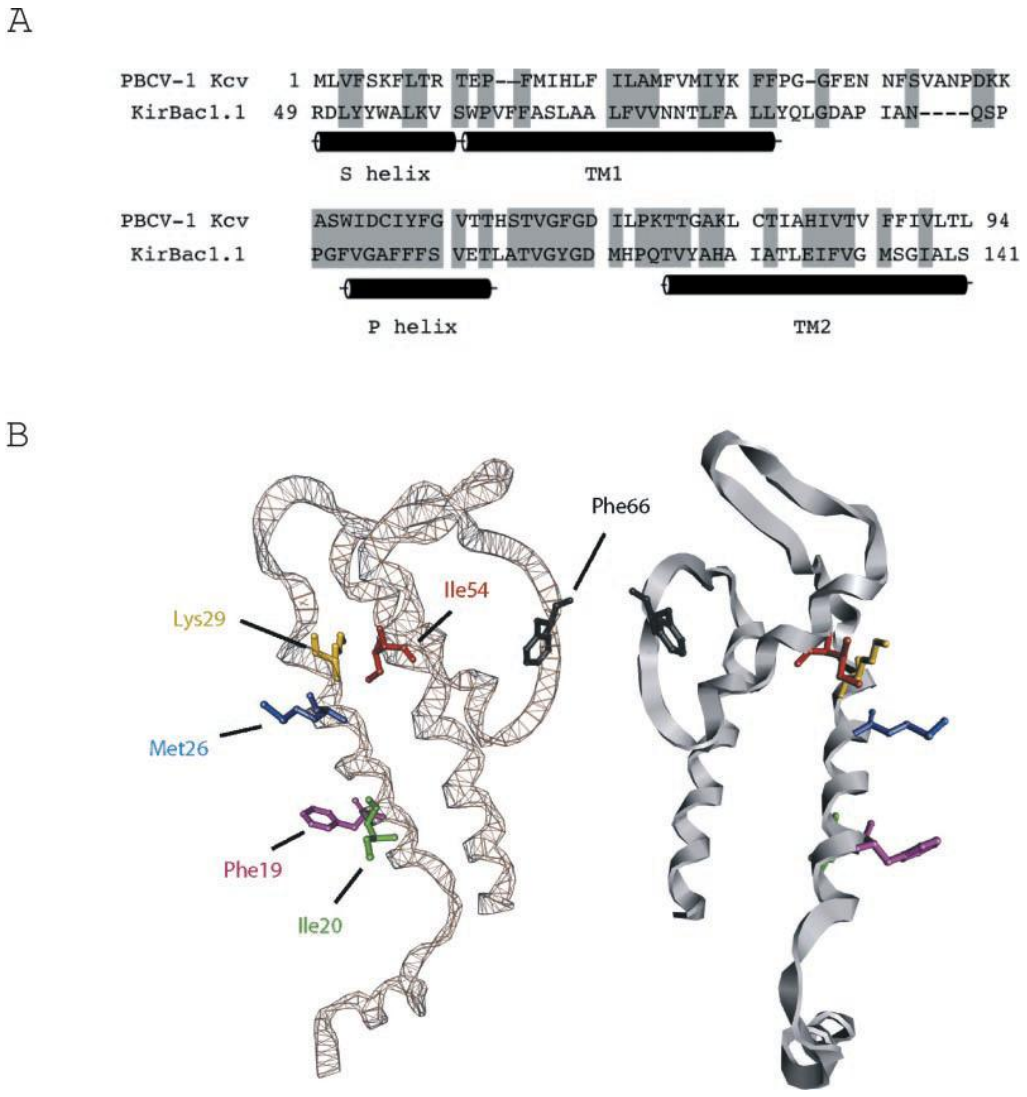

Fig. 11. Putative locations of key amino acid residues of PBCV-1 Kcv. A) Alignment of PBCV-1 Kcv to KirBac1.1. Identical amino acids and conserved substitutions are highlighted in gray. B) Structural model of PBCV-1 Kcv obtained by homology to the KirBac1.1 pore structure. Two of the four subunits are shown. Six residues are highlighted: Phe-19, Ile-20, Met-26, and Lys-29 in TM1, Ile-54 in the pore helix, and Phe-66 in the filter.

Mutational analysis allowed to determine whether amino acid substitutions in each set contributed singly or in combination to the channel property. The results indicate that none of the properties resulted from a single amino acid substitution. Three sets of amino acid substitutions associated with three specific channel properties were identified [Gazzarrini et al., 2004]:

1) K^+ current inactivation: influenced by three mutations in three different domains of the protein: the TM1 domain (amino acid 19), the pore helix (amino acid 54), and the selectivity filter (amino acid 66).
2) High Rb^+ permeability: suggested by an interaction between the pore helix (amino acid 54) and the selectivity filter. Position Leu-54 in the pore helix is next to two aromatic amino acids (Tyr and Phe) that are highly conserved among all K^+ channels. This suggests that the pore helix interacts with the selectivity filter as in KcsA crystal structure [Doyle, 1998].
3) Block by Cs^+: influenced by mutations all located in TM1 (amino acids 19 in MA-1D, 20 and 29 in PBCV-1) which presumably forms the outer helix. This is a third example of a long-range interaction. Therefore, a feature such as a channel block, which must occur inside the pore [Ichida et al., 1996; Becker et al., 1996; Garofoli et al., 2003], is affected by a distant domain. Amino acid 19, 20 or 29 must interact with the inner pore to change the sensitivity to Cs^+. However, when the structure of the bacterial K^+ channel KirBac1.1 is used as a reference to predict the structure for Kcv (fig. 8B), amino acid 19 is neither near nor associated with the selectivity filter or the inner pore domain; this result suggests that amino acid 19 is coupled indirectly to the pore domain.

Correlations between amino acid substitutions and the new properties displayed by these channels guided site-directed mutations that revealed synergistic amino acid interactions within the protein as well as previously unknown interactions between distant channel domains.

The sodium permeability and the barium block were not influenced by any of this amino acids substitution in the Kcv-like channels.

Barium it is known as a blocker of a wide number of potassium channels [Armstrong and Taylor, 1980; Eaton & Brodwick, 1980; Armstrong et al., 1982; Vergara & Latorre, 1983; Benham et al., 1985; Miller, 1987; Neyton & Miller, 1988; Zhou et al., 1996; Harris et al., 1998; Vergara et al., 1999] and it was found to bind the site 4 of the selectivity filter of KcsA channel in its crystal structure in presence of $BaCl_2$ [Jiang & MacKinnon, 2000]. Mutation of the aminoacid T75, that provide the carbonyl oxygen for the site 4 binding site, reveal a loss of tetramer stability in the presence of the ion that results in thermal destabilization of the native form of the protein [Krishnan et al., 2008].

Randomized mutagenesis combined with yeast complementation assays and PCR-backcrossing technique allowed to identify in PBCV-1 Kcv the amino acid responsible for barium binding and resulting block [Chatelain et al., 2009].

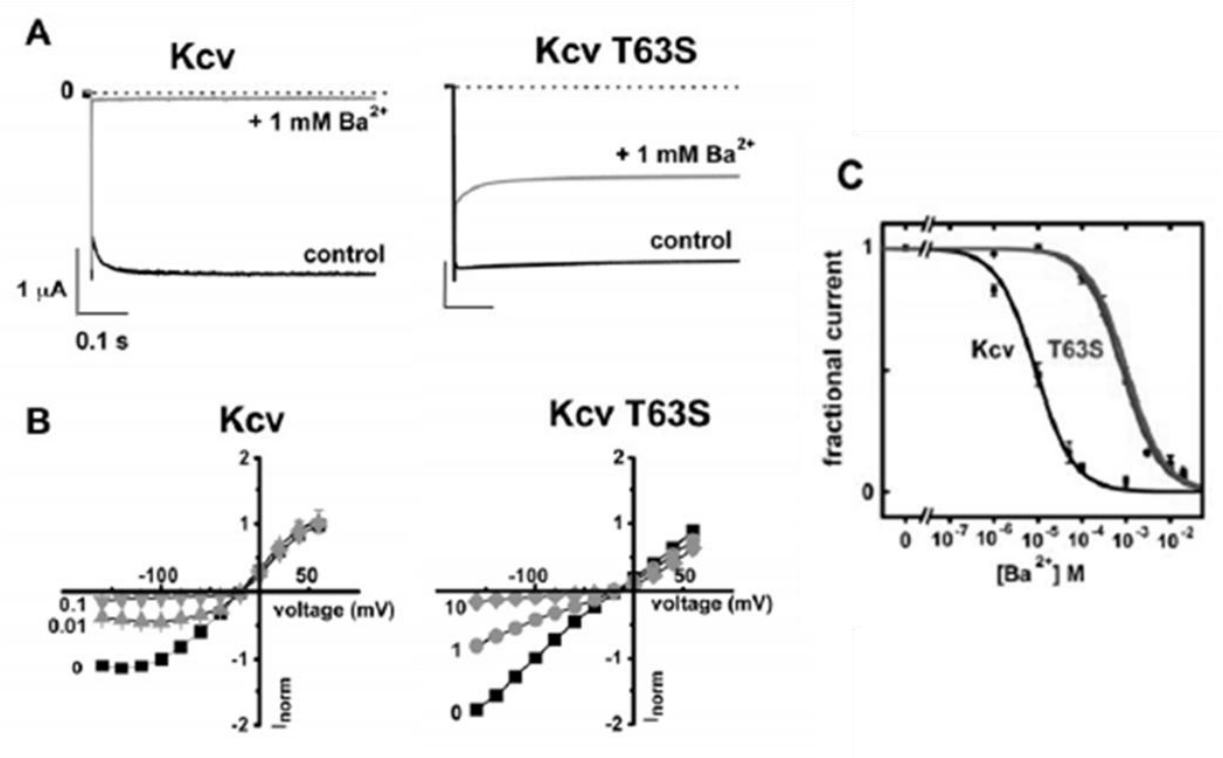

Fig. 12. Functional characterization of Kcv mutant T63S. A) Exemplary currents of PBCV-1 Kcv WT and T63S measured with two electrode voltage clamp in 50 mM potassium and with 1 mM Ba^{2+}. B) Current-voltage relation of Kcv and T63S in presence of increasing barium concentration. C) Comparison of the barium affinity of the two channels at -80 mV.

The mutation of the identified amino acid T63 in a serine, although does not influence the coordination side chain oxygen, strongly affects the channel block, resulting in a loss of sensitivity for barium, as confirmed also by tetramer stability assays in presence of Ba^{2+}.

Since the same mutation in Kir2.1 has not the same strong effect (affinity more than 10 times higher for Kcv), it was taken into consideration the fact that in the adjacent position, the 62 in Kcv, there a serine and not a threonine as in the majority of potassium channels. The effect of this amino acid was analyzed by mutating it into a Thr, and the result was that the effect of T63S mutation was partially reduced resembling the Kir2.1 behavior. This analysis revealed the coupling of the position

62 and 63 in respect to barium binding and suggested that the presence of a methyl group in the site 4 has a role in the ion coordination [Chatelain et al., 2009].

Viral potassium channels: MA-1D Kcv

Between Kcv-like channels MA-1D Kcv results to be the one that exhibits the larger functional distance with higher diversity from PBCV-1 Kcv. It differs in fact in all the three properties, but with the fewest amino acids substitution (19, 20, 26 and 29 in TM1 and 54 in the pore).

The mutations are not independent, but they interplay to generate a different channel behavior.

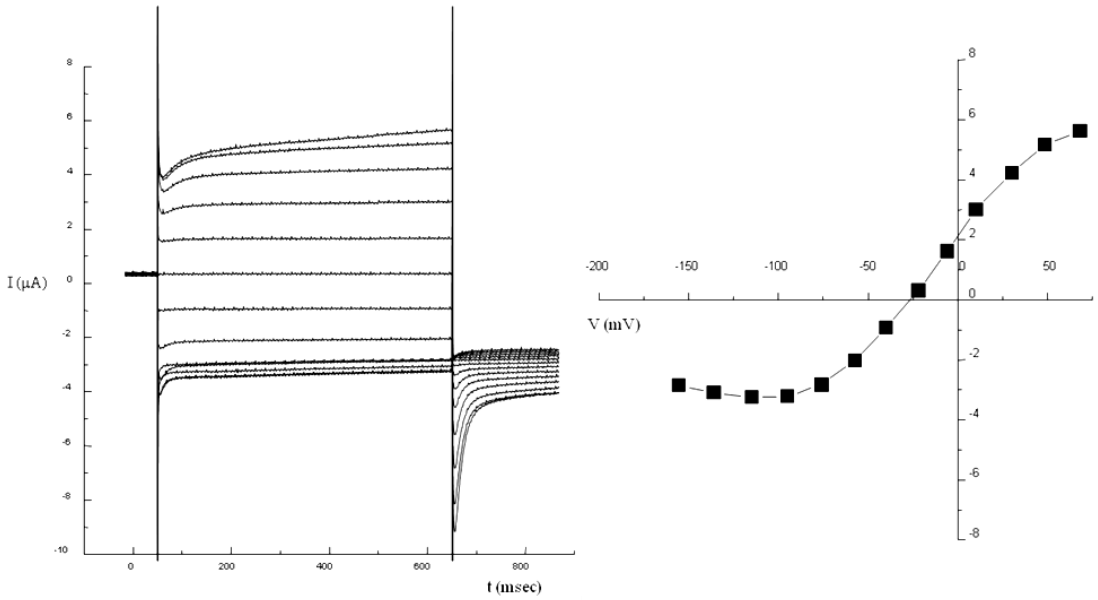

Fig. 13. Exemplary currents recorded from –180 mV to +80 mV and relative current-relation of MA-1D Kcv expressing in *Xenopus* oocytes (external solution contained 50 mM KCl).

Converting the different amino acids in those present in the PBCV-1 Kcv channel the phenotype is partially reverted, confirming that these amino acids are responsible for functional properties of the channels.

Viral potassium channels: MT325 Kcv

K^+ channels can be found also in other phycodnavirae, like MT325, which infects another host strain, *Chlorella* Pbi, also a symbiont of *Paramecium bursaria* [Gazzarrini et al., 2006].

Virus MT325 ORF M183R encodes a 95 amino acids protein, named MT325 Kcv with the 50% of identity to the other Kcv channels. The predicted structure is significantly different because it lacks 10 amino acids at the N terminus forming the slide helix in PBCV-1 Kcv and contains 10 amino acids at the C terminus absent in the PBCV-1 Kcv [Gazzarrini et al., 2006] (fig. 14).

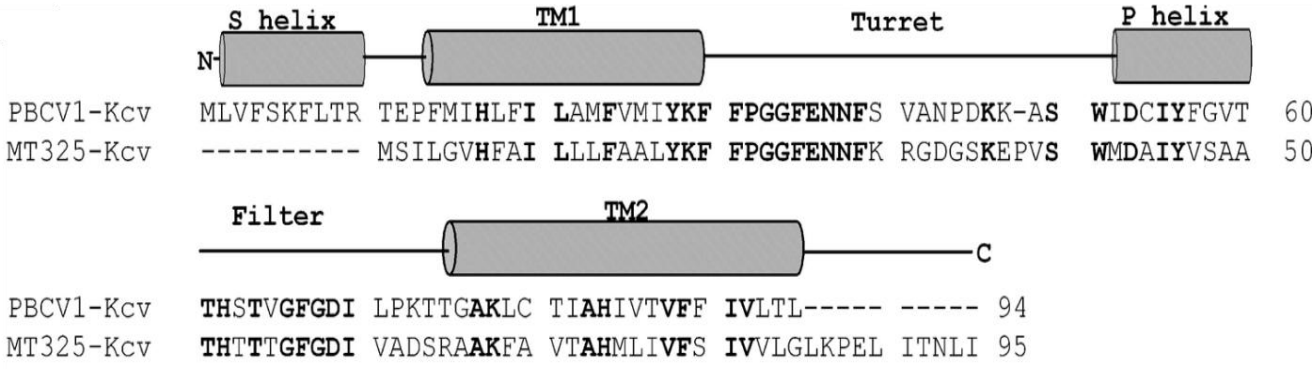

Fig. 14. Sequence alignment of MT325 Kcv with PBCV-1 Kcv. Identical amino acids are in boldface. The putative structural domains are based on homology with KirBac1.1.

Despite the structural differences with Kcv, MT325 Kcv expressed in oocytes produced a functional outwardly rectifier K^+ channel, inhibited by classical K^+ channel blocker Ba^{2+}, and selective for K^+ [Gazzarrini et al., 2006]. Figure 15 clearly shows the lack of voltage-dependent current in this channel and the typical bending of the I/V relationship at negative potentials.

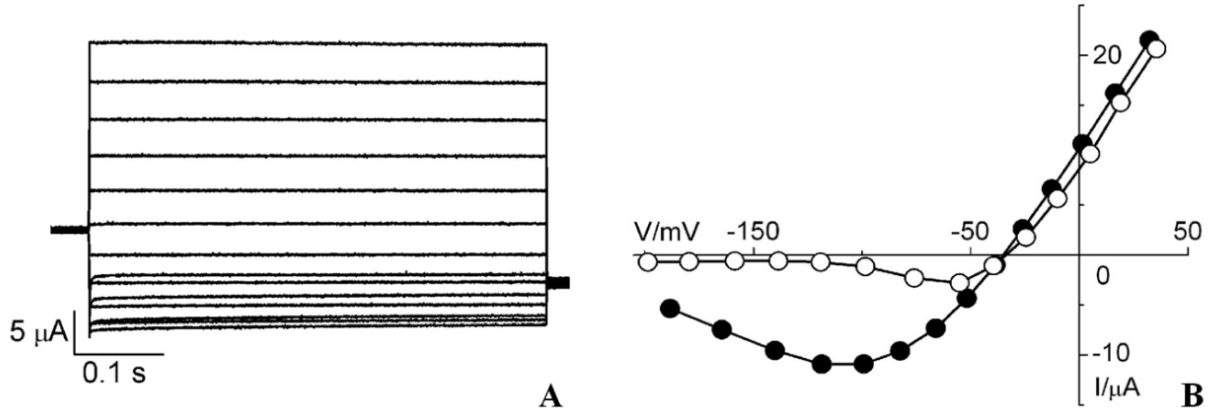

Fig. 15. A) Exemplary macroscopic current traces recorded by voltage-clamp from a MT325 Kcv injected oocyte in 20 mM external K^+. B) I/V current relationship of the measurement showed in A (in black) compared with currents in presence of 2mM Ba^{2+} in the external solution.

Viral potassium channels: ATCV-1 Kcv

ATCV- 1 is another member of the Phycodnaviridae family that attacks a *Chlorella* strain SAG 3.83 that lives in symbiosis with a protozoan, *Acanthocystis turfacea*. Also in virus ATCV-1 was found an ORF Z585R that encodes for a Kcv channel [Fitzgerald et al., 2007]. The sequence is only 82 amino acids, 12 amino acids less that the Kcv-like channels and comparing the structures it has a shorter turret and lacks at all cytoplasmatic domains (fig. 16). In the signature sequence, ATCV-1 Kcv has the Y instead of the F as all the other viral potassium channels.

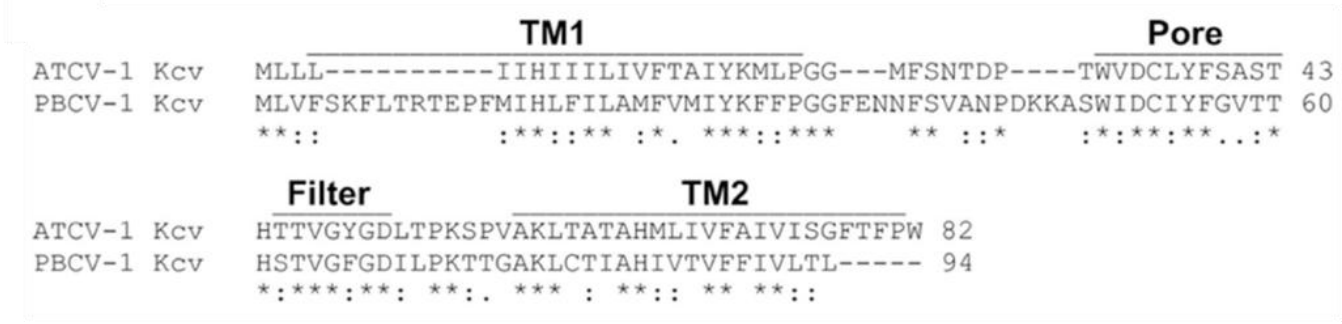

Fig. 16. Sequence alignment of ATCV-1 Kcv with PBCV-1 Kcv. Asterisks and colons indicate identical and conserved residues respectively. The putative structural domains are highlighted by horizontal line.

Fist indications that ATCV-1 Kcv forms a functional potassium channel comes from complementation of yeast *S. cerevisiae* Δ trk1, Δtrk2, a mutant that lacks endogenous K^+ uptake system [Gazzarrini et al., 2010]. The transformants are able to grow in low potassium concentration and the growth is inhibited by K^+ channel blockers $Ba2^+$ and Cs^+ confirming that the channel is expressed.

The channel was also expressed in oocytes and macroscopic currents with voltage clamp technique and single channel measurement, with patch clamp method in cell attached configuration, confirm that ATCV-1 Kcv forms a functional K^+ channel, selective for K^+ and blocked by conventional blockers (fig. 17).

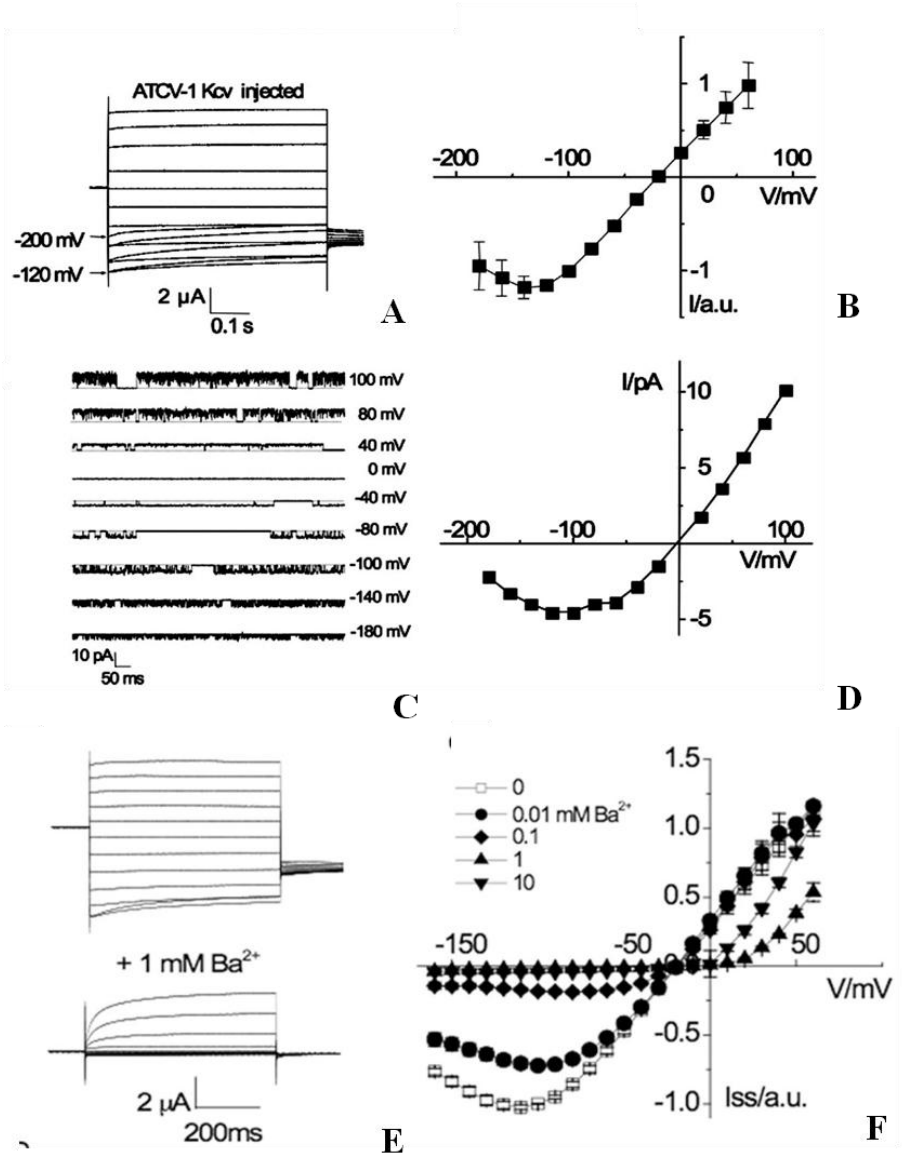

Fig. 17. A) Exemplary macroscopic currents traces recorded by voltage-clamp from an ATCV-1 Kcv injected oocyte in 50 mM external K^+. B) I/V current relationship of the measurement showed in A. C) Exemplary single channel fluctuation recorded at different voltages in cell attached configuration from an oocyte expressing ATCV-1 Kcv. D) I/V current relationship of single channel showed in C. E) Effect of 1mM Ba^{2+} on ATCV-1 Kcv currents recorded in 50 mM K^+. F) I/V current relationship of ATCV-1 Kcv in different external Ba^{2+} concentration.

In spite of its small size, this protein has all the essential feature of a K^+ channels and it is the smallest functional K^+ channel discovered.

Viral potassium channels: Kesv

A viral potassium channel was also identified in Ectocarpus *siliculosus* virus-1 (EsV-1) [Chen et al., 2005] a member of the Phycodnavirae family, which infects a filamentous marine brown alga [Van Etten et al., 2002].

Using KcsA as a probe an ORF coding a 124 amino acids protein was found in the virus genome.

Kesv is 29% homologue to PBCV-1 Kcv at the amino acid level. Together with the Kcv channel from virus ATCV-1 it is the only viral channel discovered until now with GYG instead of GFG in its signature sequence in the selectivity filter [Gazzarrini et al., 2009]. In this sense Kesv filter is similar to the filter sequence of most prokaryotic or eukaryotic potassium channels.

The alignment of the sequences of Kesv and Kcv showed that the former channel it is 23 amino acids longer at the N-terminus cytoplasmatic domain and 7 amino acids longer at the C-terminus (fig. 18).

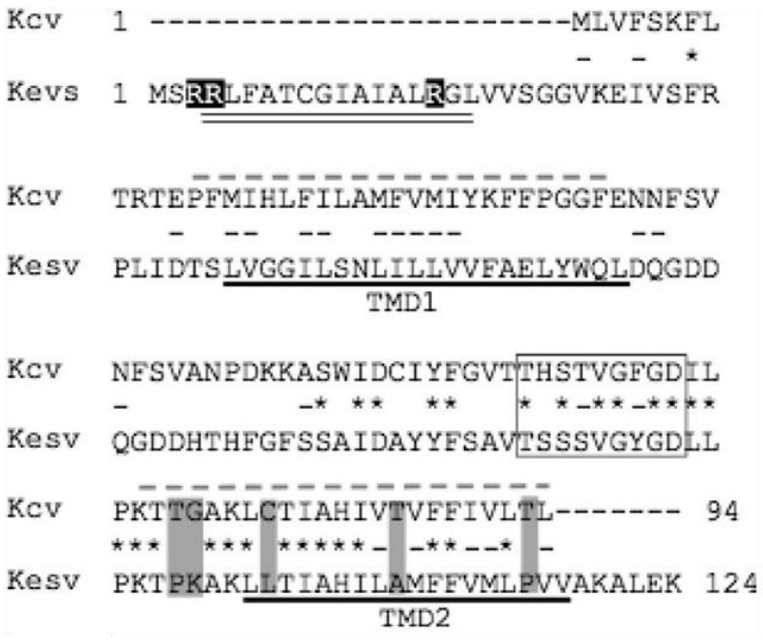

Fig. 18. Sequence alignment of Kesv with PBCV-1 Kcv. Both sequences have an overall 55% similarity (_) and 29% amino acid identity (asterisk). The position of the selectivity filter is boxed. The positive amino acids highlighted in the N terminus of Kesv are critical for the signal peptide nature of this domain.

Despite their similarity, Kcv and Kesv are sorted in heterologous expression systems to different cellular compartments. Kcv is sorted into the ER and reaches the plasma membrane, while in the

case of Kesv, it was discovered that the channel is sorted to the mitochondria (fig. 19) [Balss et al., 2008].

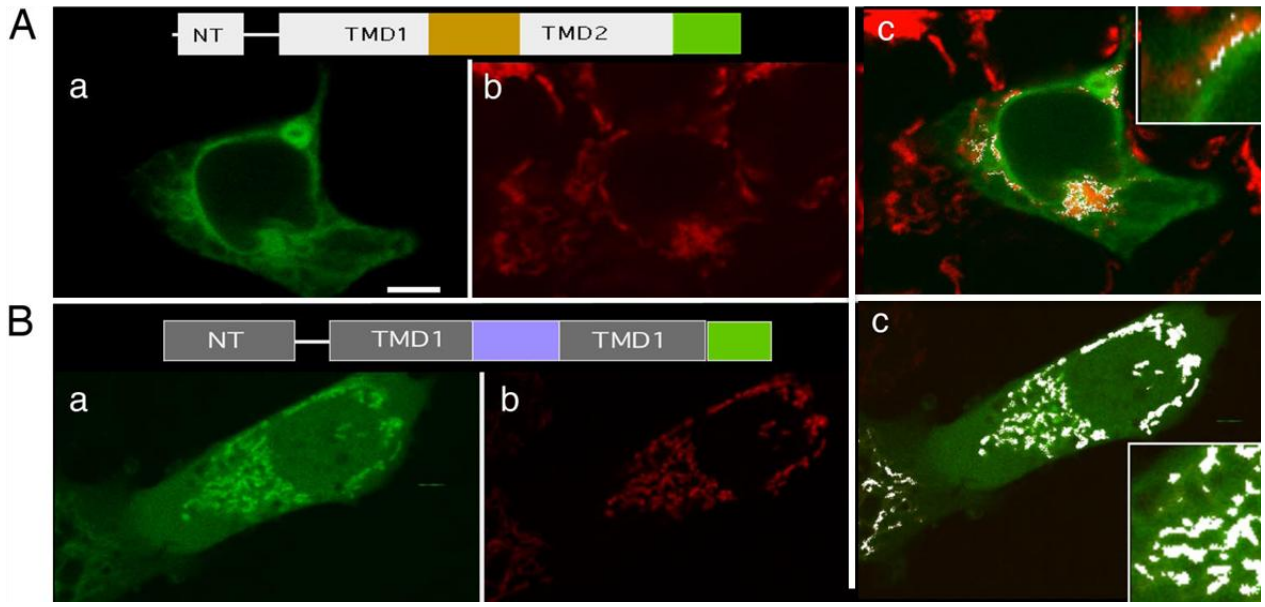

Fig. 19. Differential colocalization of Kcv:GFP and Kesv:GFP with MitoTracker in HEK293 cells A) Color-coded structural elements of Kcv:GFP chimera comprisingTM1and TM2, N-terminal domain (NT) (all in light gray), pore (orange), and GFP (green). Confocal image of exemplary HEK293 cell expressing Kcv:GFP (Aa) and staining of the same cell with MitoTracker red (Ab). Overlay of the 2 images in which colocalization of the 2 colors is shown in white (Ac). Inset magnifies a region of the cell and shows that the green and red fluorescence are well separated. The apparent colocalization only results from an insufficient resolution of the red-stained mitochondria and the green-stained perinuclear ring. (B) Color-coded structural elements of Kesv:GFP chimera comprising TM1 and TM2, N-terminal domain (NT) (all in dark gray), pore (blue), and GFP (green). Confocal image of exemplary HEK293 cell expressing Kesv:GFP (Ba) and staining of the same cell with MitoTracker red (Bb). Overlay of the 2 images in which colocalization of the 2 colors is shown in white (Bc). Inset magnifies a region of the cell and shows that the green and red fluorescences colocalize.

It was shown that by manipulating the length of the second transmembrane domain, it was possible to re-direct the channel from the mitochondria to the plasma membrane. Such a dual sorting is also known for other similar membrane proteins that are targeted to different compartments [Miyazaki et al., 2005; Karniely & Pines, 2005].

Although some measurement of Kesv activity in *Xenopus* oocytes have been published [Chen et al., 2005], they were in contrast with results from our lab. In our hands neither Kesv alone nor its chimera with the GFP were expressed at the plasma membrane of oocyte or HEK239 cells. This is in accordance with the intracellular localization of Kesv and it has been argued that the published data are endogenous currents from the oocytes and not related to Kesv activity [Balss et al., 2008].

This interpretation is also consistent with yeast complementation of mutants lacking the K^+ endogenous uptake systems. Growth of these yeast mutants on selective medium can be rescued by expressing Kcv but not by Kesv [Balss et al., 2008]. These results are consistent with the evidence that Kesv protein is imported into the mitochondria and it is not possible to measure its activity in the plasma membrane with voltage clamp on oocyte and HEK cells membranes.

In order to understand why the two viral channels are differently sorted, different chimera between Kcv and Kesv and some mutant of Kesv were tested. In these experiments it was found that a chimera of Kcv with the pore of Kesv (Kcv(P)Kesv) or a Kesv channel with an extended TM2 (Kesv113IVL) were redirected from the mitochondria to the plasma membrane of yeast and HEK293 cells. These two channel constructs were also found to be functional in yeast complementation assays and in HEK cells where there current could be recorded with voltage clamp measurement [Balss et al., 2008].

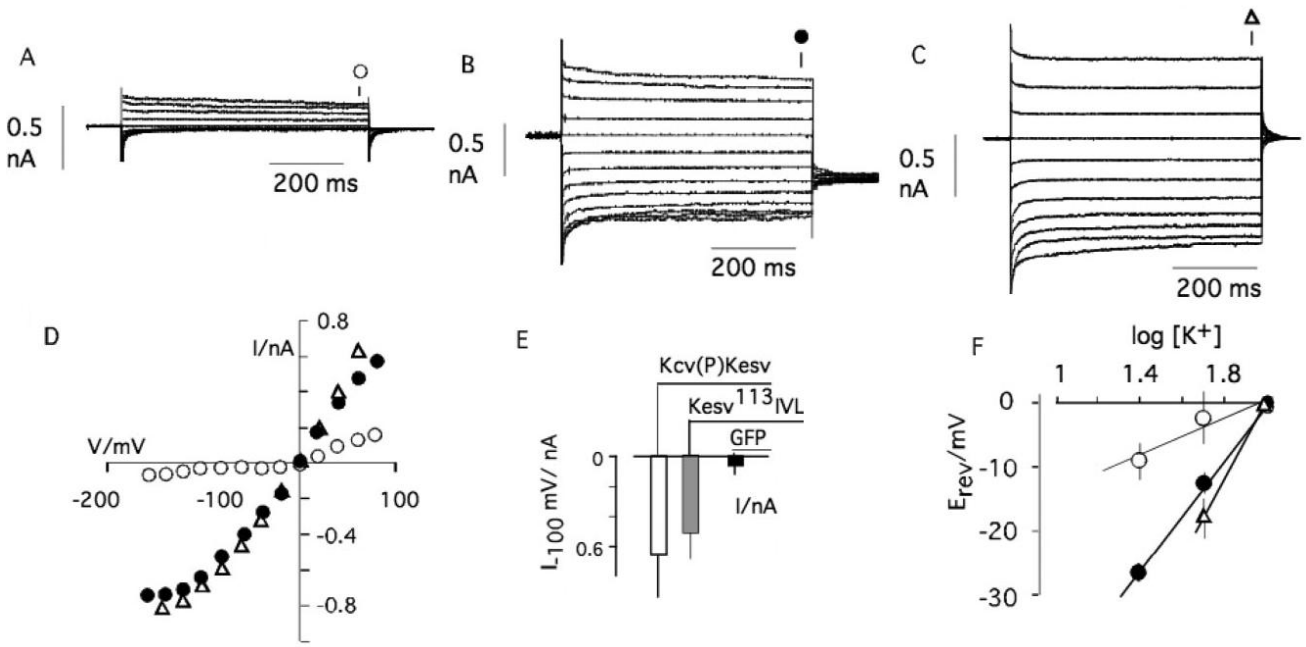

Fig. 20. Fig Kesv mutants with altered sorting signals generates conductance in HEK293 cells. Representative current responses to standard clamp protocol in a HEK293 cell transfected with only GFP (A), with Kcv(P)Kev:GFP (B), or a mutant of Kesv:GFP with an extension of TM2 by 3 aa (Kesv113IVL:GFP) (C). D) Corresponding steady-state current/voltage (I/V) relations. E) Mean steady-state currents at 100-mV test voltage from cells transfected with Kcv(P)Kev:GFP or Kesv113IVL:GFP compared with GFP-transfected. (F) Nernst plots of mean reversal voltages obtained from instantaneous I/V relations in bath solutions with different K^+ concentrations from HEK293 cells transfected with Kcv(P)Kev:GFP (filled circle), Kesv:GFP113IVL (open triangle), or mock-transfected cells (open circle).

Kcv(P)Kesv and Kesv113IVL mutants with GFP of the Kesv channel when transfected into HEK293 cells generated currents different from the GFP alone (control) transfected cells. These currents are similar to those of Kcv GFP transfected cells [Hertel et al., 2006] and generate I/V curves with typical Kcv channel feature. Current of transfected cells is 10 times higher of those of the control cells, and the conductance is K^+ concentration dependent. That means that both the proteins are functional K^+ channels.

Heterologous expression system: *Pichia pastoris*

The production of proteins for structural and functional analysis is related to the cellular machinery of the heterologous organism chosen for the expression. Among the many systems available *E. coli* is one of the more frequently used organism for heterologous expression of proteins since its genome has been entirely mapped, it is easy to handle, grows rapidly, and allows simple recovery of the target protein [Makrides, 1996; Baneyx, 1999; Sorensen & Mortensen, 2005]. However, since *E. coli* is a prokaryote and its lack of intracellular organelles, such as the endoplasmic reticulum and the Golgi apparatus that are present in eukaryotes and that are responsible for post-translational modifications or glycosylation, it often causes the production of non functional eukaryotic proteins since these modification cannot occur.

To overcome problems encountered with the use of *E. coli* to produce eukaryotic proteins, other organisms have been studied as suitable replacements. Mammalian, insect and yeast and cells are the best substitute of *E. coli* system for the expression of eukaryotic proteins.

Yeast is one of the most used organism because it combines the simple genetic manipulation and the rapid growth characteristics with the machinery for performing post-translational protein modification [Clare, 1991].

Many heterologous proteins have been successfully produced in the yeast *Saccharomyces cerevisiae*. The system has however the limitations of low yields, because of the stress caused by introduction of a foreign gene, and the proteolytic degradation that is often encountered.

The methylotrophic *Pichia pastoris* has been developed as an alternative expression system to produce milligram-to-gram quantities of proteins using the methanol-induced alcohol oxidase (AOX1) promoter, which controls the gene that codes for the expression of alcohol oxidase, the enzyme which catalyzes the first step in the metabolism of methanol [de Hoop et al., 1991]. The system has been developed since *Pichia pastoris* alcohol oxidase promoter was isolated and cloned [Buckholz and Gleeson 1991; de Hoop et al. 1991]. The use of AOX1 as a promoter, that is strong and highly regulated, allows to control the expression of the proteins since they are induces only when a high cell density is obtained. The other advantages to use *Pichia pastoris* are that it is a GRAS (Generally Recognized As Safe) organism, it grows on minimal mediums, it's easy to scale-up the fermentation, the gene is integrate in *Pichia* chromosome and it's more stable that a plasmid and it produces higher yield compared to *Saccharomyces cerevisiae* [Macauley-Patrick et al., 2005].

Cell-free expression systems

Sometimes, the overexpression of heterologous proteins, especially of membrane proteins, affects the cell physiology leading to low expression, aggregation and unfolding of the proteins or even toxic effects [Bannwarth et al., 2003]. Cell-free (CF) provides a powerful tool in order produce the protein in milligrams amount for structural and functional studies allowing to eliminate the living host environment and to have open access to the reaction for adding beneficial compounds at defined concentration and at any stage of the protein synthesis. Protease inhibitors, ligands, cofactors, or substrates that might be helpful in stabilizing the translated proteins can be added to the reaction mixture that is separated by a dialysis semipermeable membrane of 10-50 kDa in two compartments for high and low molecular weight compounds. The coupled transcription-translation machinery can be extract by *E. coli*, or wheat germ, or it could be done combining in vitro individually purified components [Schwarz et al., 2007]. The template of the reaction can be a plasmid or a PCR product both containing the gene to be expressed. In the P-CF expression the protein is produced as a precipitate (P) since almost all the hydrophobic compounds are removed from the cell extract. The precipitate is then solubilized with detergents, although sometimes functional protein can be already present in the precipitate [Elbaz et al., 2004; Sansuk et al., 2008]. This P-CF reaction mode allows to get high yield of protein because there are not additional compounds that can inhibit the reaction. If the P-CF does not result in folded and functional protein, an artificial hydrophobic environment can be provided by adding detergents (D-CF) or lipids (L-CF) to the reaction mixture. The limit of D-CF is that not all the detergents are tolerated in the reaction and the yield is lowered, while for the L-CF the presence of the lipids can even have beneficial effects on the reaction although it is not yet a well established technique and problems of translocation of the protein can occur [Schwarz et al., 2008].

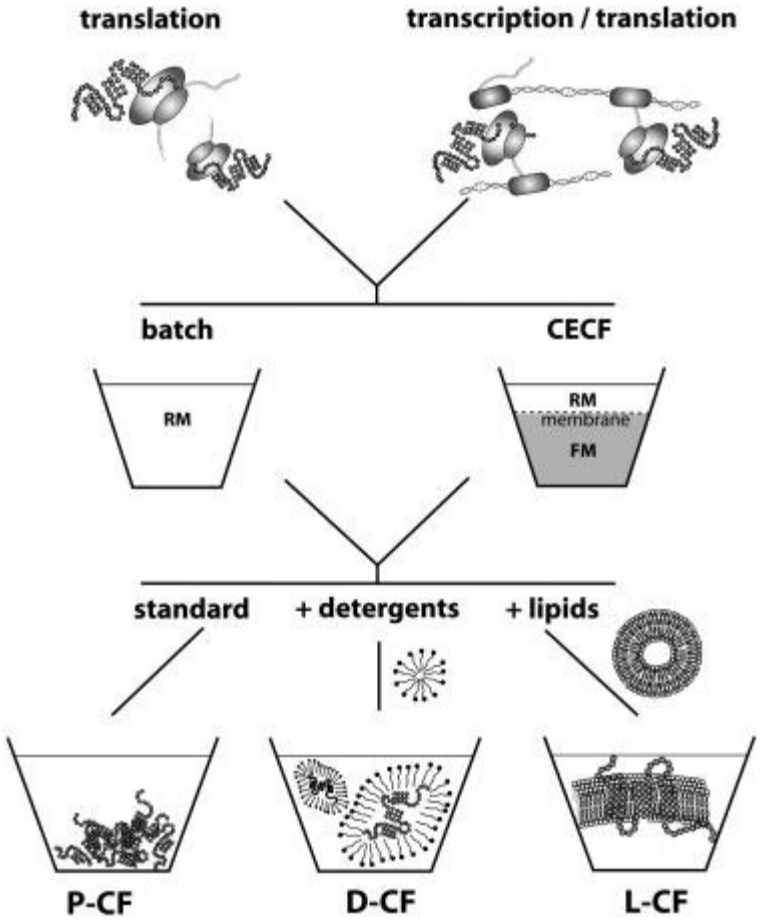

Fig. 20. Versatility of CF expression system. Most commonly used reaction type: translation and coupled transcription and translation, reaction configuration: in batch of CECF (continuous exchange cell free) and expression type: P-CF (Precipitate), D-CF (Detergent) and L-CF (Lipid).

Aim of the PhD

Since viral Kcv is one of the smallest functional potassium channel, that correspond to the pore module of more complex prokaryotic and eukaryotic potassium channels, it will be interesting to crystallize it and resolve the structure to compare these information with all the knowledge on its functions.

The aim of my PhD has been to try to prepare protein sample suitable for crystallization. The protein should be pure and homogeneous and in enough quantity to make crystallization screenings since a lot of conditions have to be tested before finding the best for crystals formation. For this reason I will first of all try to increase the quality and the yield of the protein produced in the heterologous system used in our lab, the yeast *Pichia pastoris*.

As the protein is really small, and hydrophilic surfaces to make protein-protein interaction for crystal growth are really shorten, in parallel will be establish a system for production and purification of Fab fragments of monoclonal antibodies that recognize the protein in its native conformation, to be used to increase the surface for proteins contacts. The system has already been used for the crystallization of the bacterial potassium channel KcsA with success and for this reason we hope that it will fit with Kcv.

As the crystallization of membrane proteins is really hard, I have therefore decide to express different viral potassium channels with high degree of homology with PBCV-1 Kcv, to increase the possibility to get a structure. Among these channel the mitochondrial Kesv will be expressed too also with the intent of study the channel from a functional point, since it was only measured as a chimera with Kcv, due to its mitochondria localization.

Considering the importance of the potassium channels in medicine, as they are involved in some human diseases, the study of blockers is really of interest. I will conduct studies on the channel blocker barium in Kcv channels and evaluated the importance of the 4^{th} binding site of the selectivity filter that has been showed to be involved into this blocking mechanism.

Materials and Methods

Molecular biology

Standard DNA manipulations and microbiological technique were performed as described in Molecular cloning [Sambrook et al., 1989].

1) DNA Cloning

Genes:

The gene of PBCV-1 Kcv is a synthetic gene designed in accordance with the codon usage of the heterologous system for protein expression *Pichia pastoris*. The synthetic gene of MA-1D Kcv has been obtained by single point mutagenesis of the 5 amino acids that are different in the two genes.

The mutant T63S and S62T-T63S are obtained with single point mutagenesis too.

The genes of MT325, ATCV-1 and Kesv are the wild type genes, isolated by the corresponding viruses and cloned in pSGEM vector, used for oocyte expression.

For the sequences see Introduction.

PCR (Polymerase Chain Reaction):

Polymerase chain reaction [Saiki at al., 1988] is used to amplify the genes with the restriction sites for cloning it into the plasmid at the 5' and 3'termini, to introduce point mutations, to check with colony PCR the success of the transformation, both in *E. coli* and *P. pastoris*.

Polymerase chain reactions (PCR) used during my PhD employs either Pfu (Stratagene) or the goTaq polymerase (Promega).

A typical reaction mixture of a volume of 50 µl containing 10-50 ng of template DNA (or 1 µl of boiled cells for colony PCR), 1X PCR buffer (as supplied by the manufacturer), 0.2 mM dNTPs, 0.8 µM of primers, $MgCl_2$ if required. The initial denaturation is carried out at 94°C for 2 min, then again 1min, then the annealing between 50-65 °C for 1 min, and polymerization at 72°C for1min all repeated for 25-35 cycles and at the end final polymerization for 5-10 min. The obtained DNA is analyzed on agarose gel.

Primers should have similar TM (melting temperature) a GC content of 50-60%. Primers for restriction site addition are designed on 5' and 3' of the gene adding the sequence of the of the desired restriction sites.

The primers used for colony PCR can be the same of the amplification of the gene or the 3'AOX1 and 5'AOX1primer of the pPIC3.5K plasmid (for *Pichia* expression, see Vectors). Cells are boiled 5 min before the colony PCR and the denaturation time is 5 min.

PCR for mutagenesis is done according to the manufacturer protocol of the kit Quickchange™ Site Directed Mutagenesis Kit (Stratagene). The specific primers, 18-25 bp, are designed on the gene sequence and carry in the middle the mutated triplet to insert the mutation in the gene through DNA amplification.

The PCR for the LIC (Ligase Indipendent) cloning has specific primers that should contain these sequences:

- Forward:5'CAAGGACCGAGCAGCCCCTCC + gene sequence 3' (15-21 bp without start codon);
- Reverse: 5' ACCACGGGGAACCAACCCTTATTA + gene sequence 3' (15-21 bp without the stop codon).

MATERIALS:

Agarose gel 1 %: 30 ml TBE buffer 0.5x (0.89 M tris-HCl, 0.89 M boric acid, 0.02 M EDTA) + 0.3 g agarose (dissolved in microwave) + 3 µl of SYBR Safe (Invitrogen). Running is performed at 100 V for 15-20 min.

DNA marker: 1kb ladder (Invitrogen).

For PCR cleaning both from reaction and from agarose gel the kit Wizard® SV Gel and PCR Clean-Up System (Promega) is used.

Vectors:

A) pPIC3.5K

Vector for DNA amplification in *E. coli* and protein expression in *Pichia pastoris*.

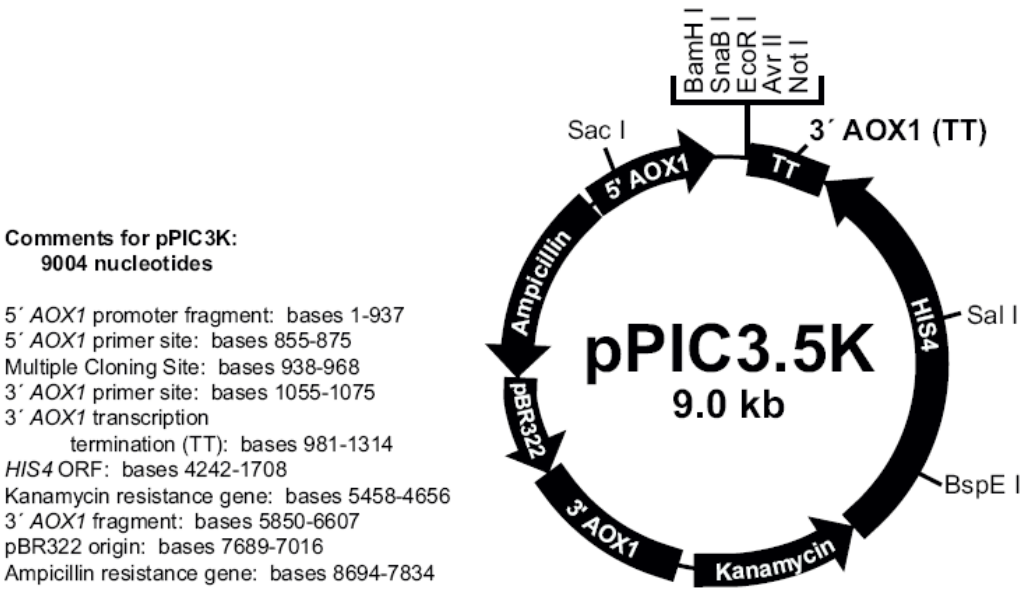

Fig. M1. pPIC3.5K vector.

The plasmid has been modified with two cassettes for the LIC (Ligase Indipendent Cloning) cloning inserted between the cloning sites BamHI and NotI.

Cassette 1: 7His-H3C

The cassette contains a 7 histidines tag, a linker (11 aa), the recognition site for the H3C protease, for the tag cleavage, and the restriction site SmaI the gene insertion with the LIC system.

Fig. M2. Scheme of the 7His-H3C tag. In black linkers are showed. The gene is cloned in the SmaI restriction site.

Cassette 2: 7His-MBP-H3C

The cassette contains a 7 histidines tag, a linker, the Maltose Binding Protein (MBP), the recognition site for the H3C protease, for the tag cleavage, and the restriction site SmaI for the gene insertion with the LIC system.

Fig. M3. Scheme of the 7His-MBP-H3C tag. In black linkers are showed. The gene is cloned into SmaI restriction site.

B) pET21CHx

Plasmid is based on the standard pET21 (Novagen). Cloning of the gene is between the restriction site of BamHI and XhoI, after removing with a silent point mutation the XhoI site at the end of the gene sequence.

C) pSGEM

Modified version of the commercial vector pGEMHE. Used for the expression of the protein in oocyte and, since it has the T7 promoter, it has been used for the CF (cell free) expression of Kesv gene cloned between restriction sites HindIII and XhoI.

D) pIVEX2.3

Plasmid provided by Dr. F. Bernhard for Cell Free expression of Kesv gene with a 10His tag at the C-terminus. The Kesv gene was cloned between NdeI and XhoI restriction sites.

Cloning

Restriction enzymes used are all provided by NEB (New England BioLabs) or Fermentas.

Digestion of the gene and the plasmid for cloning is performed as suggested by the manufacturer with double or subsequent digestions to generate sticky 5' and 3' termini.

For the LIC cloning digestion of the plasmid is done only with the SmaI restriction enzyme (NEB) that generates blunt ends.

The ligation of the DNA fragment with the plasmid is done with the ligase of Promega or NEB as suggested with plasmid/gene ratio:

(ng vector * bp gene/ bp vector) * 3 = ng gene.

2) Transformation of *E. coli*

Competent cells of *E. coli* DH5α strain are used for standard DNA amplification, XL1 Blue (Stratagene) for amplification of DNA after mutagenesis.

BL21 pLysS strain that contains the plasmid pLysS, which carries the gene encoding T7 lysozyme, is used to lower the background expression level of genes under the control of the T7 promoter.

50 µl of competent cells are incubated for 30 min on ice with the DNA construct, then subject to 40 sec heat shock at 42°C and supplemented with 1 ml SOC-medium. The cells are transferred in to a falcon tube (15ml) and incubated 1 hour in an incubator at 37 °C, 200RPM. The cell are then plated on LB+Amp plates and incubated overnight at 37°C.

MEDIA:

- SOC (1l): Tryptone 20 g, Yeast extract 5 g, NaCl 0.8 mM, KCl 0.2 mM, Glucose 1.6 mM, $MgSO_4$ 0.8 mM, $MgCl_2$ 0.8 mM. Fill up to 1 with H2O, autoclave.
- LB+Amp (1l): Tryptone 10 g, Yeast extract 5 g, NaCl 5 g, NaOH 0.009 mM, Ampicillin 50 µg/ml. fill up to 1L with H_2O and autoclave. For Agar plates add 15 g agar.

DNA extraction is done with the kit QIAfilter Plasmid Midi Kit (Qiagen).

DNA concentration is determined with the spectrophotometer at λ=260nm.

3) DNA Sequencing

The sequencing of all construct was performed by BMR Genomics, Padova.

Protein Expression

1) *Pichia pastoris* transformation

Pichia pastoris strain SMD1163 (his4-pep4-pbr1) is used because it lacks 3 endogenous proteases, which may aid production of full-length protein and the enzyme histidine dehydrogenase for the synthesis of histidine amino acid. *Pichia pastoris* cells are transformed with the Pichia Easycomp kit (Invitrogen) with 3 µg of PmeI linearized DNA using conditions recommended by the manufacturer. The transformation is checked with colony PCR.

After initial selection for His^+ transformants, multicopy integrants were selected by their resistance to increasing concentrations of geneticin G418. Clones resistant to 0.5–1.0 mg/ml of G418 were selected.

MEDIA:

- YPD (Yeast Peptone Dextrose Medium) (1l): 10 g Yeast extract, 20 g peptone, fill with H_2O and autoclave. Add 100 ml of 20% sterile dextrose. For plates YPD + Geneticin add 20 g of agar and 0.25-0.5-0.75-1-2 mg/ml G418 (Sigma).
- RDB (Regenerate Dextrose Medium) (1l): 186 g Sorbitol, 20 g of agar. Fill with H_2O and autoclave. At 60°C add a pre-warmed at 45°C solution of: 100 ml of 13.4% YNB; 100 ml of 20% dextrose, 2 ml of 0.02% biotin; 10 ml of amino acids mix (0.5% of L-glutamic, L-methionin, L-lysin, L-leucin and L-isoleucin).

2) Protein production

Small scale production in *Pichia pastoris*

Starting culture:

Transformed *Pichia pastoris* SMD1163 cells are grown at 30°C 200RPM in 10ml of MGY medium to an absorbance at 600 nm (A_{600}) >1. Store at 4°C.

MEDIUM:

- MGY (Minimal Glycerol Medium) (1l): 100 ml of 13.4% YNB (Yeast Nitrogen Base), 100 ml of 10% glycerol, 2 ml of 0.02% biotin, fill with H_2O.

Growing for biomass:

The cell culture volume (V cell culture) is calculated to get OD (N) = 2-6 in 50-200 ml MGY-medium in 19-20 hours:

N_0wished = N / e^{rt} (exponential growth formula):

where N = 2-6,

t - time in hours (20h)

r – growth rate in MGY (according to David Parcej for MGY = 0.231)

V cell culture to be added in to 50-200 ml MGY-medium in a flask

V cell culture = $N_{0\ wished}$ * 50 ml / $N_{0\ measured}$

50-200 ml MGY-medium are inoculated in a 250 ml-2 l flask with the calculated amount of cell and the flasks are kept in the shaker for 20 h.

For glycerol stock: Pellet the cells and resuspend in MGY + 15 % Glycerol at a final volume with OD 50-100, store 1 day at -20°C and then froze in liquid nitrogen and keep at -80 °C.

Methanol induction:

The cell culture volume is calculated to get OD = 1 in 50-200 ml and inoculate it in 50-200 ml of MM for 24 hours. The cells are collected and centrifuged. Pellets are stored at -80°C.

V cell culture = 1* 50-200 ml / $OD_{measured}$

MEDIUM:

- MM (Methanol Medium) (1l): 100 ml of 13.4% YNB (Yeast Nitrogen Base), 100 ml of 5% methanol, 2 ml of 0.02% biotin, fill with H_2O.

Large scale production in *Pichia pastoris*

Large scale fermentation is conducted in a 7 l bench-top fermenter (STR HT Labfors 3, Stirrer Tank Reactor). The conditions required by *Pichia*, monitored in the fermenter are: pH 5, 29°C, 1100 rpm stirring and dissolved O_2 > 20%.

The process is divided into two phases:

1) Growth in glycerol (Basal Salt Medium) to obtain biomass;
2) Methanol induction with increasing methanol concentration: 0,1-0,3-0,5-0,7% MetOH/IFV (Inner Final Volume).

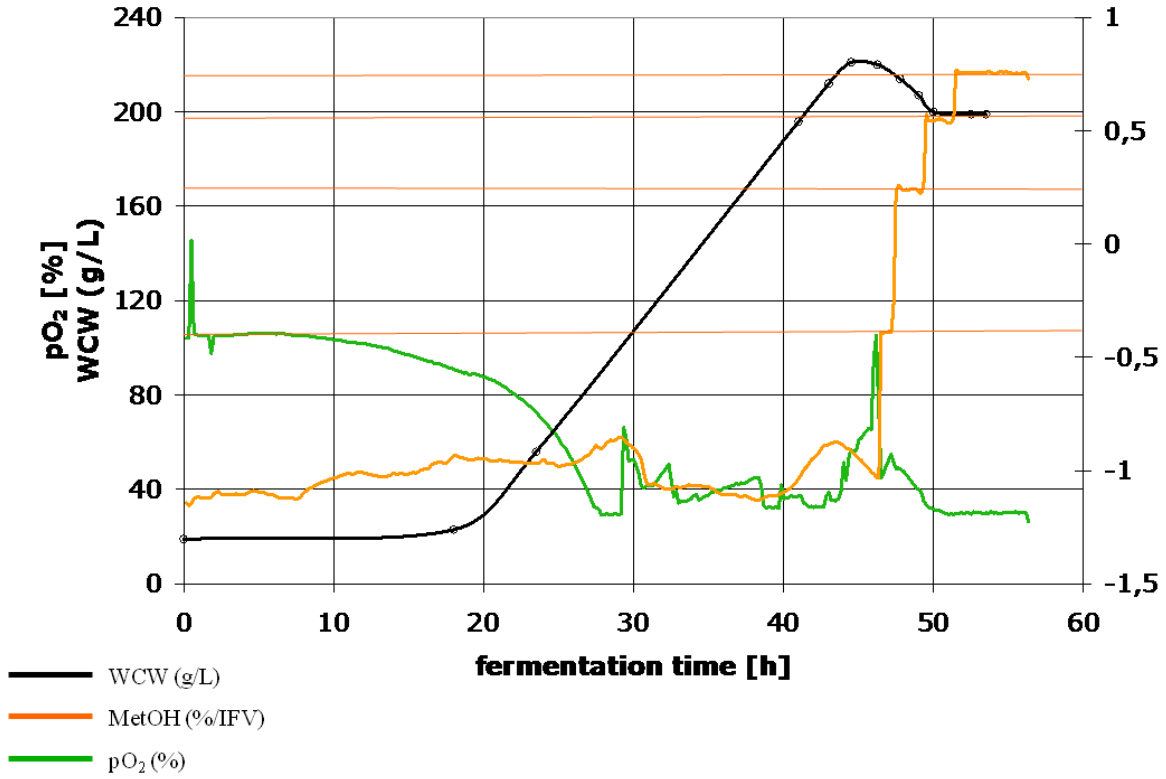

Fig. M4. Graph of fermentation of *Pichia pastoris*. In black the cell growth curve (WCW, wet cell weight), in green the O_2 uptake (pO_2,) and in orange the supply of methanol (MetOH).

800-1000 g of cells are collected and stored at -80°C.

MEDIUM:

- Basalt Salt Medium: 40 g/l Glycerol, 0,93 g/l $CaSO_4$-$2H_2O$, 18,2 g/l K_2SO_4, 14,9 g/l $MgSO_4$-$7H_2O$, 1 ml/l Antifoam, 25 g/l Na+-polyphosphate, 9 g/l $(NH_4)_2SO_4$, traces of salts.

Protein purification

1) Protein extraction

Small scale membrane preparation with glass beads

Pellets of small scale flask culture, up to 400 ml volume, are suspended in breaking buffer 1:1. An equal volume of ice-cold, acid-washed glass beads (Sigma) was added and the cells were broken by vortex mixing for 20 min (30 sec bursts separated by 30 sec cooling on ice) or by using of Bead Beater (3 min, 2 min of rest, 3 min). Glass beads, unbroken cells and other cell debris removed by centrifugation at 1500 x g for 10 minutes and the pellet washed with an equal volume of buffer and recentrifuged. The supernatants are combined.

BUFFERS:

- Breaking buffer^{+inh} : 50 mM NaH_2PO_4 , 1 mM EDTA, 5% glycerol pH=7.4 with NaOH + inhibitors in stock DL-Dithiothreitol DTT (5mM), Trypsin inhibitor (0,1 mg/ml), Benzamidine (1 mM), Pefablock (0.1mM), PMSF (1 mM).
- Glass Beads: 0.25–0.5 mm diameter. Washed 2 times with sterile H_2O, 2 times with HCl 1 M and 2 times again with H_2O.

Large scale preparation of membranes using a Cell Disruptor

Pellets of cells grown in a fermenter are suspended in breaking buffer^{+inh} in 1: 10 ratio. The cells are then passed through a cell disruptor (TS Series bench top) that breaks the cells applying high pressure (40KPa). The system is refrigerated at 4°C.

The broken cells are centrifuged at 4200 x g for 10 min.

2) Microsomes preparation

PEG 8000(polyethylene glycol) and NaCl were added to final concentrations 5% (w/v) and 200 mM respectively, in order to precipitate the crude membrane fraction. After incubation for 20 min at 4°C, the mixture is centrifuged at 29500 g for 40 min.

The pellet is resuspended in a breaking buffer without EDTA and the protein content determined using the standard DC protein assay (BioRad).

3) Solubilization

3% w/v of DDM (n-dodecyl-ß-D-maltoside) is added to the microsomes with a protein concentration of 20 mg/ml. The solubilization is performed for 4 hours at 4°C in agitation. Centrifugation at 75000 x g for 1 hour at 4°C is performed and the supernatant is collected.

BUFFER:

- Solubilization buffer (2x): 1200 mM NaCl, 400 mM KCl, 100 mM of Imidazole-HCl pH 7.5, 6% (w/v) of DDM.

4) Protein purification with affinity column

The principle of this chromatography is the affinity between histidine with Co^{+2} (Porath et al, 1975). The proteins after binding the resin can be eluted either increasing imidazole concentration.

Column preparation

1 or 3 ml of His-Select™ Nickel Affinity Gel (Sigma) are packed either into disposable polystyrene column.

The Ni^{+2} was washed away with 3.5 or 10 ml of EDTA 0,1 M. after washing with 3.5/10 ml of water, the resin is regenerated using 3.5/10 ml $CoCl_2$ 0.2 M and then washed again with water.

The resin can be stored at 4º C in Ethanol 20% or used immediately.

Before purification the Co^{+2}-NTA column has to be equilibrated with the solubilization buffer 3% DDM.

Protein-resin interaction and protein elution

The solubilized material and the resin are incubated at 4°C ON in agitation.
The resin is then loaded on the column and washed with 3.5/10 ml of solubilization buffer with DDM 0.1% (2 mM), 3.5/10 ml of washing buffer with DDM 0.1%, 3.5/10 ml of solubilization

buffer without DDM, 3.5/10 ml of elution buffer with DDM 0.5 mM and 3.5/10ml of ultrapure water. The protein eluted is collected in 135/400 µl fractions.

BUFFERS:

- Solubilization buffer (2x): 1200 mM NaCl, 400 mM KCl, 100 mM of imidazole-HCl pH 7.5, 6% (w/v) of DDM.
- Elution buffer (2x): 600 mM imidazole, 400 mM KCl at pH 7.5 with HCl.
- Washing buffer (2x): 2000 mM NaCl, 400 mM KCl, 150 mM imidazole at pH 7.5 with HCl.

Protein analysis

1) BIORAD

Total protein concentration in the microsomes is determined with the BioRad assay.

Standard with 0, 2, 4, 8, 16, 32, and 64 µl of γ-IgG (1 mg/ml) + water up to 800 µl + 200 µl of BioRad are prepared to make the curve.

Sample of microsomes diluted 1:100 with 10, 20, 30, 40 µl + water and BioRad are prepared.

After 40 min absorbance at 595 nm is determined at the spectrophotometer and the standard slope is designed and used to estimate protein concentration.

2) SDS-PAGE gel electrophoresis

SDS-PAGE analysis is performed using the discontinuous method (Laemmle 1970). For discontinuous electrophoresis, pre-cast polyacrylamide gels are used (Anamed 4-20% Tris-glycine, Invitrogen SDS-PAGE 4-12% Bis-Tris (MES)). The samples were mixed with 25% of sample buffer Laemmli.
The electrophoresis is conducted at 150 mV for 30min-1 hour

BUFFERS:

- Sample buffer Laemmli (4X): 0.5 M Tris-HCl , pH 6.8, 50% (v/v) glycerol, 10% SDS, bromo phenol blue.
- Running buffer: 25 mM Tris, pH 8.3, 192 mM glycine, 0,1% SDS.
- MES running buffer: 1 M MES, 69 mM SDS, 1 M Tris base, 10 mM EDTA.
- MOPS running buffer (Invitrogen).

Markers used are:

- Pre-stained Protein Marker, 6-175 kDa (NEB);
- Prestained Protein Ladder, Broad Range, 10-230 kDa (NEB);
- Novex® Sharp™ Pre-stained (Invitrogen)
- ColorPlus Prestained Protein Marker, Broad Range 7.5-126 kDa (NEB)

Relative molecular weight of the protein bands is calculated on the basis of the relative migration of the bands at known molecular weight (marker). The migration of the proteins of the marker is plotted towards the log of their molecular weight. The migration of the sample protein is plotted too and its molecular weight derives from the curve.

3) Native-PAGE gel electrophoresis

To check the tetrameric form of Kesv non denaturing Novex Bis-Tris Native-PAGE gel 4-16% (Invitrogen) are used.

Samples are prepared as suggested by the manufacturer with Invitrogen sample buffer and additive.

NativeMark™ Unstained is the marker used.

4) Coomassie staining

For Coomassie blue staining the gel was incubated for 30-60 min with coomassie stain solution under continuous shaking. Then the gel was washed with destaining solution and water until the background is clear.

SOLUTIONS:

- Coomassie staining: 0.1 % coomassie blue, 10% acetic acid, 40% EtOH.
- Destaining: 40% EtOH, 10% acetic acid.

5) Silver staining

Silver staining of the SDS/Native-PAGE gels is done with Sigma ProteoSilverTM Silver Stain Kit following the manufacture protocol.

6) Western blot

Nitrocellulose membrane pre-hydrated in water, 4 pieces filter paper and 2 pads are soaked in transfer buffer and assembled in the transfer apparatus.

The transfer of the proteins to the membrane is performed for 45 min at 30 mV. Dry blot with iBlot (Invitrogen) can also be performed.

After the transfer, the membrane shacked for 45 min in blocking buffer and then washed 1 min in TBS, 5 min in TBS-Tween, 15 min in TBS-Tween and 5 min in TBS. The primary antibody is added and incubated for 2 hours or overnight at 4°C. The membrane was washed again 1 min in TBS, 5 min in TBS-Tween, 15 min in TBS-Tween and 5 min in TBS and incubated for 1 hour with secondary antibody. The membrane is washed again and incubated with developer buffer until the protein bands appear.

BUFFERS:

- Transfer buffer: 25 mM Tris, 192 mM Glycine or 25 mM Bicine, 25 mM Bis-Tris, 1 mM EDTA.
- TBS (10x): 200 mM Tris, 9% NaCl, pH 7.5 with HCl.
- TBS-Tween: TBS 1x + Tween-20 0.01%.
- Blocking buffer: TBS 1x, Tween-20, 0.2%, 3% (w/v) BSA.
- Primary antibody (monoclonal ab anti-polyhistidine from mouse): 1:1000 in TBS 1x, Tween-20 0.01% e 3% w/v BSA.
- Secondary antibody (anti-mouse conjugated with alkaline phosphatase): 1:2000 in TBS 1x, Tween-20 0.01%, 3% w/v BSA.
- Developer buffer: 1 tablet of BioRad BCIP/NBT (SIGMAFAST®) in 10 ml of sterile water.

7) Gel filtration

In the gel filtration chromatography the proteins are separated by their differences in size and shape. The process involves partitioning of the protein between a stationary phase and a mobile phase that passes over its surface. The stationary phase consists of porous beads of a hydrophilic polymer, such as cellulose or some other type of carbohydrate polymer, with a well defined range of pore sizes. Proteins that are small enough can fit inside all the pores in the beads and are said to be included. These small proteins have access to the mobile phase inside the beads as well as the mobile phase between beads and elute last in the gel filtration. Proteins that are too large to fit inside any of pore are said to be excluded. They have access only to the mobile phase between the

beads and, therefore, elute first. Proteins of intermediate size are partially included-meaning they can fit inside some but not all of pores in the beads. These proteins will then elute between the large ("excluded") and the small ("totally included") proteins.

Gel filtration chromatography is used to verify the quality of the protein and separate the tetrameric form from the others.

Before loading the sample on gel filtration it should be concentrate to 200 µl with Centrifugal Filter Devices Amicon Ultra (Millipore) with a cut off f 30 kDa.

The columns Superdex 200 (HiLoad 16/60, 10/300 and 5/150 GE HealthCare) is then equilibrated in elution buffer and the sample loaded and collected into fractions.

BUFFER:

- Elution buffer: 300 mM of imidazole, 200 mM KCl at pH 7.5 with HCl, DDM 2mM /0.3mM or L-Dao

Tag removal

The removal of the 7His-H3C tag is done with the human rhinovirus 3 C protease produce in the lab.

1) H3C protease expression

The production of the H3C protease is done in *E. coli* BL21(DE3) pLysS transformed with the plasmid pET28a(+) (Novagen), containing the gene coding for the protease. The cells, after they reach high biomass, are induced with 0.4 mM IPTG at 22°C.

The cells are centrifuged and the pellet is resuspended in lysis buffer. The cells are broken with sonication for 4 min. The broken cells are centrifuged 30 min at 20000 x g. The protease is purified from the centrifuged extract on Co^{2+}-NTA column as showed before.

The protease is eluted with 5 ml of Buffer A and 5 ml of Buffer B. The content of the elution fractions is checked by SDS-PAGE gel decorated with silver staining and the richest fractions are dialyzed overnight in dialysis buffer and frozen at -80°C.

BUFFERS:

- Lysis buffer: 50 mM Tris-HCl, pH 8, 500 mM NaCl, 20 ng/µL lysozyme, 1 mM Phenylmethanesulsonyl fluoride PMSF.
- Buffer A: 50 mM Tris-HCl, pH 8, 300 mM NaCl.
- Buffer B: 50 mM Tris-HCl, pH 8, 300 mM NaCl, and 300 mM imidazole.
- Dialysis buffer: 50 mM Tris-HCl, pH 8, 150 mM NaCl, 10 mM EDTA, 5 mM DTT, 20% glycerol.

2) Tag removal reactions

Different conditions for the tag removal are tested.

Since the protein elution buffer (300 mM) can inhibit the protease activity, imidazole concentration in the protein sample is reduced below 10 mM by repetitive steps of dilution and concentration with a cut-off filter of 30 kDa (Millipore). Reaction with 30 mM imidazole is performed too.

The conditions tested are the following: digestions of 20, 100 and 500 µg of protein with 1 µl of protease and of 500 µg of protein with 10 µl of enzyme in digestion buffer (final volume of the reaction 100 µl). The reaction is incubated at 4°C for 16 hours or at room temperature for 2 hours.

The reaction is checked n SDS-PAGE decorated with silver staining or western blot.

BUFFER:

Digestion buffer: 50 mM Tris-HCl, pH 7, 150 mM NaCl, 1 mM DDT, 50mM Trizma Base, 1 mM EDTA.

Fab production

1) Production and selection of monoclonal antibodies

The monoclonal antibodies are produced by hybridoma cells provided by the EMBL Monoclonal Core Facility.

These hybridoma cells are immortal cell lines obtained by fusing myeloma cells with the spleen cells of a mouse previously immunized with the MA-1D Kcv with the 7His tag to increase the immunogenic response. The resulting cell lines have been screened by ELISA to select those lines that produced antibodies specific for the tetrameric and not the monomeric form of the protein (non-boiled and boiled protein samples). A second screen was performed in order to discard those cell lines producing antibodies that recognized the tag (comparison between full length MA-1D Kcv 7His-H3C and the same protein after tag removal).

At the end of the screening procedures, EMBL Monoclonal Core Facility sent us 26 clones.

A second screening is done incubating the western blot membranes of SDS-PAGE gel with MA-1D Kcv with or without tag and unboiled (tetramer) or boiled (monomer) with the sera as primary antibody.

The selected sera are cultivated for Fab production. The cell are kept in liquid nitrogen in FBS+DMSO, so they have to be gently defrosted at 38°C in water bath and then DMSO have to be removed with D-MEM medium + 20% FBS (H2M20). The cells are spinned down and the pellet resuspended in fresh H2M20/1% HybER, transferred into 100 mm culture dishes and incubated at 37°C with 10% CO_2. After they reach a confluence of 90% they can be splitted 1:5 every 3 days several times decreasing HybER concentration.

When the desired amount of cells is reached they can be collected by centrifuged to extract the antibody.

MEDIA:

- D-MEM without Pyruvate with 4.5 g/l of glucose and L-Glutamine (Gibco);
- FBS: Foetal Bovine Serum (Hyclone);
- HybER: Culture medium additive (Statens Serum Istitut, Denmark).

2) Fab fragment preparation

Fabs are produce according to the manufacture instruction of the Fab Preparation Kit (Thermo Scientific). Antibody is purified on protein A-resin and then digested with Papain that produces Fab and Fc fraction. Fabs are purified again through protein A-resin that binds Fc and uncut antibody. The Fabs are treated with DTT to break the disulphide bonds and incubated with the protein to make the complex in a ratio 1:4. The complex is checked by gel filtration.

Crystallization screenings

Crystallization screening is done 96 well plates (Greiner) at 4°C using the Orxy 8.0 crystallization robot (Douglas Instruments). The crystals are grown with the sitting-drop vapour diffusion technique. This technique allows a drop containing purified protein, buffer, and precipitant being allowed to equilibrate with a larger reservoir containing identical buffers and precipitants in higher concentrations.

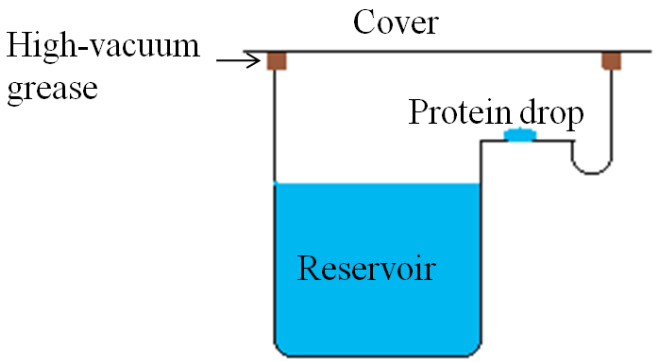

Fig. M5. Diagram of sitting drop method. In this method, the protein drop sits on a pedestal above the reservoir solution.

Initially, the droplet of protein solution contains an insufficient concentration of precipitant for crystallization, but as water vaporizes from the drop and transfers to the reservoir, both the precipitant and protein concentration increase to a level in which the protein starts to crystallize (supersaturation. Fig. M6). [Rhodes, 1993; McRee, 1993].

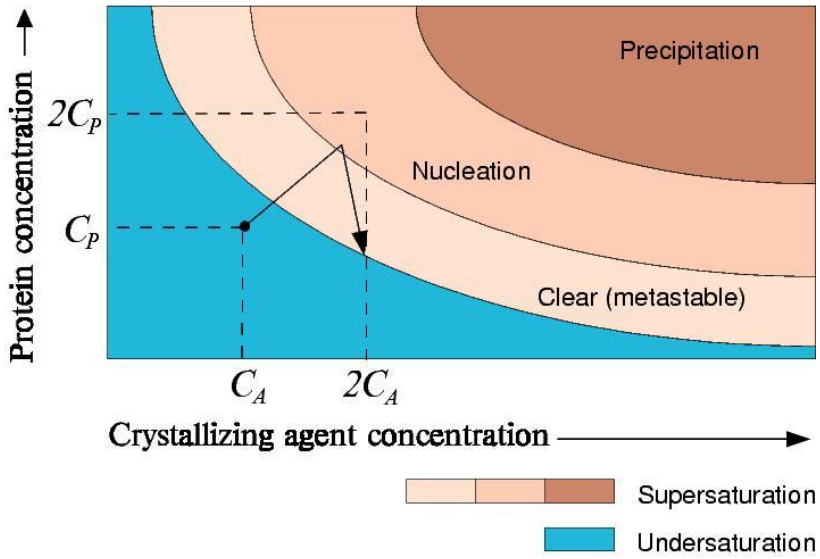

Fig. M6. Phase Diagram for vapour diffusion experiment.

In our crystallization screenings the drop is 0,3 µl and it is composed 50% protein-50% precipitant solution, 70%-30% or 25%-75%, with a protein concentrated at least 8 mg/ml.

The screenings in 96 wells are done with commercial kits: PROPLEX (Molecular Dimensions)specific for complex, PEG/ION SCREEN (Hampton Research), JBS 1, JBS 2, JBS 3 and JBS 5 (Jena Bioscience), Crystal screen (Hampton Research) and MEMBFAC (Hampton Research).

Once some interesting conditions in which some crystals are found, the crystallization screening is refined in 24 wells-plates (sitting-drop) with drops of 2 µl (1µl protein, 1µl precipitant), to obtain larger crystals analyzed with synchrotron radiation (ESRF, Grenoble, France).

Crystals are cryo-protected in 30% glycerol and frozen in liquid nitrogen.

Cell free

The production of the Kesv protein is done in Dr. Bernhard lab in Frankfurt by Dr. Roos with the P-CF (Pellet Cell-Free) technique as described in Swartz et al., 2007.

The expression was carried out in the continuous exchange configuration based on the E. coli S30 extract. A reaction mix (RM) which holds the expression machinery (origin from the S30 extract) is separated by a semi-permeable membrane from the feeding mix (FM). The FM holds all low molecular components and supplies the reaction with e.g. energy and amino acids via dialysis. In addition by-products like inorganic phosphate can dialyse out of the reaction to make a longer expression period possible which results in higher yields of protein. The reactions were incubated for 16 h at 30° C in a water bath with shaking device.

The reaction is carried out in the P-CF mode. That means the expression of the hydrophobic membrane protein takes place in the absence of any hydrophobic environment. Therefore the protein can be centrifuged down (15 min 13.000 x g, 4°C); the pellet is washed twice with the S30 buffer and then sent to our lab.

Tetrameric protein reconstitution

For the reconstitution of the protein produced with P-CF solubilization with different detergents and in different condition is performed.

Solubilization with 20x CMC final concentration in Solubilization buffer: Tris/HCl 20 mM, NaCl 150 mM (+ or substituted with 300 mM KCl), pH 7.5 + detergent to a 30 x CMC concentration.

Detergents used:

- LPPG (1-palmitoyl-2-hydroxy-sn-glycero-3-[phospho-rac-(1-glycerol)]);
- LMPG (1-myristoyl-2-hydroxy-sn-glycero-3-[phospho-rac-(1-glycerol)]);
- SDS (Sodium-n-dodecylsulfate);
- β-OG (*n*-octyl-β-D-glucopyranoside);
- DM (n-decyl-β-D-maltoside);
- DDM (n-dodecyl-β-d-maltoside);
- Triton (polyethylene glycol P-1,1,3,3-tetramethyl-butylphenyl ether);
- L-Dao (Lauryldimethylamine-N-oxide).

Conditions:

- 2 h 30°C;
- ON 4°C;
- ON 30°C.

A step of TFE (2,2,2 Trifluoethanol) denaturation for 2 hours is done before the solubilization with 33% of TFE. Solubilization buffer, that also dilute TFE concentration to a 16% non-denaturing concentration, is added to solubilize the protein at 30°C for 2 hours or ON.

Single channel measurement in artificial planar lipid bilayer

The planar bilayer is an extremely reduced artificial system for single channel measurements, free of any cellular components. It offers a high accessibility for exchanging solution (although sometimes it can lead to contaminations).

Experiments with planar lipid bilayer are performed as described by Schrempf et al., 1995 by the Montal-Müeller technique [Montal & Müeller, 1972]

1) The set-up

The system consists in a measure chamber that contains two small chambers, named cis and trans, filled with 3 ml of buffer solution and separated by a teflon foil with a small hole (Ø100 µm) in it.

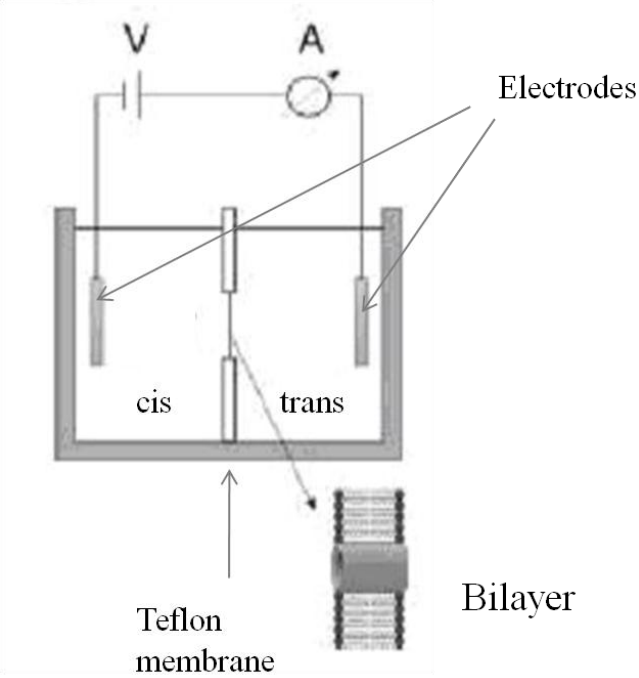

Fig.M7. Schematic representation of the bilayer set-up.

The Ag/AgCl electrode in the trans-compartment is directly connected to the head stage of a current amplifier (EPC 7, List, Darmstadt, Germany); the electrode in the cis-compartment is connected to the ground. At positive potentials the electrode in the trans-compartment was positive and the

electrode in the cis-compartment negative. In order to prevent surface-potential effects, both electrodes were connected with the bath solution via an agar bridge (2% agarose in 2 M KCl).

Lipid, 100 mg/ml L-α-phosphatidilcoline (Sigma-Aldrich), stored in chloroform: methanol (1:1) are dried in a vacuum pump for 10 min; the lipids are then resuspended in µl n-Decan (Merck) (final concentration 0.4 mg/ml). The lipids are applied to the teflon hole at both sides using the Hamilton syringe. After 2 hours of incubation buffer is added to both chambers and the lipids are washed with a pipette to form the bilayer.

The hole and the formation of the bilayer can be controlled via a binocular at the 100-fold magnification.

2) Protein reconstitution into liposomes

Protein can be added directly in the chamber (when solubilized in L-Dao addition of 5 ng of protein can be enough) or can be reconstituted into liposomes.

20 ng/µl of purified protein (200 mM KCl, 300 mM imidazole, pH 7.5) are mixed with L-α-phosphatidilcoline 20 mg/ml (Sigma) in lipid buffer + 0.09% DDM. The protein/lipid molar ratio is 1/1000. Bio-Beads (BIO-RAD) are washed twice with Et-OH, twice with water and once in lipid buffer. Bio-Beads were then added to the protein-lipid mixture and shacked 2 hours at room temperature twice and then O.N. at 4ºC.

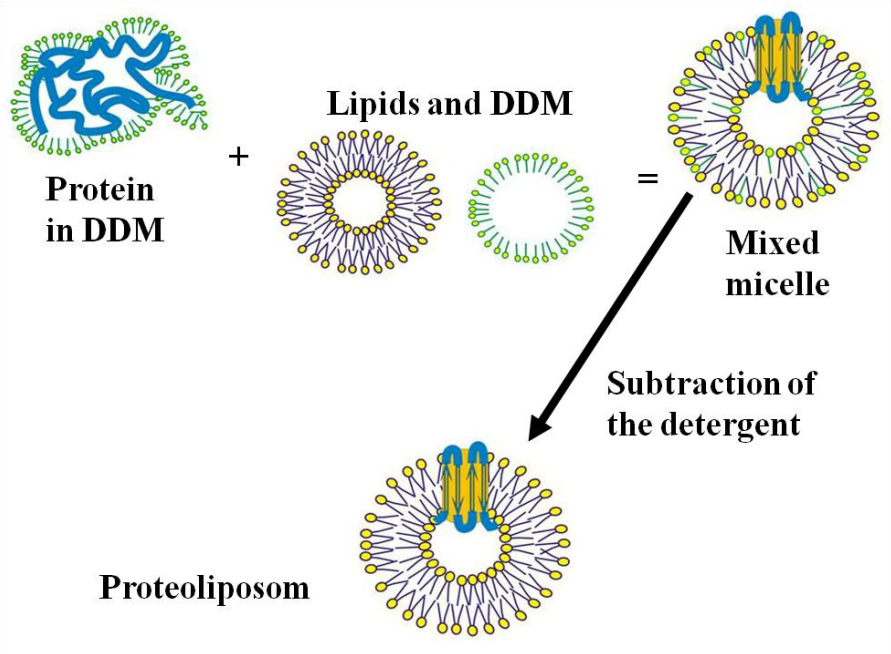

Fig.M8. Scheme of protein reconstitution is liposomes.

Aliquots of reconstituted protein are stored at -80ºC.

BUFFER:

- Lipid buffer: 20mM KCl, 10mM M/T, pH 7, 0,009 % DDM (Dodecyl-β-D-maltoside)

3) Measurements

Currents are recorded and stored by an analog/digital converter (LIH 1600, HEKA electronics, Germany) at 4 KHz after low pass filtering at a frequency of 1 kHz.

The chambers are filled with 500 mM KCl, 10 mM Mops/Tris pH 7.

Before adding the protein to the trans chamber the bilayer conductance was recorded for some time in order to exclude artefacts evoked by contaminations. Only perfectly silent bilayers are used.

Proteoliposomes are added in the trans chambers and potentials from -160 to 120 mV are applied.

When the channel fused with the bilayer, the current flowing through the channel is recorded by the amplifier.

To analyze selectivity, asymmetrical solutions are used in the two chambers (250/500 mM, 250/1000 mM 10 mM Mops/Tris pH 7 cis/trans chambers).

To study barium block increasing concentration of $BaCl_2$ are added to both chambers, and to revert the block barium is precipitated by adding 10 mM $NaSO_4$ to both chambers.

4) Data analysis

Data analysis performed by Patchmaster and Fitmaster softwares (HEKA electronics), QuB (University of Buffalo), ClampFit (Axon Instruments, Inc.), Excel (Microsoft) and Origin (Microcal Sofware, Inc.).

I/V-curves are created in Origin by determining the apparent single channel currents by visual inspection with Patchmaster software. Conductance is calculated with the linear fit of the I/V curve in the linear range with Origin.

Mean/standard deviation plot was done using Excel software.

Open probability is determined with QuB or Clampfit.

The reversal potential is calculated through the Nerst equation:

$$\mathrm{Er} = \frac{\mathrm{RT}}{\mathrm{zF}} \, \mathrm{x} \ln \frac{[\mathrm{Kout}]}{[\mathrm{Kin}]}$$

Results and Discussion

Part 1.

Strategies for Kcv channels crystallization

Aim of Part 1

In the last ten years several crystal structures of potassium channels have been obtained, mainly from prokaryotic channels but, a few also from eukaryotic [Doyle et al., 1998; Kuo et al., 2003; Long et al., 2005; Nishida et al., 2007; Tao et al., 2009; Ye et al., 2010]. These structures are often obtained from channels that are difficult or impossible to measure with the classic electrophysiological techniques, i.e. patch clamp on cell membrane. Most of the functional data are obtained after reconstitution in artificial lipid bilayer and quite often, radioactive Rb^+ uptake into proteoliposomes as a measure of K^+ permeability is the only available functional data of the reconstituted channel [Heginbotham et al., 1998; Nimigean, 2006]. We therefore consider the crystallization of Kcv worth pursuing because Kcv is very easily expressed in several heterologous systems (oocytes, mammalian cell lines, yeast) and we can accurately measure biophysical properties of the channel by a variety of electrophysiological techniques: voltage and patch clamp [Plugge et al., 2000; Abenavoli et al, 2009], planar lipid bilayer [Pagliuca et al., 2007], GUV (giant unilamellar vesicles) [Regueiro et al., 1996; Varnier et al., 2010], automated port'a patch [Brüggemann et al., 2008], yeast complementation [Gazzarrini et al., 2009; Chatelain, et al., 2009]. Beside this, we have a complete repertoire of Kcv mutants that have been tested already and that display a variety of properties of any relevant function: gating, selectivity, open probability and so on. Besides this, it remains interesting to try the crystallization of viral Kcv-like potassium channels, also because they are still the smallest functional channels (the smallest functional channel being ATCV-Kcv, 82 aa long [Gazzarrini et al., 2009]), that correspond to the pore module of more complex prokaryotic and eukaryotic potassium channels.

The goal of this part of my PhD work has been to improve the quantity and the quality of the purified proteins expressed in *Pichia* in order to get crystals for structural studies.

I have chosen to start to work with the already mentioned channel MA-1D Kcv and to try to reduce the amount of protein that aggregates, in order to increase the quantity of available protein.

Another goal of my work has been to try the crystallization of the channel in complex with the Fab fragment of monoclonal antibodies. The use of Fab fragments to improve the crystal growth of membrane proteins is a new successful technique in crystallization [Ostermeier et al., 1995; Zhou et al., 2001; Dutzler et al., 2002]: the presence of the antibody increases the hydrophilic surface and the crystal contacts of the otherwise hydrophobic membrane protein. This is relevant for protein such as Kcv that is almost all hydrophobic and does not have cytosolic domains that can mediate inter-subunit contacts in the crystal. Fab fragments can also help in stabilizing the membrane

protein in a defined conformational state (open or closed, [Zhou et al., 2001; Uysal et al., 2009]). For this reason antibodies against MA-1D Kcv have been produced and their Fab fragments purified and selected to make complex with the protein that will be used for crystals growth.

Finally, given the possibility that also in the best possible conditions the protein does not crystallize, the expression of other viral potassium channels has been developed to increase the chances to get a structure.

State of the art: MA-1D Kcv crystallization trials

In the past few years the crystallization of the viral potassium channel MA-1D Kcv, has been tried unsuccessfully. The trials have been performed with a recombinant Kcv protein purified from the *Pichia pastoris* yeast that formed irregular and/or amorphous and fragile crystals that were not diffracting at the synchrotron (fig. 1.1 A). This protein had a 9His-tag fused at the N-terminus and will be mentioned after as our control protein in the subsequent attempts to optimize protein quality and yield.

Optimization of sample preparations (extraction and purification), lead to crystals of better quality but still diffracting at too low resolution to get any structure information from them.

A **B**

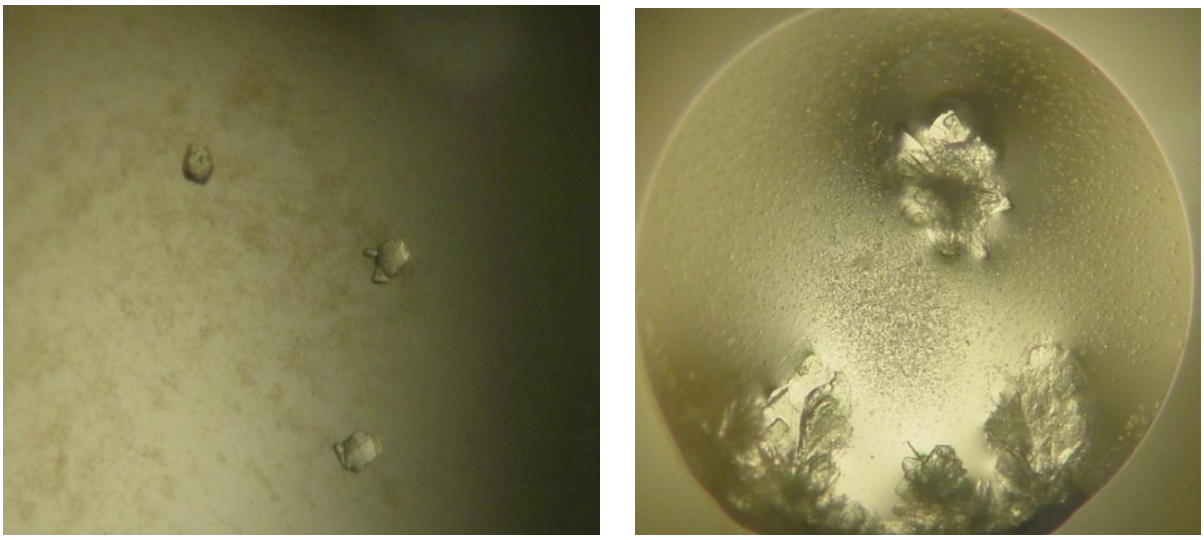

Fig. 1.1. First crystallization attempts on MA-1D Kcv. A) Non diffracting amorphous crystals. B) Diffracting multi-layered crystals.

To increase the quality of the crystals the work should focus on the sample quality, that should be pure and homogenous, and on crystal formation procedure. In this regards the protein must be in adequate amounts, 2-5 mg for each preparation, in order to test the widest range of different crystallization conditions at each trial [Michel, 1983; Ostermeier and Michel, 1997].

The problems of the yield was that, although the scaling-up of the expression in *Pichia pastoris* in a 7 liter fermenter had been optimized already, the yield was nevertheless enough for a full

screening of crystallization conditions because nearly half of the extracted protein was lost as aggregate before the final concentration step.

The quality of the sample was also a problem, because of the 28 amino acids tag added to the protein for immunodecoration and purification steps that was supposed to negatively influence the crystallization process by adding flexibility and leading to disordered crystals.

The problem introduced by the tag was expected to be solved by removing it with the specific proteolytic enzyme. Several attempts were conducted with the specific enterokinase as well as with the unspecific thrombin proteases and in different reaction conditions, but they didn't work. We think that may be the recognition sequence was not accessible to the proteases due to the detergent micelle that surrounds the protein.

An alternative solution was to prepare a protein with a shorter tag of 7 histidines only, but this led to a protein that was aggregating even more than the protein with the longer tag. This protein was nevertheless used to make some crystallization screenings but with no better results.

Fig. 1.2. Crystallization attempts of MA-1D Kcv with 7His tag.

Results

Increase of protein yield: His-tag removal by H3C protease

1) Expression of MA-1D Kcv with the removable 7His-H3C tag in *Pichia pastoris*

To solve the problem of the removal of the tag, that can influence the quality of the protein sample for crystallization, the synthetic gene sMA-1D Kcv has been cloned in the vector for *Pichia pastoris* expression with a 7His tag fused at the N terminus provided of a recognition site for the Human rhinovirus 3C protease to remove the tag (see M&M, fig. M2). The H3C protease is known to be a rather active enzyme, even in the presence of large amounts of detergent [Wang & Johnson, 2001].

The synthetic gene was designed in order to remove the A+T rich stretches, that can negatively influence the expression in yeast [Sreekrishna et al., 1997; Romanos et al., 1992; Scorer et al., 1993], and also taking into account *Pichia pastoris* preferred codon-usage. We designed a synthetic gene because in our previous experience we had obtained some improvement in the expression of another viral channel, PBCV-1 Kcv [Pagliuca et al., 2007].

The transformed *Pichia* cells were selected on high antibiotic concentration (1 mg/ml geneticin instead of 0,25 mg/ml, because high resistance is thought to be associated with multiple copies of the gene), and then some colonies had been screened on a small scale to check if they express the protein. Microsomes purified from methanol-induced *Pichia cells* were prepared (see M&M) and loaded on SDS-PAGE gel and the protein was analysed by western blot using the anti-his tag antibody (fig. 1.4)

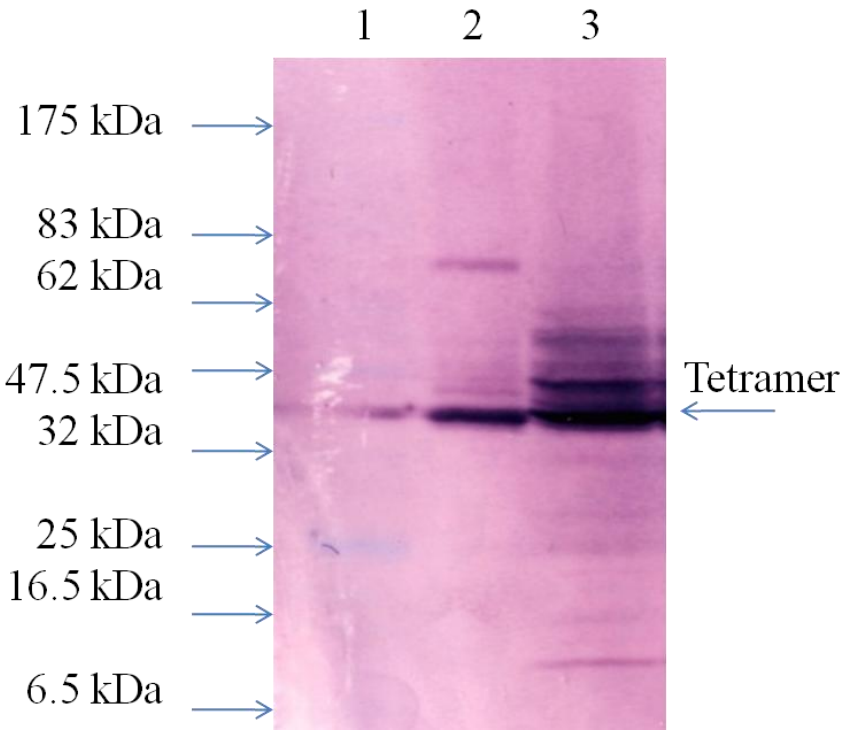

Fig. 1.4. Expression of MA-1D Kcv 7His-H3C. Lane 1: marker 5 µl; lane 2: 1 µg of purified protein of MA-1D Kcv 9His-EK as control; lane 3: 15 µl of microsomes of MA-1D Kcv 7His-H3C. Western blot of the SDS-PAGE 4%-20% gel immunodecorated with anti-polyHis antibody.

In the western blot of the SDS-PAGE gel, where the microsomal fraction of MA-1D Kcv 7His-H3C was loaded (fig. 1.4), a band can be seen in lane 3 at the same molecular weight of the tetramer of the purified protein with the 9His-EK tag used as a control in lane 2. The real molecular weight of both proteins should be around 55-56 kDa but from previous experience on 4-20% SDS gel, we know that the Kcv tetramer runs between 47.5 and 32 kDa at around 40 kDa. This is a property common to many membrane protein on SDS-PAGE gel [Rath et al., 2009; Dornmair et al., 1990] and tetrameric potassium channels in particular [Cortes et al., 1997; Heginbotham et al., 1997].

From the western blot we concluded that the protein is expressed and so the production of MA-1D Kcv in *Pichia* was scaled up in a 7 litre fermenter.

The cell yield of a 7 litre fermentation is usually about 800 g. Microsomes from the cells have been prepared and frozen in small aliquots at –80°C. The proteins were further solubilized from the membranes by means of a standard procedure, previously optimized, that is based on the use of the DDM (dodecyl-β-d-maltoside) detergent. DDM, a non ionic detergent, was used because it is a mild

detergent suitable for crystallization or easy to exchange with other detergent by affinity chromatography. Furthermore, in solubilisation screenings done with different detergents, DDM was found to give acceptably good extraction of Kcv protein from the membranes.

The solubilized protein was purified by affinity chromatography on Co^{2+}-NTA column (see M&M) and loaded on SDS-PAGE gel (fig. 1.5).

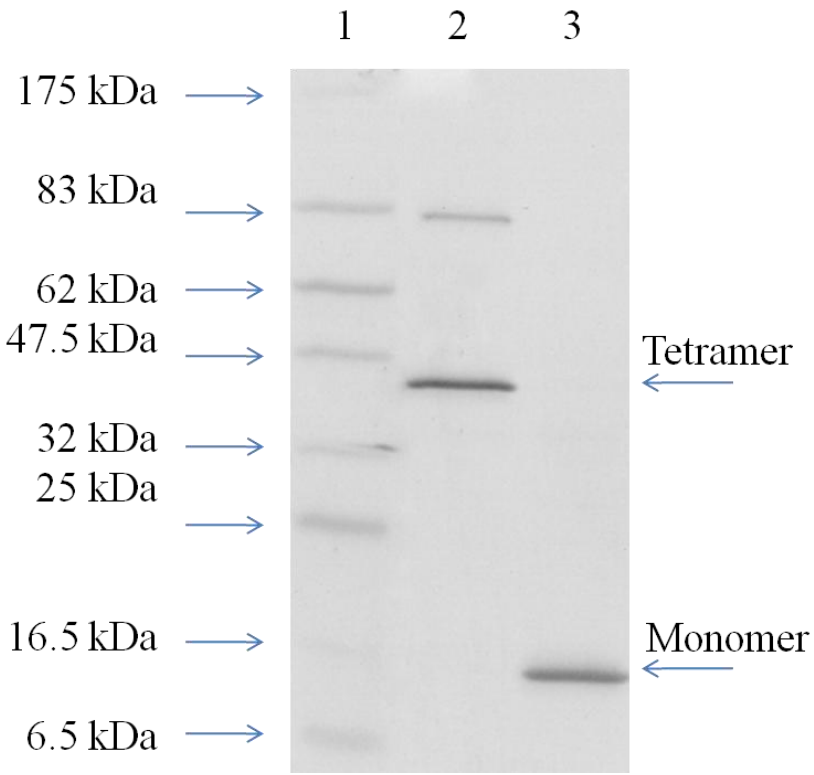

Fig. 1.5. Purified MA-1D Kcv 7His-H3C samples eluted from Co^{2+}-NTA column. Lane 1: marker 5 µl; lane 2: 2.5 µg of MA-1D Kcv; lane 3: 2.5 µg of MA-1D Kcv boiled 5'. Silver staining of SDS-PAGE 4%-20% gel.

Lane 2 shows a prevalent band corresponding to the tetramer, running between 32 and 47.5 kDa. A higher molecular weight band is also present, presumably corresponding to the aggregate form. In lane 3 a boiled sample has been loaded: in this case the protein runs as a monomer, between 6.5 and 16.5 kDa (the theoretical molecular weight of this monomer is 14 kDa). It is already known for PBCV-1 Kcv that channel proteins are stable in SDS and that the monomeric form can be obtained by heating the sample [Cortes et al., 1997; Pagliuca et al., 2007]. It is worth noting that boiling the sample seems to dissolve the aggregate, too.

Following affinity chromatography, the quality of the protein was checked by size exclusion chromatography (hereafter mentioned as gel filtration, GF) on a superdex 200 column (fig. 1.6).

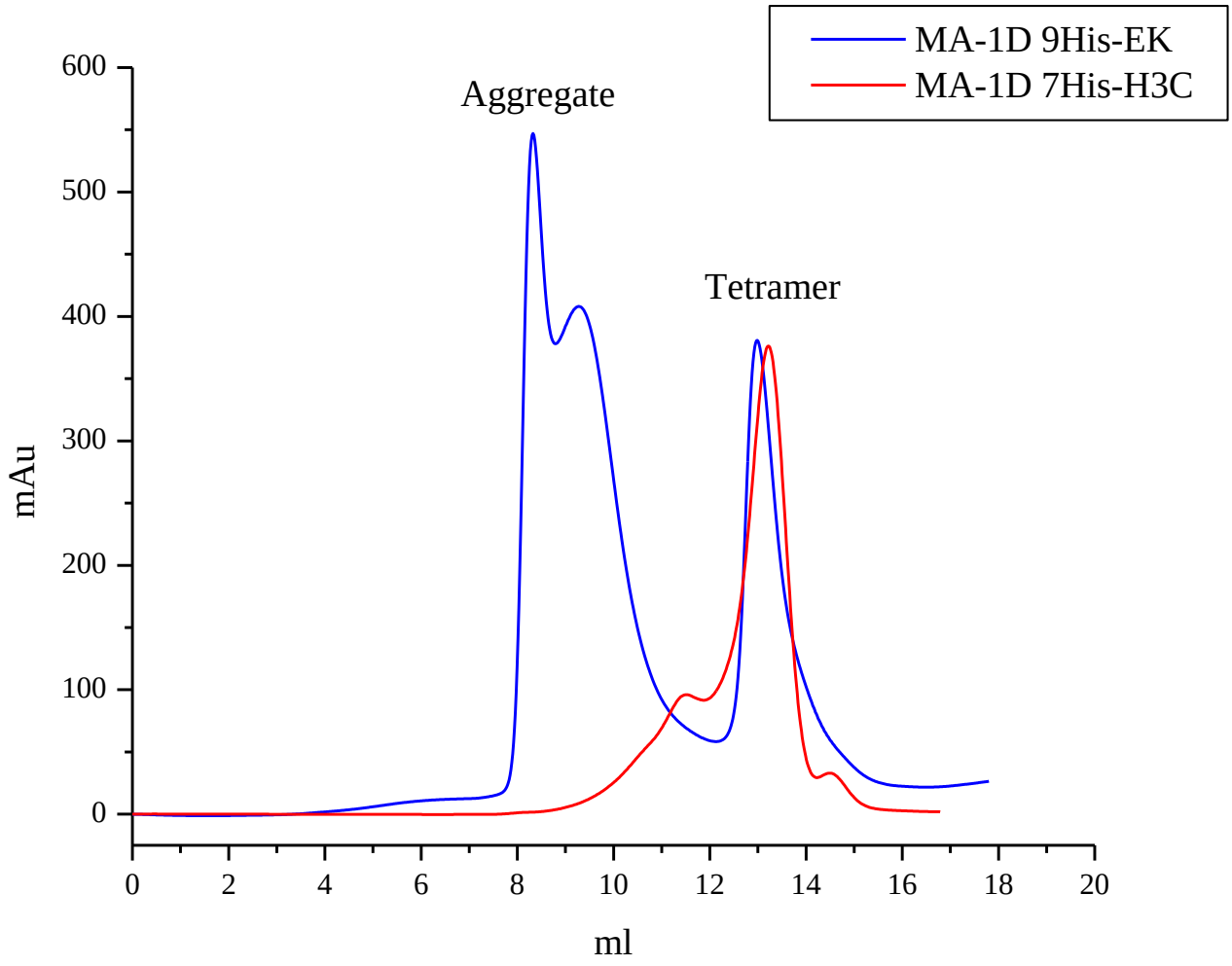

Fig. 1.6. Chromatogram of the gel filtration of the purified MA-1D Kcv 7His-H3C (in red) compared to the MA-1D Kcv 9His-EK tag (in blue). The amount of loaded protein is not comparable.

From the gel filtration of MA-1D Kcv 7His-H3C in figure 1.6 is evident that the quality of the protein has improved, compared to that of MA1D 9His-EK, even before the removal of the tag. The peaks corresponding to the tetramer of the two proteins with different tags elute at the same volume (about 13 ml) but the construct with the 7His-H3C tag has only a small amount of aggregate form (visible as a peak at lower elution volumes, between 8 and 10 ml), compared to MA-1D Kcv with the 9His-EK tag. We know that the first elution peak correspond to the aggregated protein because the corresponding fractions were loaded on SDS-PAGE gel and they were running at high molecular weight under the 80 kDa band if the marker (data not showed). From this gel filtration is

evident that an increase in quality and yield has been already obtained just by changing the construct, because starting from the same amount of solubilized protein, the tetrameric form useful for crystallization screenings is doubled compared to the old protein construct.

2) Optimization of reaction conditions for the 7His-H3C tag removal

Several experiments have been done to test the best conditions for the removal of the 7His-H3C tag. The parameters that were changed were the protease/protein ratio, the temperature, the time of incubation and the imidazole concentrations.

The first condition tested was the protease/protein ratio because the activity of the 3C protease is unknown, since is produced in the lab (see M&M), and needs to be tested after each preparation. Since the high imidazole concentration present in the protein elution buffer (300 mM) can inhibit the protease activity, imidazole concentration in the protein sample was first reduced below 10 mM by repetitive steps of dilution and concentration with a cut-off filter of 30 kDa (Millipore).

The conditions tested were the following: digestions of 20, 100 and 500 µg of protein with 1 µl of protease and of 500 µg of protein with 10 µl of enzyme.

After incubation of the reaction at 4°C for 16 hours, the samples were loaded on SDS-PAGE gel and silver staining and western blot were performed (fig. 1.7).

A

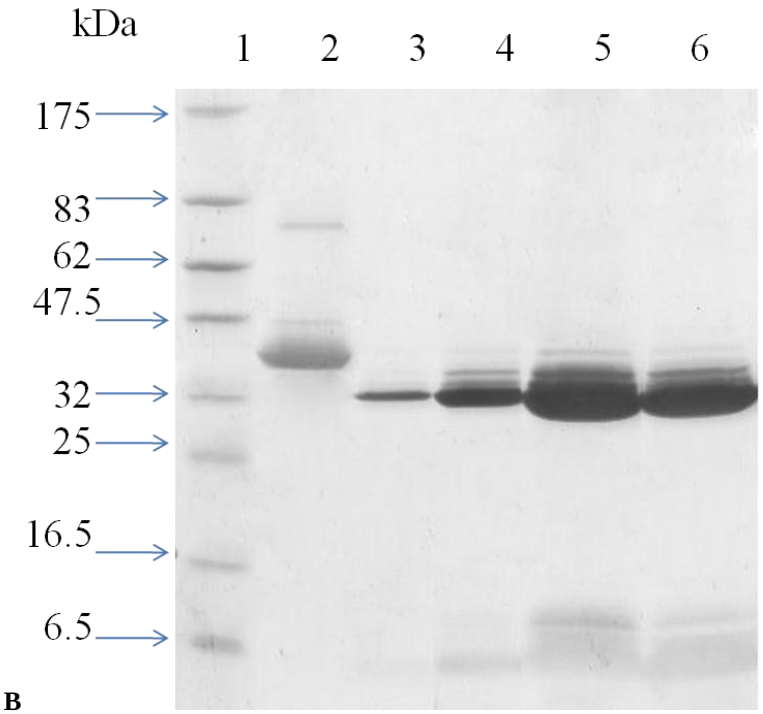

B

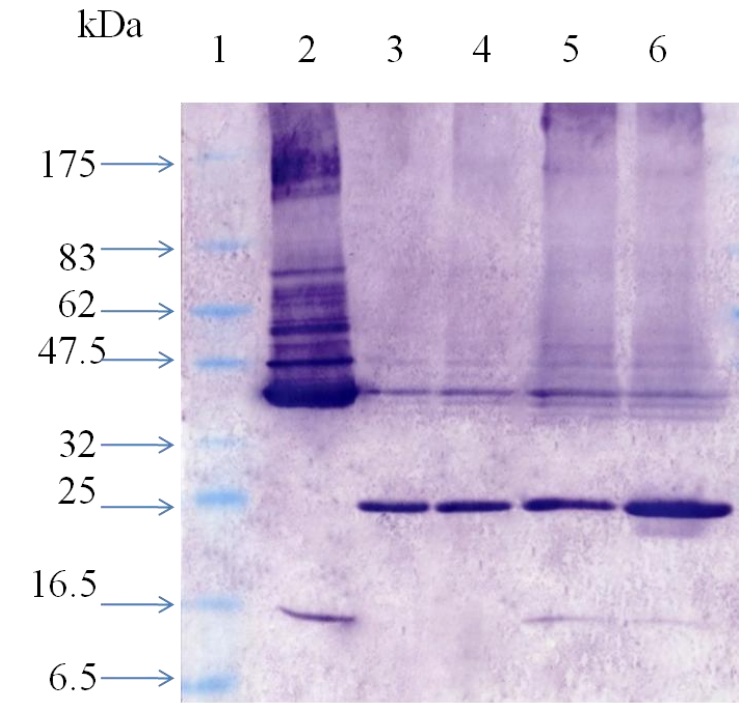

Fig. 1.7 A and B. Tag removal with H3C protease: protease-protein ratio screening. Lane 1: marker 5 µl ; lane 2: 100 µg of MA-1D Kcv 7His-H3C as control (protein before protease digestion); lane 3: 20 µg of Ma-1D Kcv 7His-H3C + 1 µl of protease; lane 4: 100 µg of Ma-1D Kcv + 1 µl of H3C protease; lane 5: 500 µg of Ma-1D Kcv 7His-H3C + 1 µl of protease; lane 6: 500 µg of Ma-1D Kcv + 10 µl protease. Silver staining (A) and western blot performed with the anti-polyHis antibody (B) of SDS-PAGE 4%-20% gel.

The silver staining of the electrophoretic migration of the protease reactions (fig. 1.7 A) shows that there's a shift of the molecular weight of the protein bands in lanes from 3 to 6 compared to lane 2, from around 44 kDa (measured with relative migration method, see M&M) corresponding to the apparent molecular weight of the tetrameric form of MA-1D Kcv with the tag, to 32 kDa that corresponds to the expected molecular weight of the tetramer without the tag. This shift of about 12 kDa is reasonable because the tag is 26 aminoacids long corresponding to 2.8 kDa for the monomer and about 11 kDa for the tetramer.

Tag removal occurred for all the conditions tested although some additional bands, corresponding to partial digestion of the tetramer, are detectable, even at the lower protein concentration tested (lane 3). The condition chosen for subsequent experiments is the reaction with 1 µl of enzyme for 100 µg of protein (lane 4).

Another interesting data that came out is that the band at a molecular weight of 78 kDa in lane 2, corresponding presumably to an aggregated form of the protein, disappeared after the protease reaction (lanes 3-6). This could denote that the tag removal led to the solving of aggregated forms of the protein.

In the corresponding western blot in figure 1.7 B it could be seen that from lane 3 to 6 there's a strong decrease but not a complete disappearance of the main band recognized by the antibody at about 44 kDa. Since the antibody recognized the histidine tag, it means that the removal of the tag was never fully achieved as already highlighted by the appearance of the multiple bands on the silver staining. The additional 25 kDa band that is visible on the western blot corresponds to the 3C protease that also has an histidine tag.

Different conditions were tested in a second experiment to check if the protein could be used with a moderately higher concentration of imidazole, 30 mM, to shorten the procedure needed in order to reduce it. The reaction was performed at 4°C for 16 hours but also at 30°C for 2 hours to check if it was possible to reduce the length of the reaction.

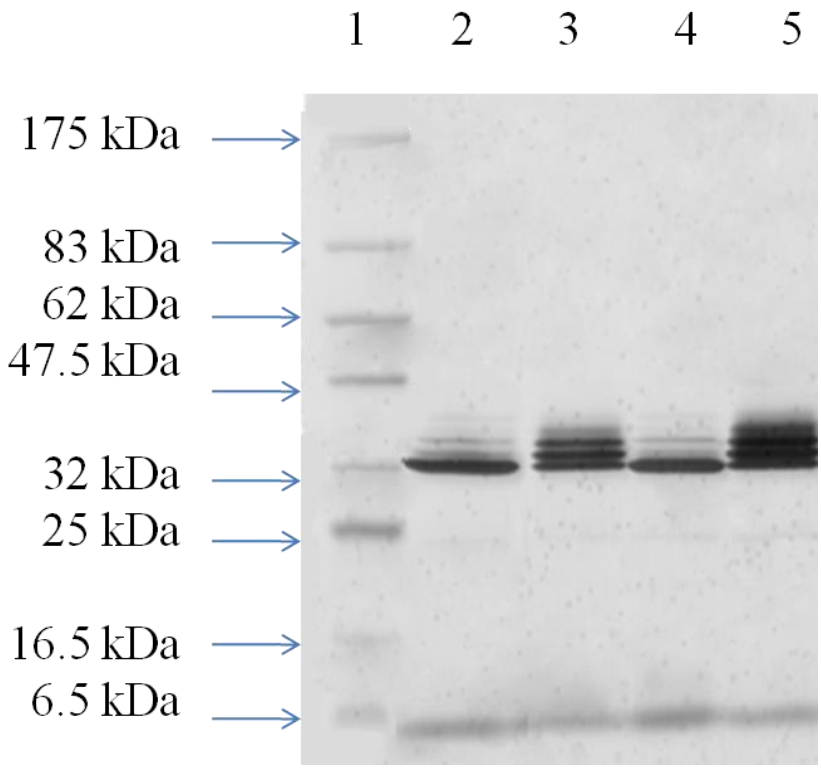

Fig. 1.8. Effect of imidazole and temperature on the 3C protease activity. Lane 1: marker 5 µl ; lane 2: 100 µg of sMA-1D Kcv 7His-H3C + 1 µl of 3C, 4°C 16 h (control); lane 3: same but 30°C 2h; lane 4: with 30mM imidazole. 4°C 16 h; lane 5: same but 30°C 2 h. Silver staining of SDS gel 4%-20%.

The silver stain of the SDS-PAGE gel (fig.1.8) shows that both the reactions at 30°C for 2 hours in lane 3 and 5 are less efficient than the corresponding reactions at 4°C for 16 hours in lane 2 and 4 because there are more bands corresponding to partial digestion of the protein and the band at 32 kDa corresponding to the complete cut protein is thinner. So the incubation of the reaction for a shorter time at 4°C is not efficient enough. In the samples treated at 4°C for 16 hours, the increase of imidazole, up to 30 mM, in lane 4 had no influence on the reaction if compared to the control in lane 2 where the sample had 7.5 mM imidazole. This means that the imidazole concentration in the protein buffer has to be reduced about 10 times, before tag removal.

3) Protein purification by affinity chromatography

At the end of the tag digestion, the protein sample was passed a second time through a Co^{2+}-NTA column to remove the H3C protease, the tags and the partially digested proteins, in order to obtain the protein sample as pure and homogeneous as possible. The protein was collected in the flowthrough and a sample loaded on SDS-PAGE gel for silver staining and western blot analysis (fig. 1.9 A and B).

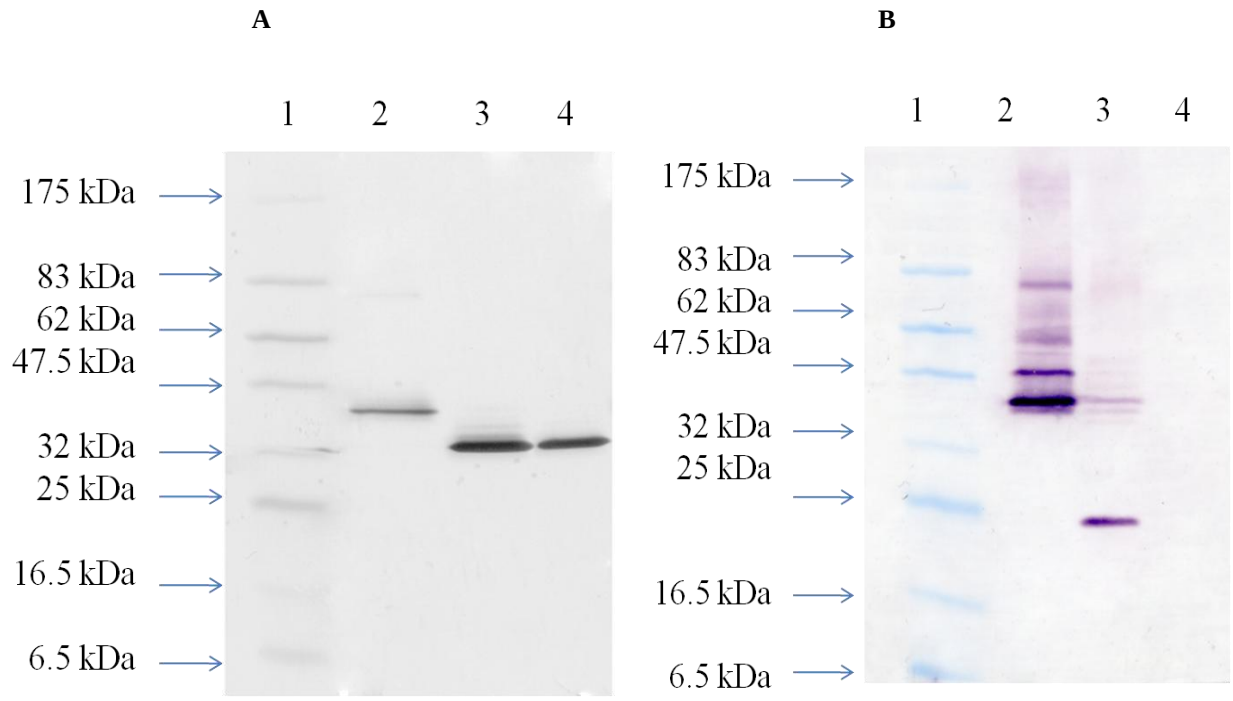

Fig. 1.9 A and B. Purification on Co^{2+}-NTA column of MA-1D Kcv 7His-H3C digested with H3C. Lane 1: marker 5 µl; lane 2: MA-1D Kcv before protease reaction as control; lane 3: MA-1D Kcv after H3C digestion; lane 4: MA-1D Kcv digested and purified on Co^{2+}-NTA column. Silver staining (A) and western blot (B) of SDS-PAGE 4%-20% gel.

The silver staining shows in lane 2 the usual bands for MA-1D Kcv: a band at 44 kDa corresponding to the tetrameric form and an upper band at 78 kDa that could be an aggregation form. Lane 3 shows the shift after the protease reaction and the disappearing of the upper band at 78 kDa, already mentioned in figure 1.7 A. Lane 4 shows the result of the purification on the Co^{2+}-NTA column: after affinity chromatography, the Kcv band is cleaner, without the partial digested protein bands. In the western blot is showed that in lane 3 the band recognized by the antibody anti

his-tag is weaker in intensity compared to the uncut protein loaded as a control in lane 2 and this means that almost all the protein is digested. In lane 3 is also visible a band of 25 kDa corresponding to the 3C protease. In lane 4, after purification the antibody recognized no band, confirming that partially digested protein, tags and the protease have been successfully removed.

4) Gel filtration

The quality of the sample in terms of monodispersion was further checked by size exclusion chromatography (gel filtration).

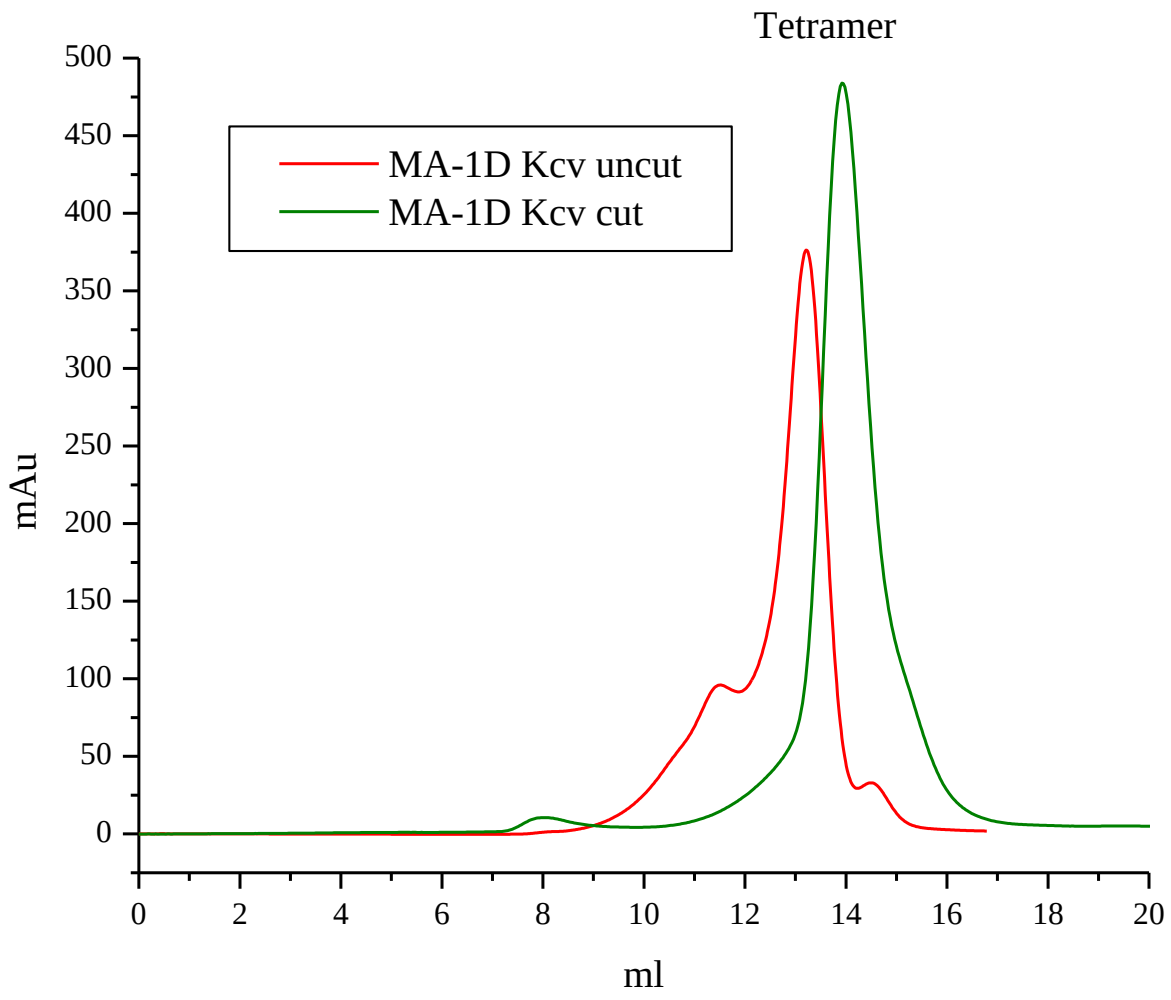

Fig. 1.10. Chromatogram of the gel filtration of the purified MA-1D Kcv without the tag (in green) compared to the uncut MA-1D Kcv 7His-H3C (in red). The amount of protein loaded is not comparable.

Figure 1.10 shows overimposed the two chromatograms obtained by gel filtration with the protein before (red line) and after (green line) the removal of the tag. There is a clear shift in the elution peak that is due to the different molecular weight of the protein (44 vs. 34 kDa). It is also clear that, after tag removal, the protein sample is monodisperse and does not show any aggregation peak at higher molecular weight.

It can be therefore concluded that a significant improvement in quality and yield of the protein has been reached by tag removal.

This protein has been further used for crystallization screening. Figure 1.11 shows exemplary crystal-like structures that we obtained after several round of crystallization trials. These pseudo-crystals were not diffracting and we therefore decided to change the crystallization strategy. Given the monodispersity and purity of the protein sample, the optimization procedure seemed not to be the limiting step anymore. We therefore decided to use this protein but to test other crystallization strategies, such as to crystallize the Kcv protein in a complex with a Kcv-specific antibody.

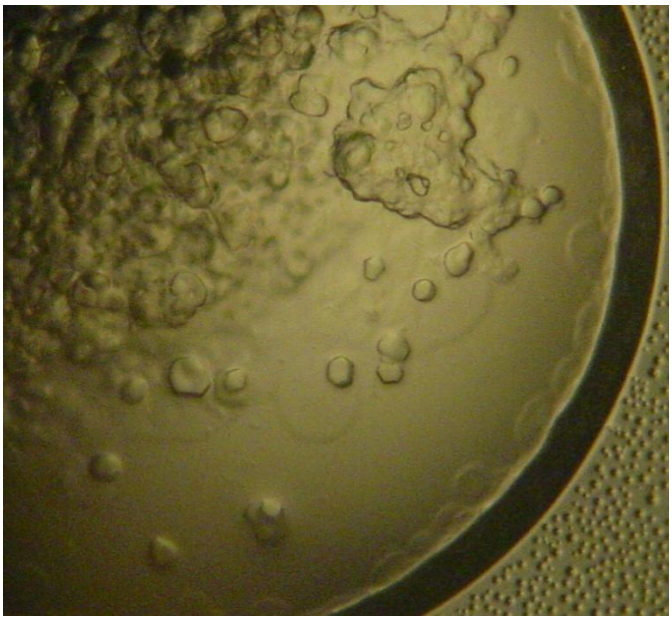

Fig. 1.11. Irregular non diffracting precipitates of MA-1D Kcv.

Use of monoclonal antibodies for crystallization

A strategy to improve crystals formation is the use of antigen binding fragments (Fabs) that can be used as chaperon of crystallization of integral membrane proteins because they bind to the protein, and enlarge the hydrophilic part of the protein, thus providing additional surface for crystal contacts [Ostermeier et al., 1995]. The Fab fragments are obtained from monoclonal antibodies produced by hybridoma cells. These immortal cell lines are obtained by fusing myeloma cells with the spleen cells of a mouse previously immunized with the antigen (see Introduction; [Köhler & Milstein., 1975]).

To produce monoclonal antibodies against MA-1D Kcv we used the protein fused to the 7 histidine tag, in order to increase the immunogenic response in mice. The procedure was run by a company, the EMBL Monoclonal Core Facility. They obtained several hybridoma cell lines that were screened by ELISA to select those lines that produced antibodies specific for the tetrameric and not the monomeric form of the protein (non-boiled and boiled protein samples). A second screen was performed in order to discard those cell lines producing antibodies that recognized the tag (comparison between full length MA1D Kcv 7His-H3C and the same protein after tag removal)

At the end of the screening procedures, EMBL Monoclonal Core Facility sent us 26 clones with these characteristics.

1) Screening for antibodies that recognize the protein without the tag

The screening done by the EMBL facility by ELISA was repeated in our lab using the sera of the hybridoma cell lines for western blot analysis.

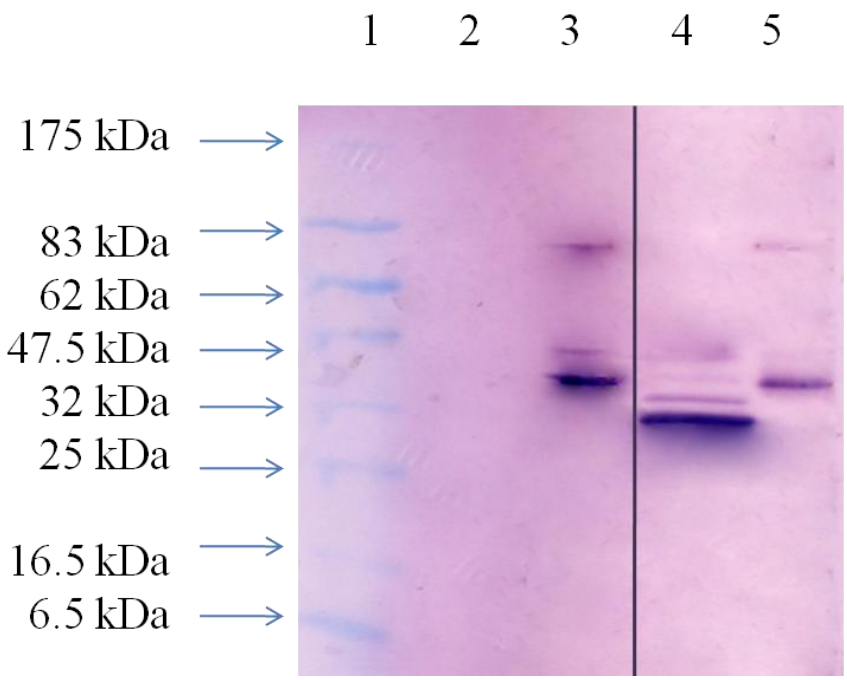

Fig. 1.12. Screening of antibodies that recognize the protein without the tag. Lane 1: marker 5 µl ; lane 2: 25 ng of MA-1D Kcv without the tag (CUT) immunodecorated with anti-polyHis antibody; lane 3: 25 ng of MA-1D Kcv with the tag (UNCUT) immunodecorated with anti-polyHis antibody; lane 4: 25 ng of MA-1D Kcv CUT immunodecorated with monoclonal antibody serum of hybridoma 20G1; lane 5: 25 ng of MA-1D Kcv UNCUT immunodecorated with monoclonal antibody serum of hybridoma 20G1. Western blot of SDS-PAGE gel 4-20%.

Figure 1.12 shows a representative example of a procedure that was performed for all 26 sera.

In the western blot in figure 1.12 the immunodecoration has been done in lanes 4 and 5 with the serum of hybridoma cell line 20GI and in lanes 2 and 3 with the anti-polyhistidine antibody as a control. It could be seen that the clone 20GI recognized both the uncut and the cut protein, lane 4 and 5 that runs at the corresponding molecular weight of 32 and 44 kDa, while the anti-polyHis antibody recognized only the uncut protein in lane 3 as expected. This confirms that the antibody doesn't react with the histidine tag but with the protein itself. Table 1.1 summarizes the results for all 26 clones.

Ab clone	UNCUT	CUT
4C5	-	-
1B9	+	+
5C6	+	+
5H3	-	+
5C10	-	-
3H12	+	+
9F11	-	-
8F3	-	-
5A10	+	+
15G8	+	+
20A2	+	+
3H7	+	+
15C7	+	+
3A1	+	+
13B3	+	+
20G1	+	+
3E7	+	+
7G7	+	+
8D6	+	+
11E2	+	+
14B5	+	+
8D3	+	+
2B2	+	+
9H5	+	+
8H7	+	+
17A2	+	+

Tab. 1.1. Summary of the western blot screening with the 26 antibodies on the cut/uncut protein.

The screening has revealed that 21 sera recognize both uncut and cut form of the protein, and this means that they recognize an epitope common to both forms and not the histidine tag. Four

antibodies don’t recognize any of the protein forms and another one recognizes only the cut protein. Since these 4 were pre-selected for positive recognition of the protein in ELISA we think that they recognize the tetramer only in its native conformation, while they do not recognize the partly-denatured form of it that runs in the SDS-PAGE gel. For what concerns the antibody that recognizes only the cut protein, we think that it reacts with an epitope of the tetrameric protein that is normally not accessible when the tag is present.

2) Screening of antibodies that recognize the tetramer and not the monomer

The sera were further screened by western blot to test and confirm those that were recognizing the protein in the tetrameric form. As previously reported, the MA-1D Kcv is stable in SDS-PAGE and the protein sample must be boiled for 10 minutes to obtain the monomer. All the 26 sera were used to immunodecorate the western blots of the SDS-PAGE gels where un-boiled and boiled protein samples of MA-1D Kcv without the tag (CUT) were loaded. In figure 1.13 two exemplary experiments are shown.

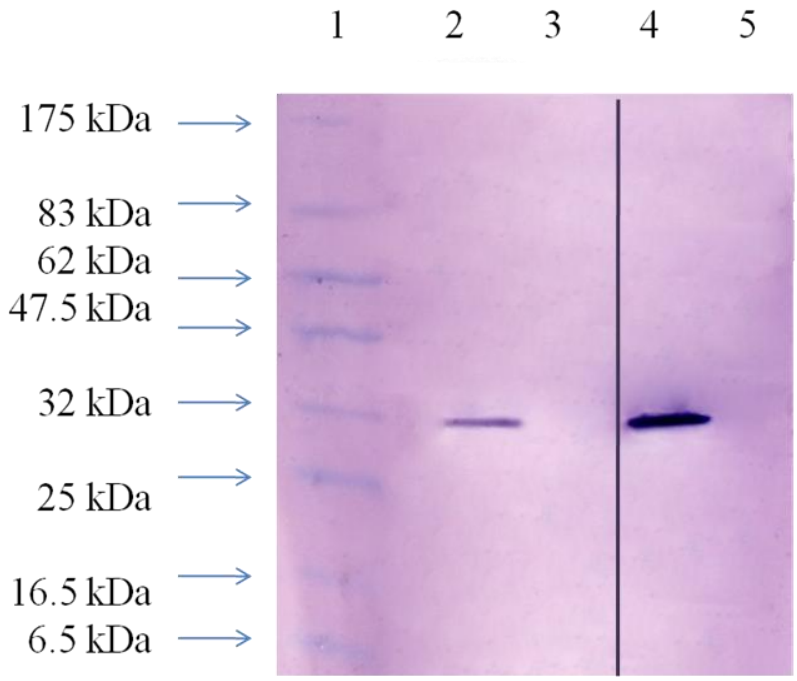

Fig. 1.13: Screening of antibodies that recognize the tetrameric protein. Lane 1: marker 5 µl ; lane 2: 25 ng of MA-1D Kcv un-boiled immunodecorated with 9H5 antibody; lane 3: 25 ng of MA-1D Kcv boiled immunodecorated with 9H5 antibody; lane 4: 25 ng of MA-1D Kcv un-boiled immunodecorated with 8D6; lane 5: 25 ng of MA-1D Kcv boiled immunodecorated with 8D6 antibody. Western blot of SDS-PAGE gel 4-20%.

The western blot screening on un-boiled/boiled MA-1D Kcv reveals that both antibodies showed (9H5 e 8D6) recognized only the tetrameric form of the protein in lane 2 and 4, while in lane 3 and 5, where boiled protein has been loaded, there are no signals at the expected molecular weight of the monomer, around 14 kDa. The monomeric protein was present, as checked on a parallel silver

staining gel where cut and purified on Co^{2+}-NTA protein and a sample boiled for 10' to get the monomer were loaded (fig. 1.14).

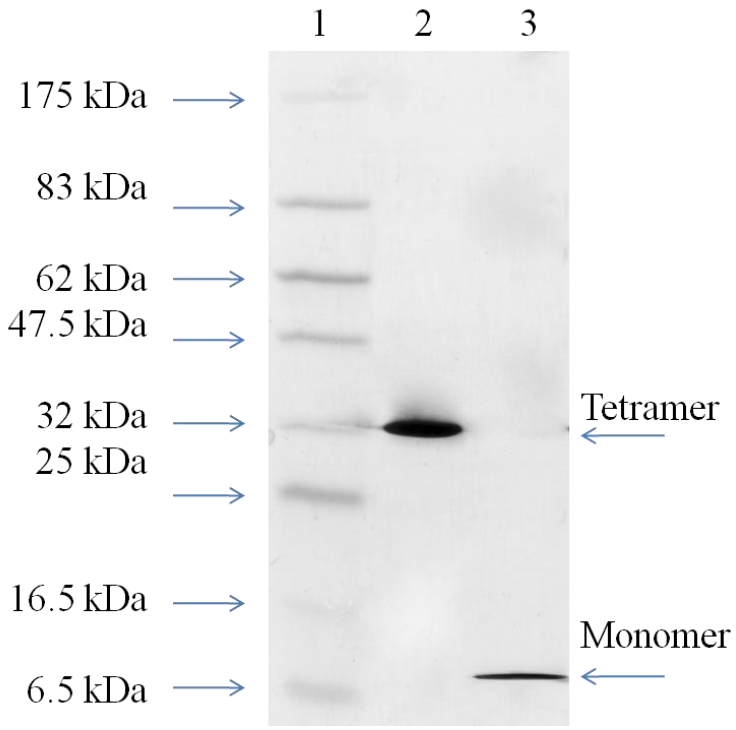

Fig. 1.14: Boiling test on MA-1D Kcv CUT protein. Lane 1: marker 5 µl ; lane 2: 100 ng of MA-1D Kcv CUT un-boiled; lane 3: 100 ng of MA-1D Kcv CUT boiled. Silver staining of SDS-PAGE gel 4-20%.

As showed by the silver staining the protein after 10 minutes of boiling is completely split into monomers that run at a molecular weight of about 10 kDa as expected, so the monomers are present but not recognized by the antibodies.

Of all the 26 sera tested, 22 have showed interaction with the tetrameric form as showed in the example in figure 1.13, and the remaining 4 showed no interaction at all. These 4 were those sera previously not reacting with the protein on western blot. The summary of the experiment is showed in table 1.2.

Ab clone	CUT TETRAMER (un-boiled)	CUT MONOMER (boiled)
4C5	-	-
1B9	+	-
5C6	+	-
5H3	+	-
5C10	-	-
3H12	+	-
9F11	-	-
8F3	-	-
5A10	+	-
15G8	+	-
20A2	+	-
3H7	+	-
15C7	+	-
3A1	+	-
13B3	+	-
20G1	+	-
3E7	+	-
7G7	+	-
8D6	+	-
11E2	+	-
14B5	+	-
8D3	+	-
2B2	+	-
9H5	+	-
8H7	+	-
17A2	+	-

Tab. 1.2. Summary of the western blot screening with the 26 antibodies on the un-boiled/boiled protein.

3) Clones selection.

Table 1.3 reports a summary of the results after the two western blot tests compared with the ELISA test.

	ELISA		WESTERN BLOT			
Ab clone	**UNCUT**	**CUT**	**UNCUT**	**CUT**	**TETRAMER**	**MONOMER**
4C5	+	+	-	-	-	-
1B9	+	+	+	+	+	-
5C6	+	+	+	+	+	-
5H3	+	+	-	+	+	-
5C10	+	+	-	-	-	-
3H12	+	+	+	+	+	-
9F11	+	+	-	-	-	-
8F3	+	+	-	-	-	-
5A10	+	+	+	+	+	-
15G8	+	+	+	+	+	-
20A2	+	+	+	+	+	-
3H7	+	+	-	-	+	-
15C7	+	+	+	+	+	-
3A1	+	+	+	+	+	-
13B3	+	+	+	+	+	-
20G1	+	+	+	+	+	-
3E7	+	+	+	+	+	-
7G7	+	+	+	+	+	-
8D6	+	+	+	+	+	-
11E2	+	+	+	+	+	-
14B5	+	+	+	+	+	-
8D3	+	+	+	+	+	-
2B2	+	+	+	+	+	-
9H5	+	+	+	+	+	-
8H7	+	+	+	+	+	-
17A2	+	+	+	+	+	-

Tab. 1.3. Summary of ELISA and western blot screenings on the 26 hybridoma clones.

In red are highlighted the sera that were positive in ELISA but were not recognizing anything in the western blots, in yellow the one that recognizes only the cut form of the protein and in green the 6 positive ones that were chosen for further tests because they gave the best signals on the gel, although the concentration was unknown and the analysis was not quantitative. The 6 clones were diluted 1:5 and tested again by western blot.

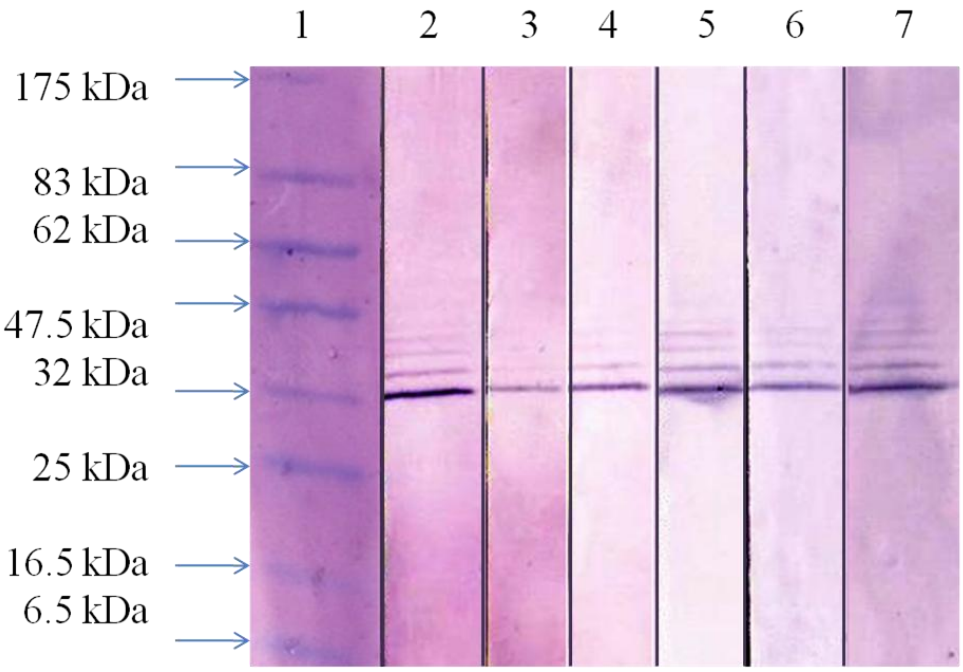

Fig. 1.15. Immunodecoration with 1:5 diluted sera of the 6 chosen antibodies. Lane 1: marker 5 µl ; lane 2: 8D6; lane 3: 15C7; lane 4: 17A2; lane 5: 11E2; lane 6: 3A1; lane 7: 20G1; in all the lanes 25 µl of MA-1D Kcv CUT but not purified on Co^{2+}-NTA resin were loaded. Western blot of SDS-PAGE gel 4-20%.

All the diluted sera still recognized the MA-1D Kcv cut protein as expected. The multiple bands visible upon the prevalent one can be partial digestion of the protein, that maybe were not removed after the purification on Co^{2+}-NTA resin. The 6 positive clones chosen have also been screened to check if they recognize other Kcv-like protein in western blot, in particular PBCV-1 Kcv that differs from MA-1D Kcv just for 5 aminoacids, and its barium insensitive mutant T63S that presents an additional mutation in the selectivity filter, the threonine 63 into serine.

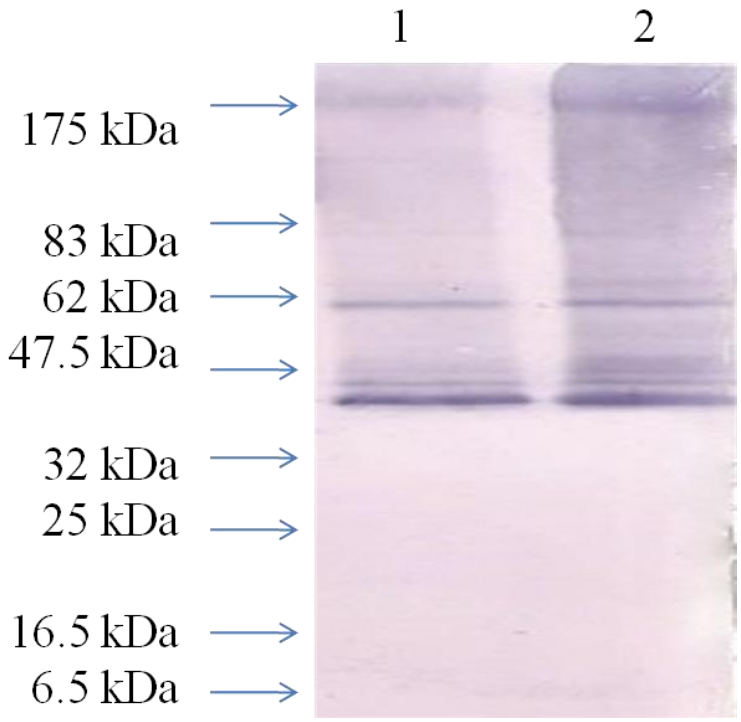

Fig. 1.16. Immunodecoration of PBCV-1 Kcv and PBCV-1 Kcv T63S with the antibody 17A2. Lane 1: 25 µg of UNCUT PBCV-1 Kcv; lane 2: 25 µg of UNCUT PBCV-1 Kcv T63S. Western blot on SDS-PAGE gel 4-20%.

Figure 1.16 shows an example of recognition of the two proteins with serum 17A2, but all 6 clones tested were recognizing both proteins. The multiple band recognition depends on the fact that these uncut protein run at different molecular weight. The tetramer is the stronger band below 47.5 and the other strong band at 62 kDa is supposed to be an aggregate. This means that the antibody recognized a common epitope in PBCV-1 Kcv and its mutant too and can be used for crystallization of these two proteins too.

Together with these 6 positive clones, also 2 (4C5 and 9F11) that gave negative results in western blot but were positive in ELISA tests, were chosen for further amplification and purification because they might recognize the protein in its native form.

4) Fab fragments production for protein-antibody interaction

The 8D6 clone

The chosen hybridoma clones were grown in order to produce and purify large quantities of the antibodies from which isolate the Fab fragments.

The first clone that was used for Fab fragment preparation was 8D6. After growing and expanding hybridoma cells, the supernatant was collected and centrifuged. The supernatant was then purified by affinity chromatography with protein A-bound resin (see M&M).

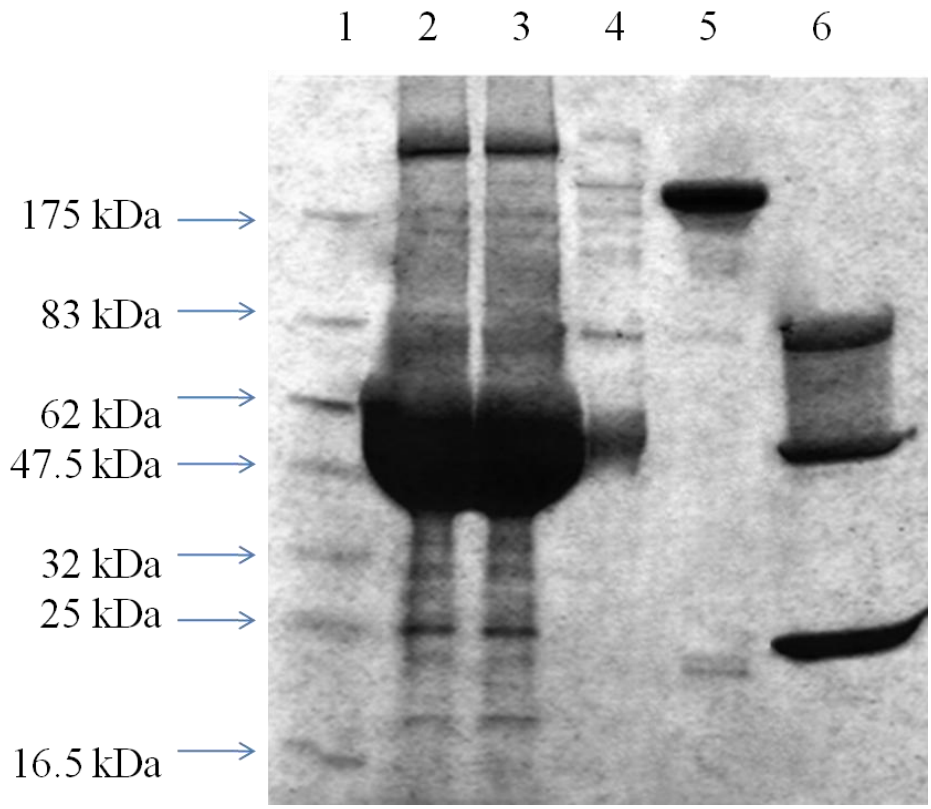

Fig. 1.17. Purification of the 8D6 antibody. Lane 1: marker 5 µl; lane 2: 5 µl of the flowthrough of the affinity column; lane 3: 10 µl of the washing step of the resin; lane 4: 22 µl of 2nd washing step; lane 5: 10 µl of the elution; lane 6: 10 µl of elution + 10 mM DTT. Coomassie staining of the SDS-PAGE gel 4-20%.

Figure 1.17 shows in lane 5 and 6 the purified antibody that runs as a single band (lane 5) at about 150 kDa in non reducing conditions, while it runs in 3 bands in lane 6 at 75, 50 and 25 kDa after

treatment of the sample with DTT that reduces the disulfide bonds in the antibody (see fig. 1.18 for a scheme). The 150 kDa band is, as expected, really faint in the lanes from 2 to 4 where the flowthroughs are loaded. The flowthrough of the column contains all the proteins that are not bound to the resin (lane 2) and the two washing steps remove proteins weakly and aspecifically bound to the protein A-resin.

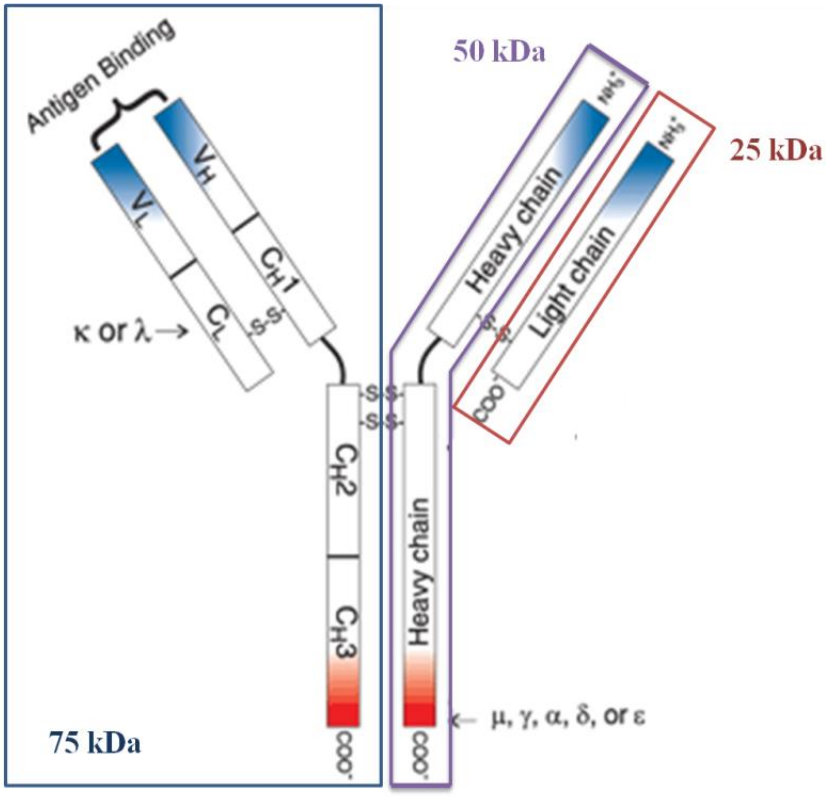

Fig. 1.18. Schematic representation of an antibody showing the disulfide bonds that connect the heavy and the light chains and the nature of the three molecular weight bands, 75, 50 and 25 KDa, appearing on the gel in reducing conditions.

The purified antibody shown in lane 5 of figure 1.17 was further subjected to a digestion step with papain, a cystein protease enzyme that cleaves the Fc (crystallizable) portion of immunoglobulins from the Fab (antigen-binding) portion. Figure 1.19 shows the cleavage scheme.

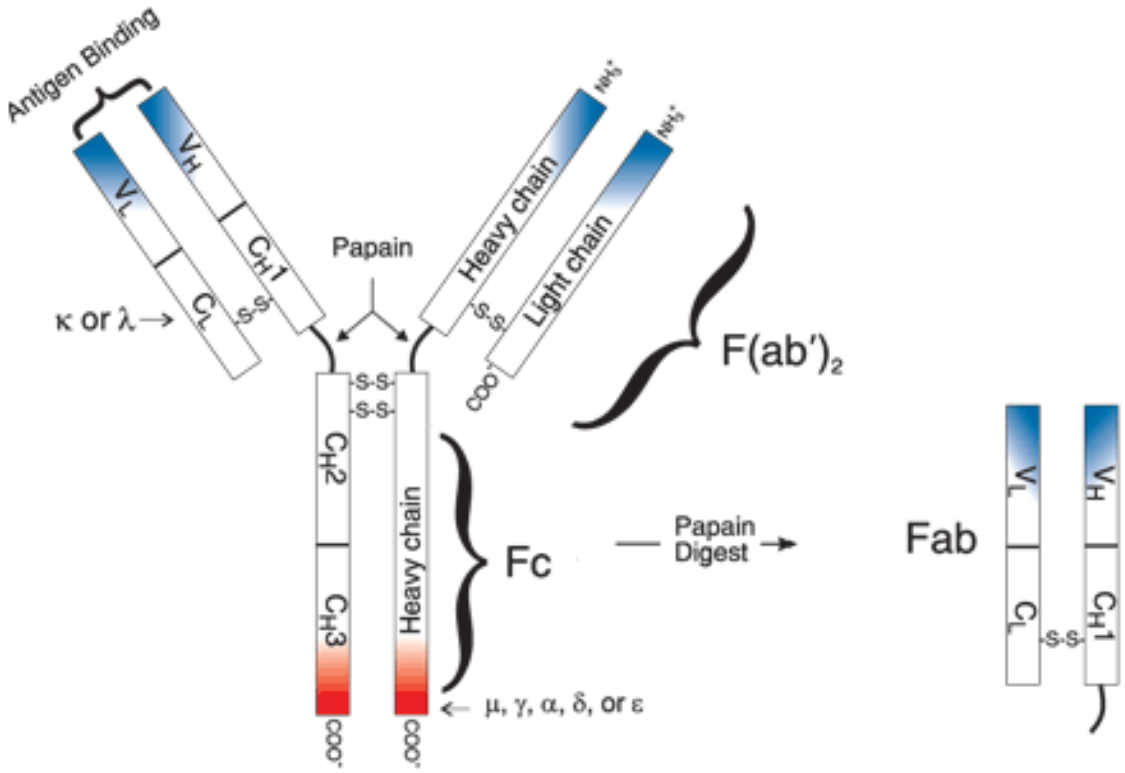

Fig. 1.19. Scheme of papain cut.

The digestion reaction was then reloaded on a new protein A-column that binds the Fc and uncut antibody and separates them from the Fab fragments that are found in the flowthrough. (see M&M).

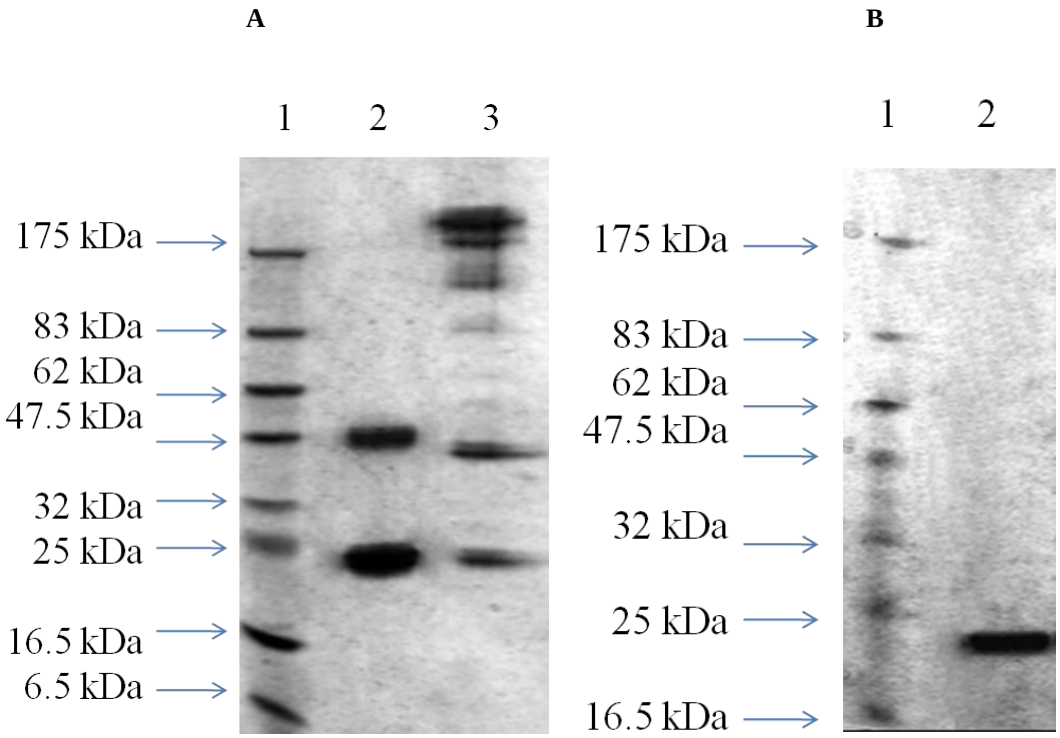

Fig. 1.19 Production and purification of Fab fragment from the 8D6 antibody. A) Lane 1: marker 5 µl; lane 2: 10 µl of the flowthrough from protein A resin loaded with the sample digested with papain in non-reducing conditions; lane 3: 10 µl of flowthrough of the regeneration of the resin with IgG buffer of protein A-resin. B) Lane 1: marker 5 µl; lane 2: 10 µl of purified Fab fragments (same sample of A, lane 2) + 10 mM DTT. Coomassie blue staining of a SDS gel 4-20%.

Figure 1.19 A shows in lane 2 the Fab fragment. The Fab fragment was obtained by papain digestion and is present in the flowthrough of the Protein A-resin. The two bands of 25 and 50 kDa represent the Fab fragments reduced and not reduced (the reduced Fab can be present also in absence of DTT). In lane 3, where an aliquot of the regeneration step of the protein A-resin, that contains the Fc and the undigested antibody, was loaded the 3 bands correspond to the uncut antibody at 175 kDa (expected molecular weight is 150), the Fc fragments at 50 kDa also binding to the protein A and some residual Fabs that was possibly retained in the resin.

After treatment of the Fab sample eluted in the flow through with 10 mM DTT, the disulfide bonds are reduced and there's only the 25 kDa band (fig. 1.19 B, lane 2).

The purified Fab fragments of the antibody 8D6 were mixed with the MA-1D Kcv protein in 1:4 ratio (see M&M) and the complex formation was checked by gel filtration on superdex 200 column (fig. 1.20).

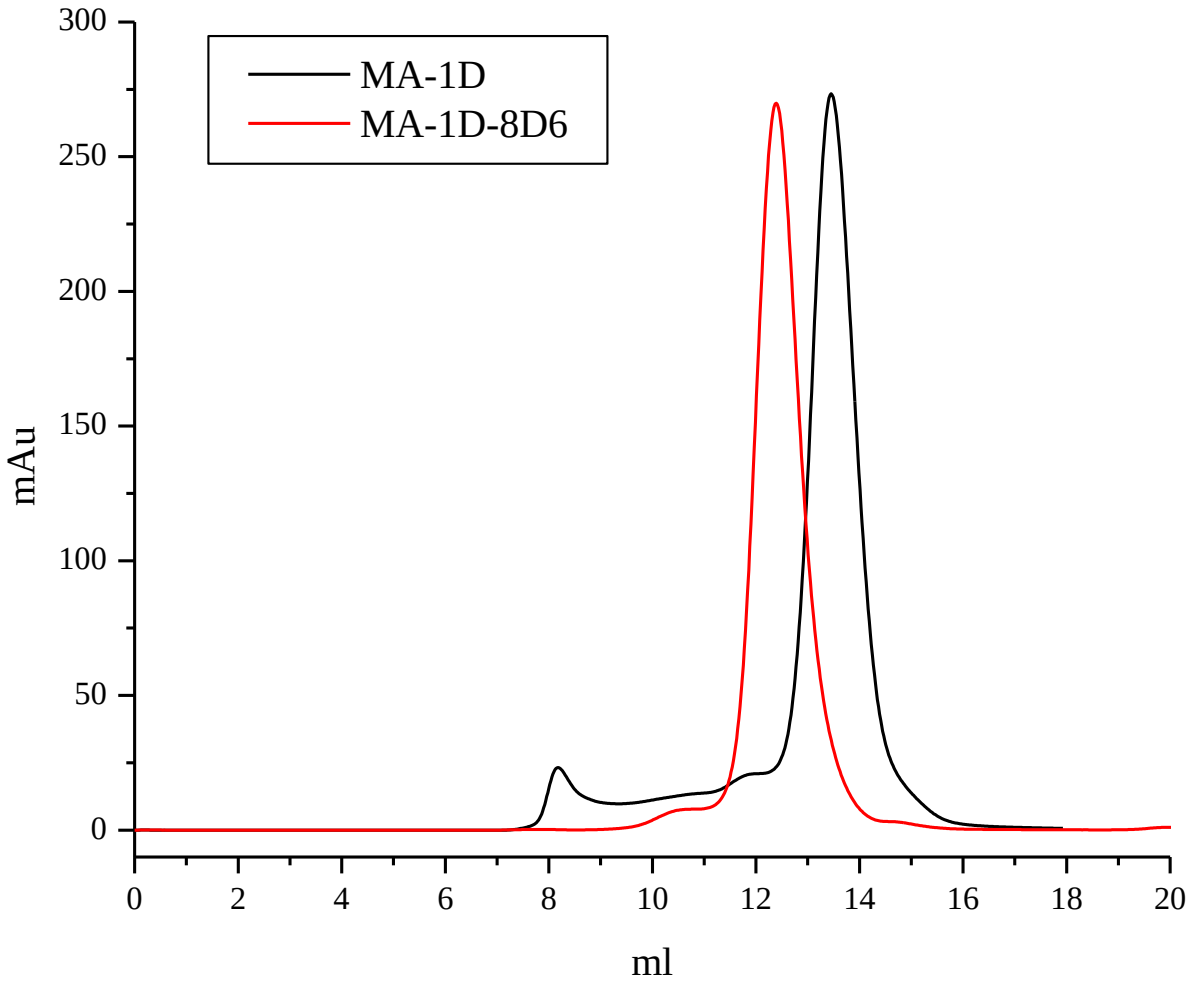

Fig. 1.20. Superimposition of chromatograms of the MA-1D Kcv protein (in black) and the complex MA-1D Kcv-8D6 Fab (in red).

In the gel filtration in figure 1.20 it is clearly evident that there's a shift to higher molecular weight in the peak of the tetramer of MA-1D Kcv alone (black), when it is bound to the Fab fragment (red). This indicates that the complex was formed although it is still not possible to know the stoichiometry: if it's one Fab fragment for tetramer or one for each protein subunit; this second possibility seems the most desirable because it would increase by 4 times the hydrophilic surface for protein-protein interaction during crystals formation.

To confirm the complex formation, the fractions corresponding to the peaks, observed in gel filtration were loaded on an SDS-PAGE gel and stained with coomassie (fig. 1.21).

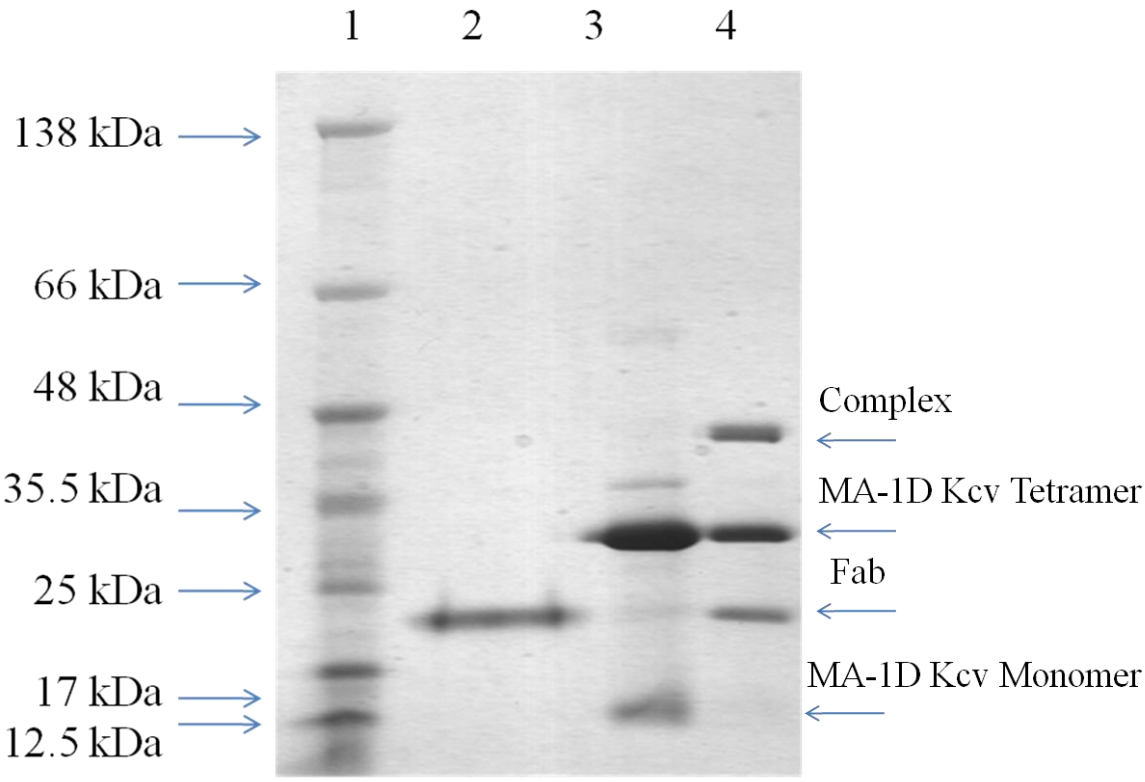

Fig. 1.21. Interaction between Fab and MA-1D Kcv protein. Lane 1: marker 5 µl; lane 2: 22ul of Fab + 10 mM DTT; lane 3: 22 µl of MA-1D Kcv from the black peak of the gel filtration shown in figure 1.20 (elution fractions 13-15 ml); lane 4: 22ul of the fractions of the red peak of the gel filtration shown in figure 1.20 (elution fractions 11-13 ml). Coomassie of the SDS-PAGE 4-12% Bis-Tris (MOPS) gel.

Figure 1.21 shows in lane 2 a band below 25 kDa that corresponds to the reduced Fab fragment; in lane 3, where a sample of the fractions eluting from 13 to 15 ml of the black GF of MA-1D Kcv were loaded, a predominant band below 35 kDa that corresponds to the tetramer of MA-1D Kcv and a faint band at 12.5 kDa that corresponds to the monomer are visible. The molecular weight where both Fab and MA-1D Kcv run are different from those showed in the SDS-PAGE gel done before, because different SDS-PAGE gel were used (4-12% Bis-Tris MOPS). In lane 4, where the fractions corresponding to the red peak (11-13 ml) were loaded, there are three bands visible: the lowest one runs as that of lane 2 and must be the Fab fragment; the middle one runs as the major band in lane 3 and must be the MA-1D Kcv tetramer; the highest one, below 48 kDa, can be the sum of Kcv and Fab fragment, as is reasonable to think that represents the complex. According to this view, the complex seems to be formed by one Fab fragment and one tetramer. This is not the most favorable situation in terms of crystal formation, as discussed earlier.

This complex has been used in crystallization screenings at 4°C with PEG or 2-propanol as precipitants at different concentrations (in total we screened 96 conditions). We did not observe any crystal formation while, in some cases, precipitates were obtained (fig. 1.22).

A **B**

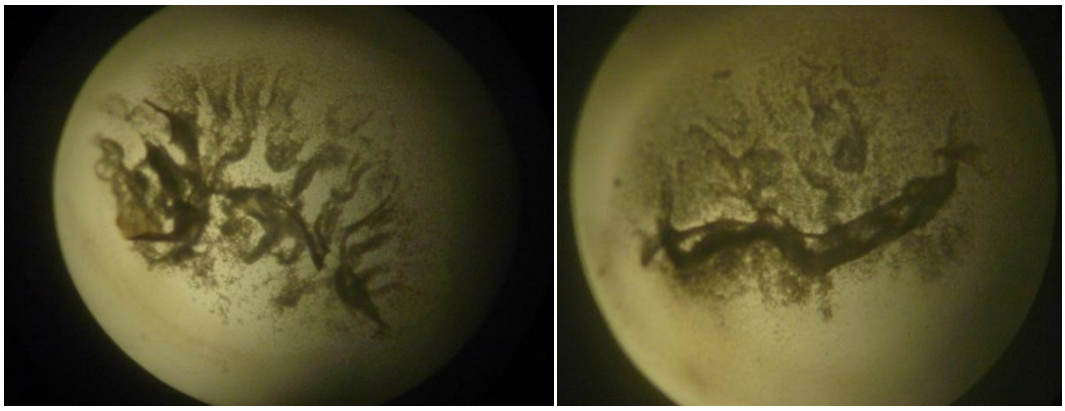

Fig. 1.22 A and B. Examples of precipitate of the protein.

From these initial partial results it is clear that that it was necessary to go on screening more conditions for this complex, as well as to produce and purify other Fab fragments from different antibodies.

4C5 and 3A1 clones

Two more antibodies had been screened in parallel with 8D6 as positive control: 3A1 that was recognizing both cut and uncut form of the tetrameric protein but not the monomer and 4C5 that was not recognizing any protein in the SDS-PAGE gel but was positive in ELISA screening, meaning that the antibody binds to the protein only in its native conformation.

The antibodies were produced in small scale, purified with protein A and digested with papain to get the Fab fragments (see M&M).

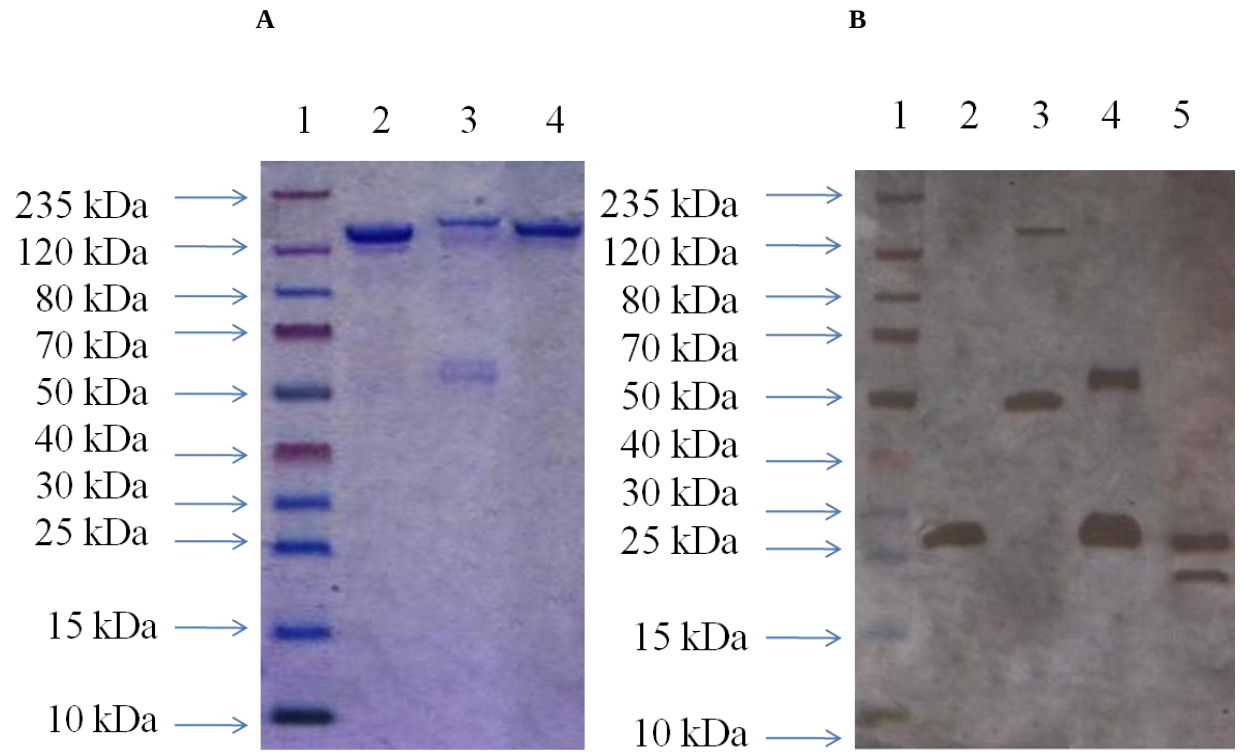

Fig. 1.23. Production and purification of Fabs of 8D6, 4C5 and 3A1 antibodies. A) Full Antibody purification with protein A-resin. Lane 1: marker 5 µl; lane 2: 10 µl of 8D6; lane 3: 10 µl of 4C5; lane 4: 10 µl of 3A1. B) Purification of Fabs in the flowthrough of the passage on protein A-resin after papain digestion. Lane 1: marker 5 µl; lane 2: 10 µl of 8D6 Fab + 10 mM DTT; lane 3: 10 µl of 4C5 Fab; lane 4: 10 µl of 4C5 Fab + 10 mM DTT; lane 5: 10 µl of 3A1 Fab + 10 mM DTT. Coomassie (A) and Silver (B) staining of SDS-PAGE 4-12% Bis-Tris (MES) gel.

From coomassie staining of the SDS-PAGE gel in figure 1.23 A we can see the 3 antibodies purified from the sera with protein A-resin. On the gel were loaded the elution fraction of the purification of the whole antibodies from the sera and after coomassie staining bands at 150 kDa molecular weight are detectable.

After digestion with papain and subsequent purification on protein A the samples were loaded on SDS-PAGE gel in figure 1.23 B. In lane 2 where 8D6 Fabs were loaded after DTT treatment, a single band at 25 kDa as expected is present. In lane 3 and 4 4C5 Fabs without and with DTT were loaded: the antibody was not completely digested and some whole antibody was not kept in the protein A-resin, in fact a band at 150 kDa is showed together with the not reduced Fabs; after DTT addition 2 bans are present in lane 4: a band at 75 kDa corresponding to half antibody because only the disulfide bond of the heavy chains has been reduced (see fig. 1.19) and a band at 25 kDa corresponding to the Fab fragments. In lane 5 where the sample with 3A1 Fabs with DTT addition,

can be seen 2 bands, one corresponding to the reduced Fab and another one at lower molecular weight unexplainable.

All the Fab fragments were used to make the complex with MA-1D Kcv protein in DDM detergent in 1:4 ratio and after the interaction all the samples were concentrated to 200 µl and loaded on a small Superdex 200 column of gel filtration (fig. 1.24).

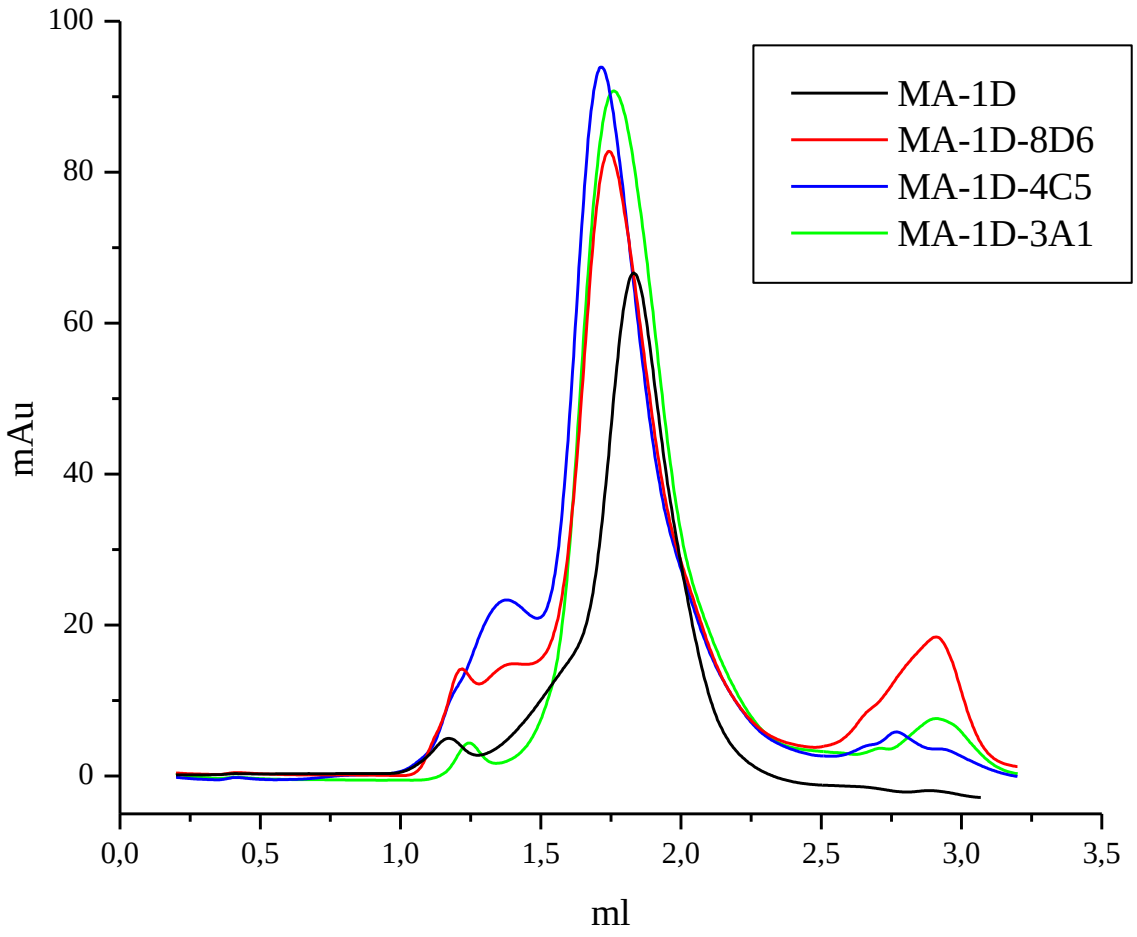

Fig. 1.24. Superimposition of the chromatograms of MA-1D Kcv (in black) and the complex with the Fab fragments of the antibodies. In red MA-1D Kcv-8D6, in blue MA-1D Kcv-4C5, in green MA-1D Kcv-3A1.

From the gel filtration in figure 1.24 all the curves of the interaction between protein and the Fab fragments of the 3 antibodies are superimposed to the curve of MA-1D Kcv alone. What can be seen is that all the 3 peaks of the interactions eluted at higher molecular weight than the protein itself and this could mean that there's the complex formation.

The MA-1D kcv-4C5 complex is the one with the peak more shifted toward higher molecular weight and that could be an indication that maybe, as hoped, there's more than one Fab fragment for each protein that could increase the protein-protein interaction for crystals formation.

This antibody was chosen for the scaling up for crystallization purpose.

Increase in protein yield: expression of other viral channels

In parallel with the strategies illustrated before other two approaches were adopted in order to increase the yield of purified protein in yeast for crystallization purpose:

- to modify the Kcv constructs by adding a maltose binding protein at the N terminus;
- to express other viral K^+ channels such as ATCV-1 and MT325 Kcv.

The expression of heterologous proteins fused to a maltose binding protein (MBP) is known to increase protein solubility [Kapust & Waugh, 1999] but also to increase the yield of protein production in *E. coli* because the juxtaposition of the ribosome binding site with the N terminus MBP domain of the fusion protein results in efficient translation initiation. It has also been observed that sometimes MBP protects its passenger proteins from proteolytic degradation in vivo. It is reported that MBP has been successfully used for expression of membrane protein for crystallization [Hilf & Dutzler, 2008]. Since recently it has been used also in yeast [Li et al., 2010], I decided to check if the presence of the MBP could increase the expression of the viral channels in *Pichia pastoris*.

The other strategy consists in expressing new viral K^+ channels. A number of different functional K^+ channels has been found in chlorella viruses. Kcv-like channels exist in 40 chlorella viruses infecting the same host, *Chlorella* NC64A [Kang et al., 2004], with differences in 16 aminoacids. These channels were classified in 7 groups that differ from each other from 4 to 12 aminoacids and they showed different properties including altered current kinetics and inhibition by cesium (see Introduction).

K^+ channels can be found also in other phycodnavirae like Ectocarpus siliculosus virus [Chen et al., 2005], which infects a marine filamentous brown alga, MT325, which infects *Chlorella* Pbi [Gazzarrini et al., 2006] and *Acanthocystis turfacea* Chlorella virus (ATCV-1), that infects a chlorella-like green alga, *Chlorella* SAG 3.83 [Fitzgerald et al., 2007; Gazzarrini et al., 2009].

Kesv will be discussed separately in chapter 3 because differently from the chlorella virus channels, it is targeted to the mitochondria.

Virus MT325 encodes a 95 aminoacids protein, named MT325 Kcv with 50% sequence identity to MA1D-Kcv. The difference with PBCV-1 Kcv is that it lacks 10 aminoacids at the N terminus and contains 10 aminoacids at the C terminus absent in the MA-1D Kcv [Gazzarrini et al., 2006].

Virus ATCV-1 encodes for a Kcv channel, ATCV-1 Kcv that is only 82 aminoacid long and compared with the other Kcv channels it has a shorter turret and no cytoplasmatic domains at all [Fitzgerald et al., 2007].

Yeast complementation assays and currents measured in oocyte with voltage clamp technique and with patch clamp method in cell attached configuration confirm that MA-1D and ATCV-1 Kcv form functional K^+ channels, selective for K^+ and blocked by conventional blockers (see Introduction; [Gazzarrini et al., 2009]).

Since I have previously demonstrated in my master degree thesis that it is also possible to express wild type channels in *Pichia pastoris* avoiding the creation of synthetic genes, I tested the expression of MT325 and ATCV-1 Kcv as wild type genes in parallel with the synthetic gene of PBCV-1 ant MA-1D Kcv.

1) Expression of Kcv channels with the 7His-MBP-H3C tag in *Pichia pastoris*

The synthetic genes MA-1D Kcv and PBCV-1 Kcv and the wild type genes of MT325 and ATCV-1 Kcv have been cloned in the vector for *Pichia pastoris* expression, pPIC3.5K, downstream of a tag including 7 histidines, the MBP and a recognition site for the Human rhinovirus 3C protease (see M&M, fig. M3).

After *Pichia* transformation the colonies were screened by colony PCR to check if they contained the gene (fig. 1.25)

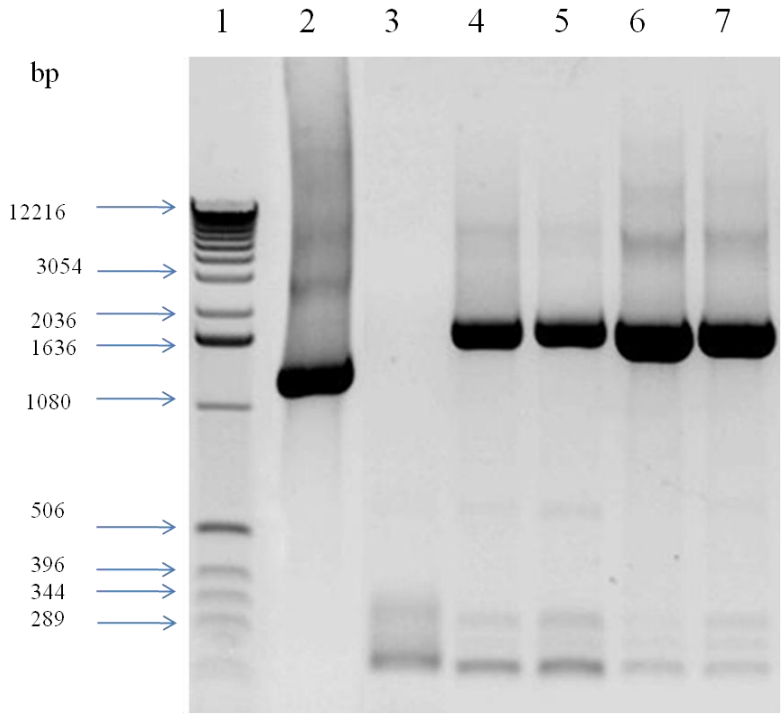

Fig. 1.25. Colony PCR of MA-1D, PBCV-1, MT325 and ATCV-1 Kcv + 7His-MBP-H3C tag. Lane 1: markers; lane 2: empty vector with MBP as control; lane 3: negative control (water); lane 4: sMA-1D Kcv; lane 5: sPBCV-1 Kcv; lane 6: ATCV-1; lane 7: MT-325. 1% agarose gel.

Figure 1.25 shows the agarose gel of the PCR products. Lane 2 and 3 are positive and negative controls, respectively. In lanes 4-7, where colony PCR products of the constructs were loaded, are visible 4 bands, one for each channel construct, at the correct molecular weight. The four positive colonies after DNA sequencing were grown in batch and protein expression was induced by methanol.

Proteins expression was checked on the purified microsomal fraction by western blot analysis with anti-polyHis monoclonal antibody but no or very little expression was found in two independent experiments, thus suggesting that MBP could not act to enhance the production of these channel proteins in *Pichia pastoris*.

2) Expression of wild type MT325 and ATCV-1 Kcv in pPIC3.5K with the 7His-H3C tag in *Pichia pastoris*

MT325 and ATCV-1 Kcv have been cloned in the vector for *Pichia pastoris* expression, pPIC3.5K with the LIC cloning system, fused at the N terminus with the 7His-H3C tag, the same used for MA-1D Kcv expression (see M&M, fig. M2).

The constructs have been confirmed by sequencing and were used to transform *Pichia pastoris*.

The colonies were checked by PCR and the positive ones were grown in batch and induced with methanol for expression of the proteins. Proteins expression was then checked on microsomes by western blot analysis by means of an anti-his tag antibody (fig. 1.26).

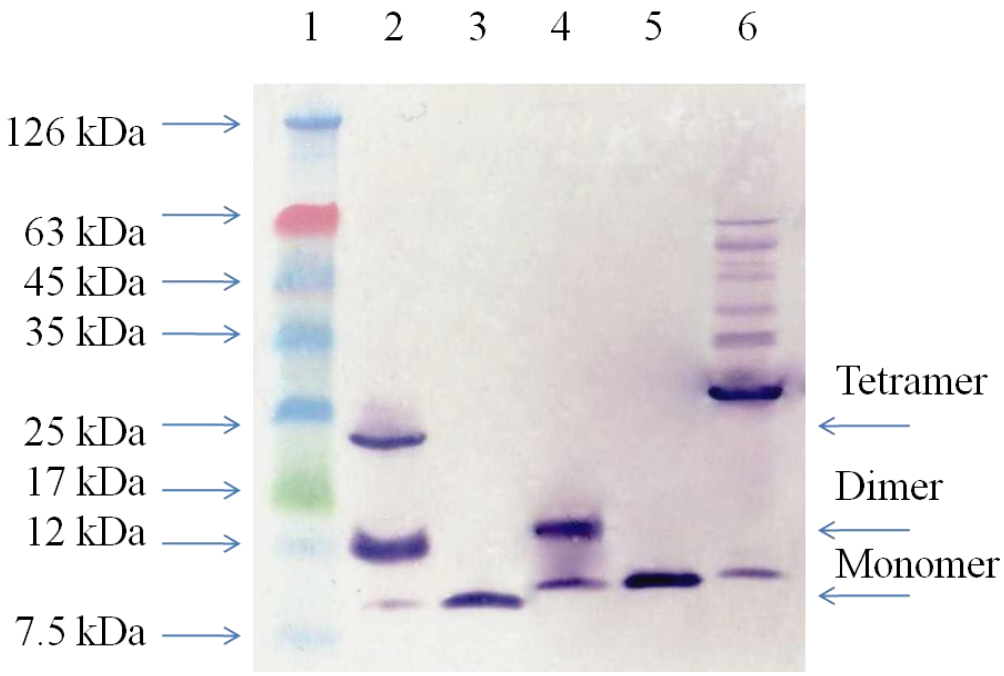

Fig. 1.26. Expression of ATCV-1 and MT325 Kcv. Lane 1: 5 µl of marker; lane 2: 15 µl of microsomes of ATCV-1 Kcv 7His-H3C; lane 3: same of 2 but boiled; lane 4: 15 µl of microsomes of MT-325 Kcv 7His-H3C; lane 5: same of 4 but boiled; lane 6: 1 µg of purified MA-1D Kcv 7His-H3C. Western blot by means of anti-his tag antibody.

Figure 1.26 shows in lane 2 and 3 unboiled and boiled microsomes expressing ATCV-1 Kcv, and in lane 4 and 5 unboiled and boiled microsomes expressing MT325 Kcv. Lane 6 shows, as a control, purified unboiled MA-1D Kcv. Both new channels are expressed and the boiled samples, 3 and 5,

show the monomer running at the expected molecular weight, with ATCV-1 Kcv being at the lowest weight. The unboiled samples, 2 and 4, show a prevalence of dimeric form for both channels, and in the case of ATCV1 only, also the presence of the tetramer. In order to see if it could be stabilize the tetrameric form also in MT325 Kcv, another electrophoretic run in the presence of barium ions was performed. Barium is a well known viral potassium channel blocker known to stabilize the tetrameric form of the protein in SDS page [Pagliuca et al., 2007; Chatelain, et al., 2009]. Figure 1.27 shows the result of an experiment in which microsomes of cells expressing MT325 Kcv were added with 1 mM $BaCl_2$. When tested by western blot after electrophoretic run on SDS-PAGE gel, we could observe the presence of the tetrameric form of the channel while very little dimeric and no monomeric forms were visible (lane 2). This result is quite important because the evidence that both new channels can be purified as tetramers and that the tetramers are rather stable form of these proteins, will prompt us to use the two new proteins in crystallization trials.

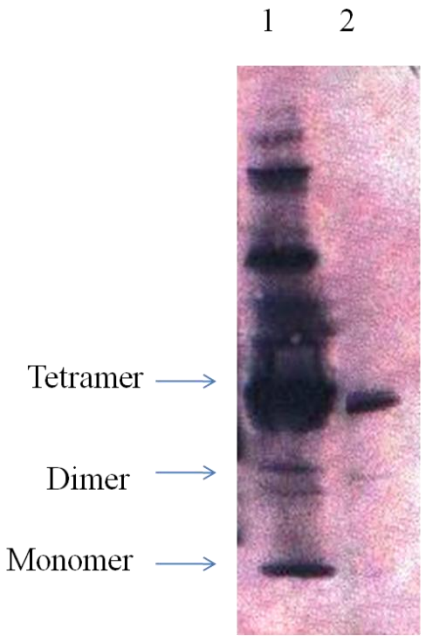

Fig. 1.27. MT325 Kcv in presence of barium. Lane 1: 1 µl microsomes of MA-1D Kcv from fermentation; lane 2: 5 µl of microsomes of MT-325 Kcv 7His-H3C. Western blot of the SDS-PAGE gel 4-12% Bis-Tris MES.

Discussion part 1

Crystallization of membrane proteins is still a demanding task since there are not standard methods for membrane protein production, purification and crystal formation. In the past years we have set the protocol for the expression of two small viral potassium channels (PBCV-1 and MA-1D Kcv) in the eukaryotic system *Pichia pastoris*. This procedure leads to purification of the protein in its tetrameric conformation that can be functionally reconstituted in planar lipid bilayer [Pagliuca et al., 2007]. Disadvantages of this procedure are:

- very lengthly, more than 15 days for fermentation and protein purification;
- low yield (10-15 mg of purified proteins from 800g of *Pichia* cells);
- half of the protein is lost due to aggregation during the last concentration step.

We could not change the expression system to improve the yield or speed up the production because *Pichia* had been selected as the best expression system, at the end of a long list of failure with other systems, among all, E. *coli*. So, in my PhD thesis, I decided to work to improve the quality and the quantity of protein obtained from *Pichia*, in order to get protein samples suitable for crystallization attempts.

One of the reasons of the low yield was that the protein was subjected to aggregation and sometimes more than half protein was lost. To avoid protein aggregation, I decided to work on the tag, anticipating that the 9His-EK tag at the N terminus could presumably cause aggregation.

For this purpose the protein was fused, at the N terminus, to a removable His tag for the purification that, differently from the previous one, could be cleaved from the purified proteins by means of a detergent resistant protease.

Surprisingly an improvement of protein purity and homogeneity was already achieved with the expression of the protein with this new tag. The amount of aggregate, detectable in gel filtration was really low compared to previous protein production. To further improve the purity of the protein, the tag was successfully removed with the H3C protease, and the protein was further purified to remove undigested forms (uncut or partially cut protein).

Despite the high monodispersity of the Kcv protein sample, the crystal-like structures obtained in some conditions, were not diffracting. After several attempts, we came to the conclusion that the propensity to form fragile and quite disordered crystals, displayed by this protein, could be related to a reduced number of inter–protein contacts. This is a very common feature of membrane proteins that are kept in solution by a surrounding shell of detergent.

To overcome this problem we decided to use antigen binding fragments of monoclonal antibodies as chaperons of crystallization [Ostermeier et al., 1995]. Monoclonal antibodies that recognized only the tetrameric form of the protein were selected on ELISA because the tetramer is the native and functional form of the protein that we want to crystallize and the same procedure had been successfully applied before to the crystallization of KcsA [Zhou et al., 2001]. The antibodies were screened also on SDS-PAGE gel and on ELISA and then screened again in our lab on SDS-PAGE gel. One of the 26 antibodies, positive both in ELISA and SDS-PAGE, 8D6 was used to make the complex with the channel for the crystallization but we did not obtain any crystal. Judging from the SDS-PAGE gel performed on the peaks isolated by gel filtration, the complex seems to show a 1:1 stoichiometry (1 Fab fragment for tetramer). This might not sufficient to increase the surface for protein-protein interaction during crystallization.

Since the antibodies that recognized the tetramer in SDS-PAGE gels can interact with a partially denatured protein, due to the presence of SDS, I decided to screen also those antibodies that were positive in ELISA but negative on SDS-PAGE gel. Probably these antibodies recognize the protein only in its native form and not when it is not perfectly folded, in presence of the denaturing agent.

The 4C5 antibody, negative in SDS-PAGE was used to make the complex with MA-1D Kcv protein and the gel filtration of this complex showed a peak that elutes at higher molecular weight compared to the 8D5 tested before. The explanation can be that maybe more than one Fab bind to the protein increasing its amphipathic surface and leading to a sample more suitable for crystal screenings.

This antibody has been produce in large scale and we are preparing complex with MA-1D Kcv for crystallization tests.

Another strategy that I have employed in order to improve the chances of getting crystals, is the expression in *Pichia pastoris* of other viral potassium channels. I focused on MT325 and ATCV-1 Kcv and on the mitochondrial viral potassium channel Kesv (discussed in part 3) because they are functional too, although Kesv was measured only as a chimera, and despite the homology they present also some differences at the structural level. An interesting side observation of this approach

has been that I have obtained expression by using the wild type genes. Expression of the wt PBCV-1 was tested before [Pagliuca et al., 2007] but without positive results. For this reason the synthetic gene with optimized *Pichia* codon usage had been designed. The success in my case can be due to the fact that I have changed the construct. In fact I have been substituting the expression vector and the tag. As reported in the literature [Tucker & Grisshammer, 1996] the tag in particular can influence protein expression increasing the expression level but also lowering or even abolishing it.

Another result is that MBP does not improve Kcv expression in *Pichia*. This was somehow expected, given the fact that MBP is a bacterial protein. Nevertheless there were reports in which MBP was improving the expression and stability of proteins in *Pichia* [Li et al., 2010]. But in this case, these were soluble proteins. In the case of membrane proteins an additional problem is that the protein has to be inserted in the membrane and the MBP at the N terminus could prevent this. The literature reports nevertheless some positive results [Hilf & Dutzler, 2008]. The difference is that in this case the expression of the pentameric receptor was obtained in *E. coli* and not in *Pichia*.

Therefore the two wt genes have been cloned without the MBP, with the same tag as MA-1D Kcv, and the expression in *Pichia* was successful. The production in the near future will be scaled up and crystallization screenings with these new proteins will be done.

Results and Discussion

Part 2.

Electrophysiological study of the barium block of Kcv channels in artificial planar lipid bilayer

State of the art: barium block of Kcv and its mutant

PBCV-1 Kcv is the prototype of a group of miniature potassium channels found in a in a number of viruses of the *phycodnaviridae* family [Kang et al., 2004]. Due to its minimal size (94 aa) PBCV-1 Kcv is an excellent model system to study ion channels structure-function relationship. An interesting property that can be analyzed, important for its pharmacological application, is the study of the channels blockers. Screening for mutant channels resistant to blockers can lead to identify aminoacids involved into the mechanism of block [Chatelain et al., 2005]. To this purpose we have adapted a yeast-based screening method established by Prof. Daniel Minor [Minor et al, 1999]. The method was applied to Kcv to study the block by barium and amantadine. A library of Kcv mutant was built by mutagenic PCR and it was screened by complementation assays in yeast. This procedure led to the identification of a single point mutation, T63S, conferring barium-resistant growth to the transformed yeast [Chatelain et al., 2009].
The mutation involved in the control of barium affects the threonine 63 that is part of the highly conserved selectivity filter and it is involved, with its lateral chain, in ion coordination as showed before also for KcsA [Zhou & Mackinnon, 2004].

Electrophysiological studies in *Xenopus laevis* oocytes with voltage clamp revealed that the T63S mutant of Kcv has a K_D for barium that is 0.81 mM, 100 times higher than that of the wild type channel (8.8 μM). Introducing this mutation in another potassium channel, the human potassium inward rectifier Kir2.1 (mutation T142S), resulted too in a decrease in barium sensitivity, of about 5 times ($K_{D\ wt}$ = 6.5 μM, $K_{D\ mut}$ = 35.6 μM). This can be due to the fact that the selectivity filters of the two channels are not identical, in fact the residue upstream of the mutated threonine (position 62 in Kcv and 141 in Kir), is a threonine in Kir2.1 and a serine in Kcv. The introduction of a threonine in position 62, reduces the effect of the mutation T63S in barium sensitivity. This study pointed out a negative coupling between the positions with respect to barium binding.

Aim of part 2

The aim of this part of my PhD thesis has been to perform a single channel study of the Kcv mutants T63S and S62T-T63S. To this purpose I was producing small amounts of recombinant proteins expressed and purified from *Pichia pastoris*. The protein channels were in turn reconstituted in proteoliposomes and incorporated in artificial planar lipid bilayer for single channel measurement.

Results

Characterization of PBCV-1 Kcv and its mutants T63S and S63T-T63S in planar lipid bilayer

The PBCV-1 Kcv protein and the mutants, obtained by point mutation of the wt genes, were expressed in the yeast *Pichia pastoris*, extracted from the membranes and purified in the presence of DDM detergent (see M&M). Therefore the three proteins were reconstituted into liposomes of L-α-phosphatidilcholine and added to the bilayer in the trans chamber in symmetrical 500 mM KCl solution. Fluctuations at different voltages, in steps of 10 mV, were recorded after the addition of the protein, between +/- 80 mV (measurements done by Dr. Henkel).

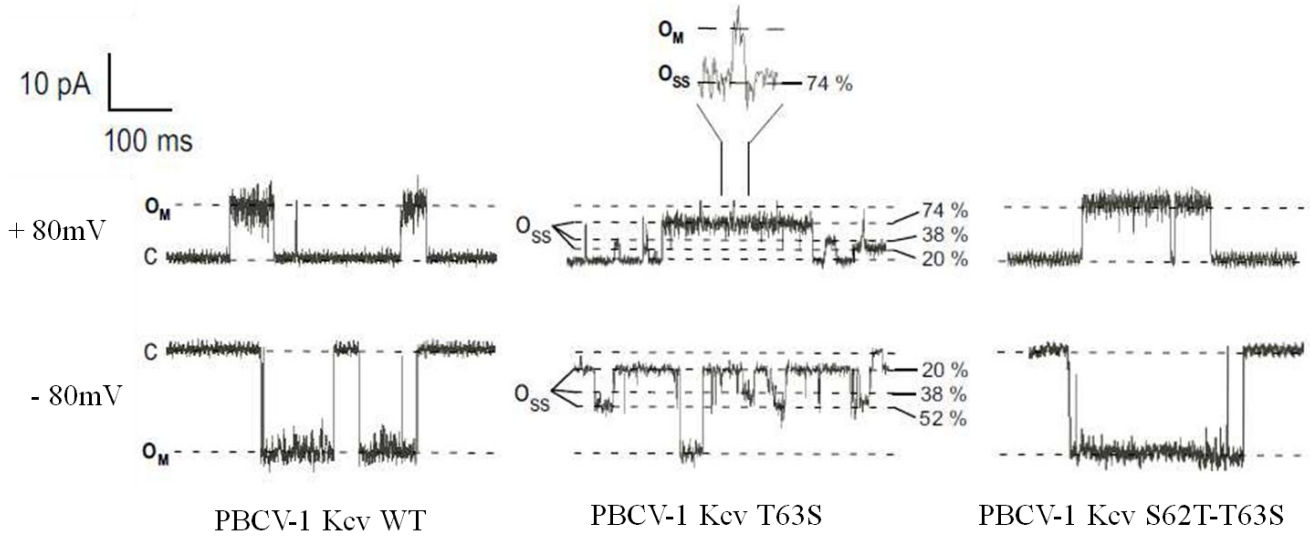

Fig. 2.1. Exemplary currents registered at +/-80 mV of PBCV-1 Kcv wt, PBCV-1 Kcv T63S and S62T-T63S. Open substates (O_{SS}), that are percentage of maximum opening (O_M), are highlighted for PBCV-1 Kcv T63S.

Figure 2.1 shows exemplary traces recorded at +80 and –80 mV from the three channels. PBCV-1 Kcv signal displays at both voltages typical transitions between a closed state and an open state. Similar unitary current fluctuations with the same conductance were also described in previous studies with wt Kcv [Pagliuca et al., 2007].

The mutant S62T/T63S shows too a typical unitary current fluctuations between a closed and open state nearly identical to the wt current. The single mutant T63S shows instead a different behavior, in fact, together with transitions between a closed state and a maximal open state, conductance substates are also present. Another feature of the T63S channels is the obvious strong increase of the overall open probability (p_o), the probability that the channel leaves the closed state to any other conductance state, when compared to the wt or to the double mutant channels.

The mean currents of the maximal opening from several experiments of the three channels were plotted against the voltage in an I/V curve relationship (fig. 2.2).

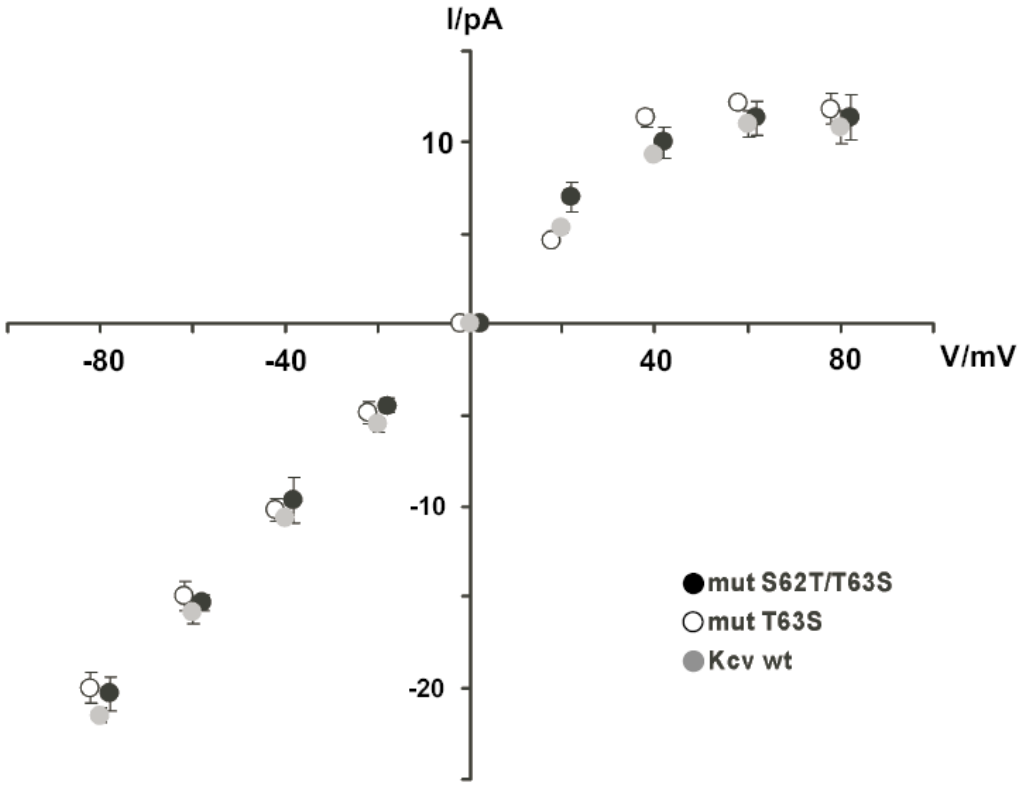

Fig. 2.2. I/V curve of the maximal single channel conductances of PBCV-1 Kcv wt (grey dots) and the mutants T63S (white dots) and S62T-T63S (black dots). Data are mean of 5 experiments in 500 mM KCl symmetrical solution. The calculated conductance is 250 pS.

The currents of the three channels give a very similar behavior. The plot is linear from +40 to –80 mV and after +40 mV there's a negative slope. This is in agreement with what shown in Figure 2.1, where the current recorded at +80 mV is clearly smaller than the current recorded at the negative voltage, -80 mV, although the reversal potential of the current is zero (symmetric K^+ conditions).

These results are again similar to those showed in a previous work on PBCV-1 Kcv wt [Pagliuca et al., 2007]. The conductance calculated in the linear range is 250 pS for all the three channels.

These experiments demonstrate that the mutation has no influence on the maximal conductance but only on the frequency of the achievement of this level by T63S mutant.

Analysis of the subconductance levels in the T63S mutant

Before analyzing the effect of barium, the presence of substates will be discussed comparing the wt to the T63S mutant. These subconductance levels can be rarely observed also in the wt [Pagliuca et al., 2007] but they are a prevalent feature of the T63S mutant but not of the double mutant. To analyze the differences between the two channels a mean/standard deviation plot was done by Dr. Schroeder with the standard deviation of 20 data points (recorded at +80 mV, symmetrical 500 mM KCl) plotted as a function of the average of the same data points (fig. 2.3).

In this graph, the x-coordinate represents the current level and lines can be interpreted as transitions between different states; the more lines between two states are present, the higher is the corresponding transition probability.

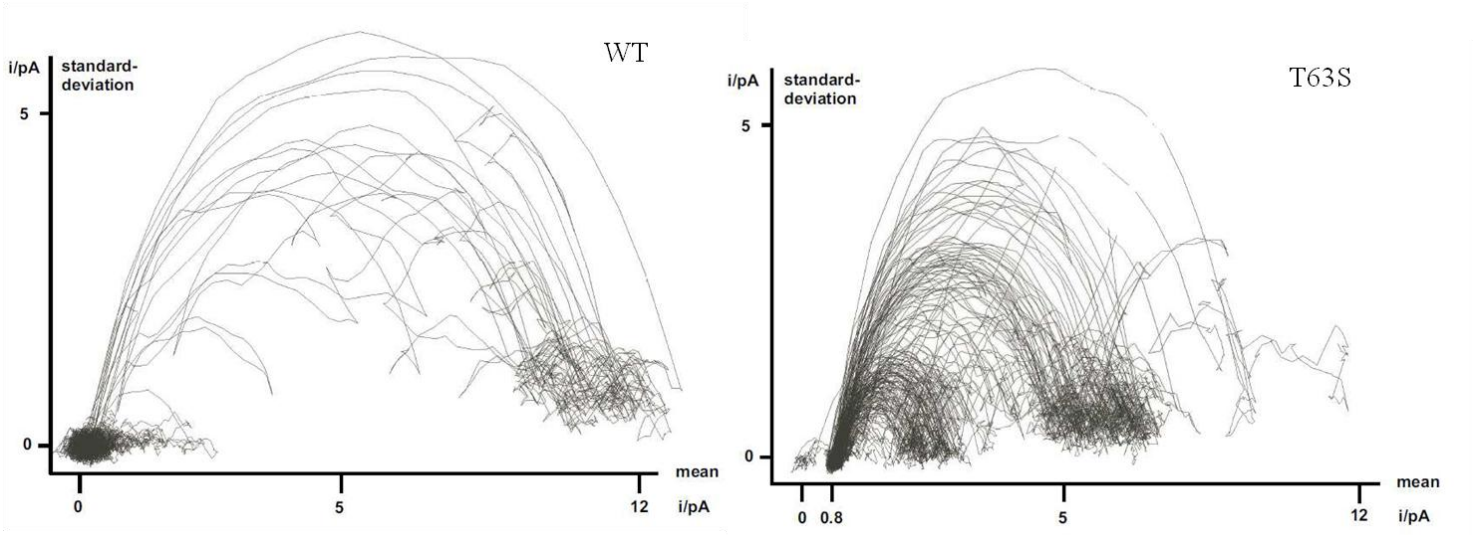

Fig. 2.3. Mean/standard deviation plots of PBCV-1 Kcv wt and PBCV-1 Kcv T63S. Lines represent transitions between states.

In the case of the wt PBCV-1 Kcv mainly transitions between the closed (0 pA) and the maximal open state (12 pA) can be observed. In contrast the mean variance plot of T63S-Kcv is less defined, and reflects the rare attendance of the closed and maximal open state. In addition to the maximal open state, some other open states can be noticed. A small substate (0.8 pA corresponding to 10 pS), occurs to be the predominant conductance level. Most transitions start from or end at this state.

Effect of Barium

The addition of barium to both chambers had immediately effect on wt and S62T-T63S currents, while the current of the single mutant T63S didn't seem to be affected (fig. 2.4).

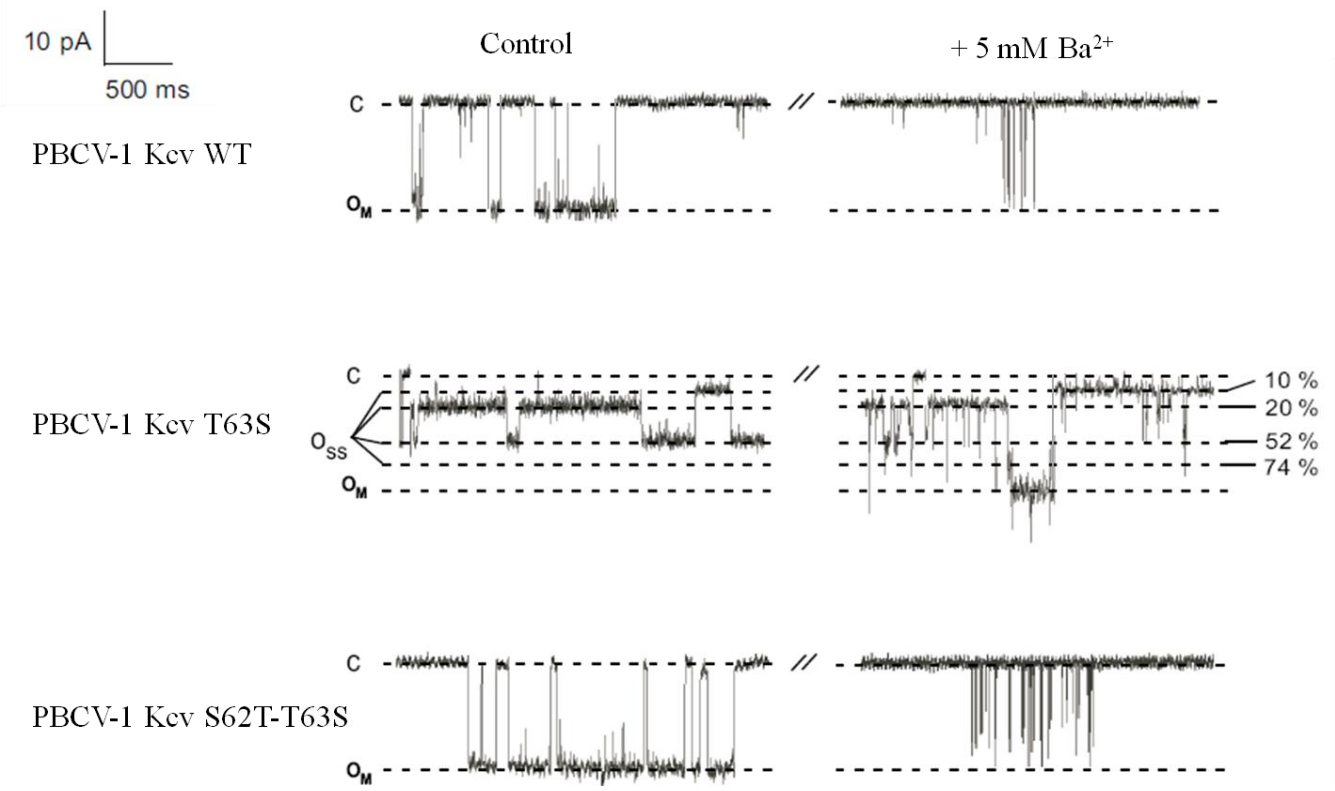

Fig. 2.4. Exemplary currents registered at +/-80 mV of PBCV-1 Kcv wt, PBCV-1 Kcv T63S and S62T-T63S without (control) and with 5 mM $BaCl_2$.

As showed in the measurements in figure 2.4 the addition of the blocker doesn't have an influence on the amplitude of the current but affects strongly the open probability of the wild type and the double mutant channels. This can be better described as a reduction of the open dwell time, the time a single channel remains in the fully open state. Such a reduction in the dwell time generating very short openings or "spikes" was already reported for the wt in previous studies [Pagliuca et al., 2007]. An increase in resolution of the spikes shows that they are channel fluctuation with a full conductance despite the short time of opening (fig. 2.5).

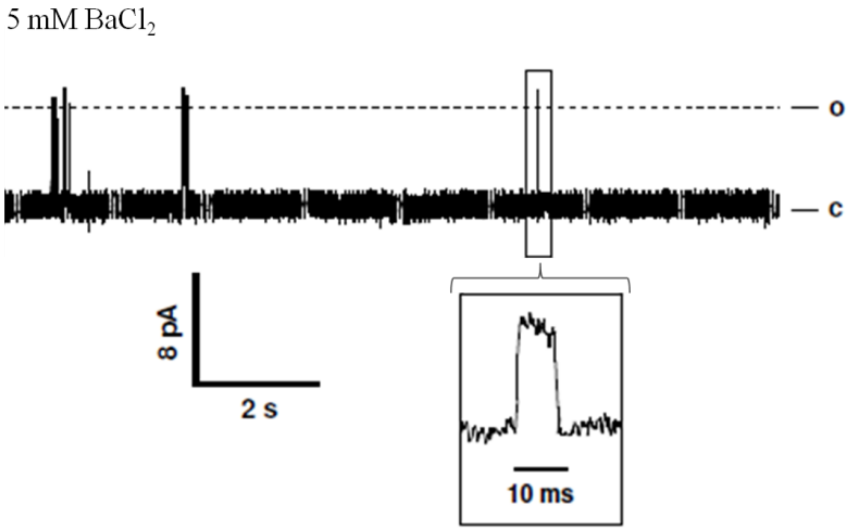

Fig. 2.5. Detailed view of a spike of S62T-T63S Kcv in presence of 5 mM barium. The enlargement shows that the spike is an opening event.

A property of the barium block that was also analyzed is the reversibility of the effect. Since in our recording system it was not possible to exchange the solution, in order to remove barium I have added 10 mM $NaSO_4$ that induces the precipitation of Ba^{2+} ions in the form of $Ba(SO_4)_2$. Figure 2.6 shows the recovery of the full open probability after the addition of the precipitant in both chambers.

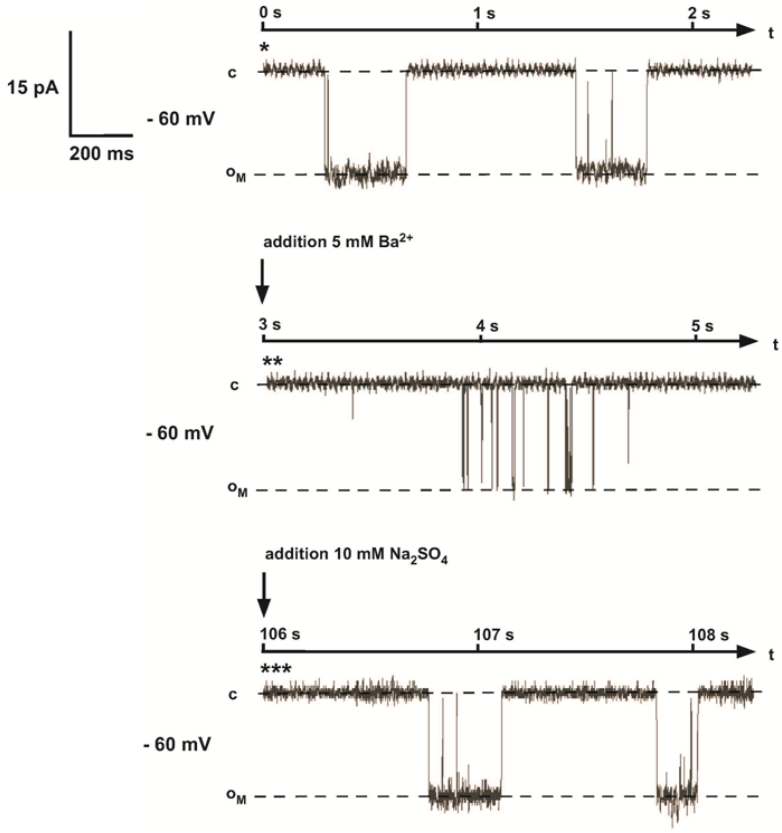

Fig. 2.6. Reversibility of barium block in PBCV-1 Kcv wt by addition of $NaSO_4$ recorded at -60 mV. In the first lane there's a recording before the addition of the blocker. In the second lane barium is added and a reduction in op can be noticed. In the third lane, after addition of the precipitant, op is recovered. The same effect was observed also at positive potentials (data not shown).

Since barium influences the open probability, to analyze differences between PBCV-1 Kcv wt and the two mutants, T63S and S62T-T63S, the open probabilities in absence and presence of $BaCl_2$ were calculated. Due to the high number of substates of PBCV-1 Kcv T63S, just the overall-open probability (p_o*) and the probability to achieve the maximum conductance level (p_o^M) were discriminated and not the p_o for each single conductance level.

Histograms of amplitudes for each time series were created and fitted with multiple Gauss-functions. Afterwards, the open probabilities were expressed as ratios of the corresponding integrals. Figure 2.7 shows open probabilities of the maximal open states as a function of voltage for PBCV-1 Kcv wt, PBCV-1 Kcv T63S and S62T/T63S in absence and presence of Ba^{2+}.

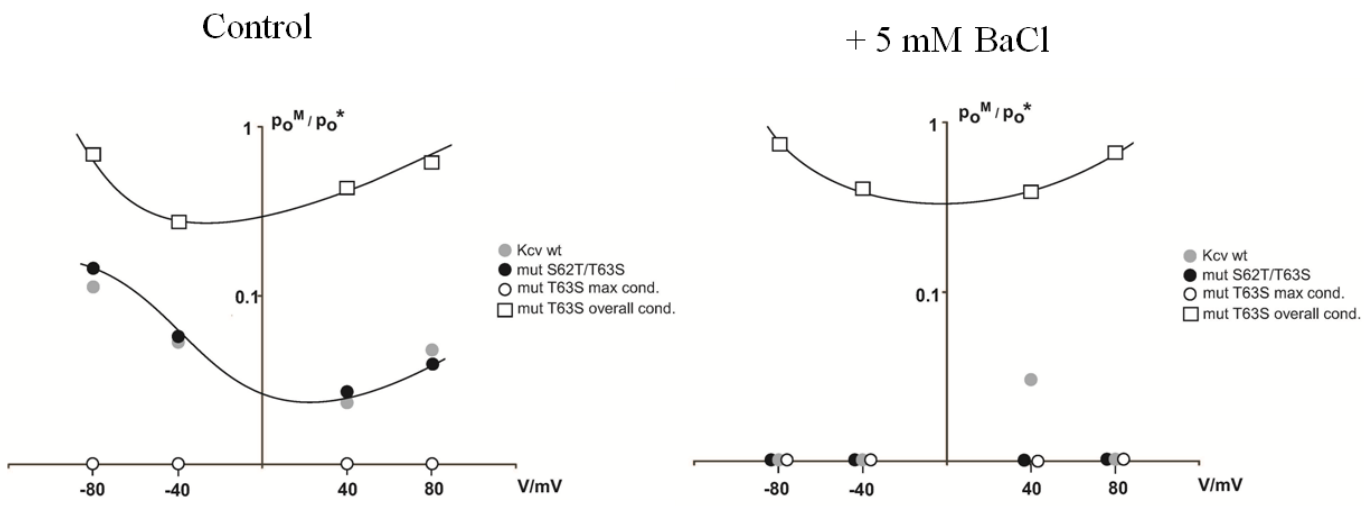

Fig. 2.7. Open probabilities as functions of voltage for PBCV-1 Kcv wt (grey dots), T63S (white dots and squares) and S62T/T63S (black dots) before and after adding $BaCl_2$. For T63S white circles represents the probability for the maximal conductance and the white squares mark the probability for the overall conductance. This overall conductance includes the occurrence of all states apart from the closed state.

In the case of T63S only, the overall open probability is also plotted.
For the wt and the double mutant the p_o^* and the p_o^M are nearly the same, because when these channels open, they usually adopt the maximum open state and substates really rarely occur. Therefore, for these two channels, we did not plot the overall po.

In the absence of $BaCl_2$, the overall open probability (po*) for T63S is at +80mV is about 15-fold higher than the open probability for the wt and S62T/T63S (0.9 for the T63S mutant and 0.04 for the wt and the double mutant).

On the contrary, its open probability for the maximal conductance level is dramatically lower than those of the wt and the double mutant. Because of the rare appearance and the very short dwell times of the maximum open state of PBCV-1 Kcv T63S, it was not possible to achieve a statistically robust value; but it is clear that the value is at least a factor of 50 smaller than the corresponding values of the two other proteins.

In presence of Ba^{2+}, the open probabilities of the wt and the S62T/T63S mutant also fall below this detection limit and the analysis does not allow to discriminate between them. The overall-open probability p_o^* of T63S seems to be unaffected by Ba^{2+}.

Mutation T63S like in other potassium channels

As mentioned before the threonine residue in position 63 is one of the most conserved in the selectivity filter of potassium channels. The same mutation T → S introduced in the mammalian inward rectifier Kir2.1 (T142S) also produced a barium resistant behavior, similar to what observed in PBCV-1 Kcv [Chatelain et al., 2009].

For this reason it was decided to analyze the mutation also in other channels and the first choice was the Kcv-like channel MA-1D Kcv that differs from PBCV-1 Kcv for only 5 aminoacids but nevertheless shows quite different electrophysiological properties [Gazzarrini et al., 2004].

Characterization of MA-1D Kcv and its mutant T63S in planar lipid bilayer

First of all I performed a characterization of the wt channel, since this protein had not been previously studied in planar lipid bilayer. The protein was produce in *Pichia pastoris* and solubilized in DDM (dodecyl-β-d-maltoside). The detergent was exchanged during gel filtration with L-Dao (N,N-Dimethyldodecylamine-N-oxide), a zwitterionic detergent that was more suitable for protein integration in the bilayer, and it was possible to directly insert the protein in the lipids of the bilayer without passing through the proteoliposomes formation step.

The experiments were done in 500 mM KCl symmetric solution in both bilayer chambers. Fluctuations at different voltages, in steps of 10 mV, were recorded after the addition of the protein between +120/-160 mV (fig. 2.8)

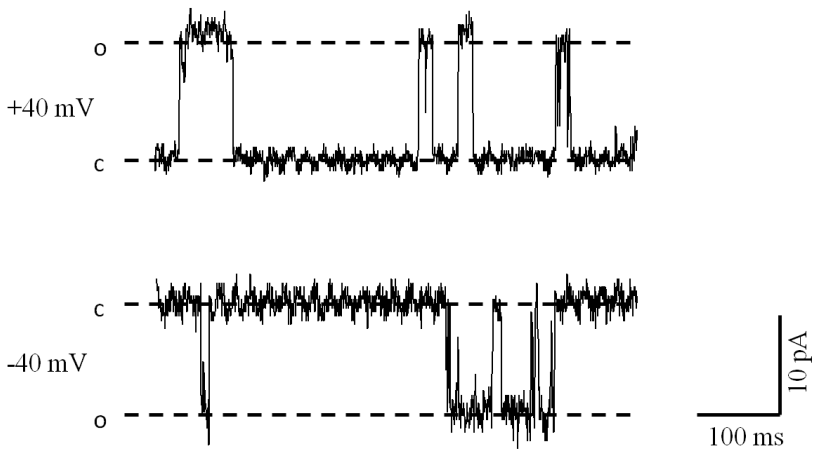

Fig. 2.8. Exemplary currents registered at +/-40 mV of MA-1D Kcv in 500 mM symmetric solution. O indicates open state, C the closed state.

The mean currents from several experiments were plotted against the voltage in an I/V curve relationship (fig. 2.9).

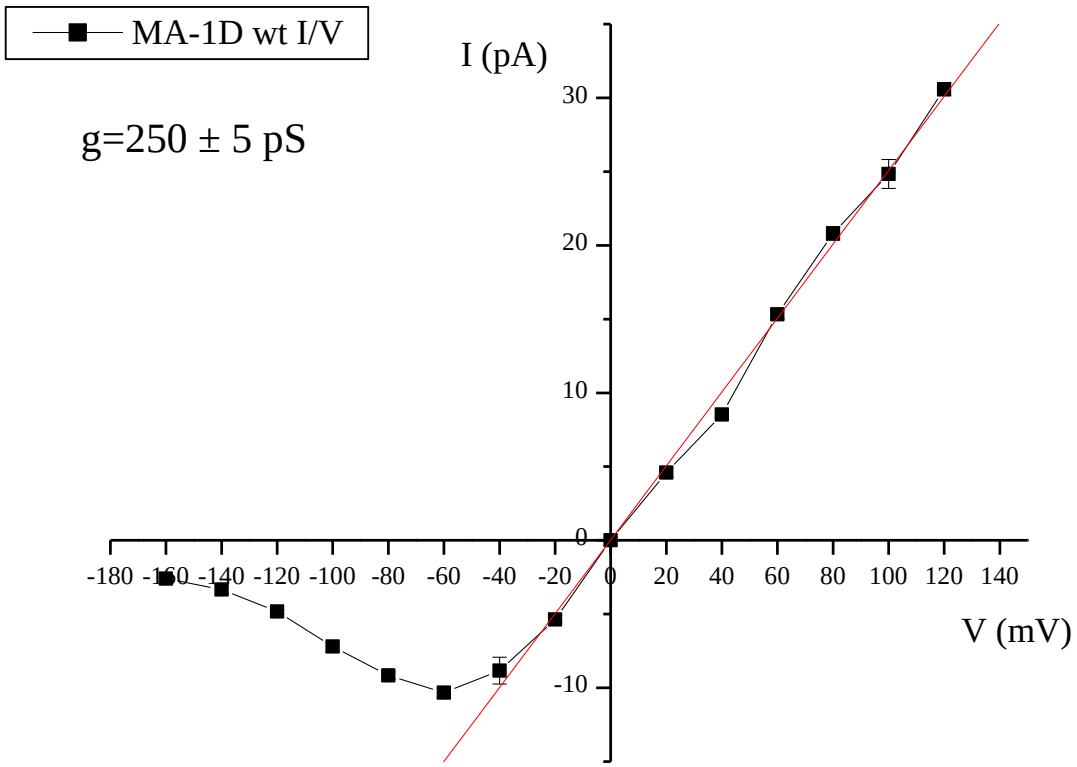

Fig. 2.9. I/V curve of the maximal single channel conductance of MA-1D Kcv wt. Data are mean of experiments in 500 mM KCl symmetrical solution. The calculated conductance g is 250 pS and is the result of the linear fitting indicated in red.

The plot of the I/V curve is linear from +140 to –20 mV, while at more negative potentials the relationship is not linear and a negative slope can be measured..

This I/V relation closely resembles that one of the MA-1D Kcv macrocurrents recorded in oocytes [Gazzarrini et al., 2004].

The effect of the barium has again as in PBCV-1 Kcv the effect to influence the open probability of the channel that decreases in the presence of the $BaCl_2$ (fig. 2.10)

I have tested the effect of 1 mM barium on the MA-1D Kcv current. Figure 2.10 shows a representative current recording obtained at +/-40 mV after the addition of barium to both chambers.

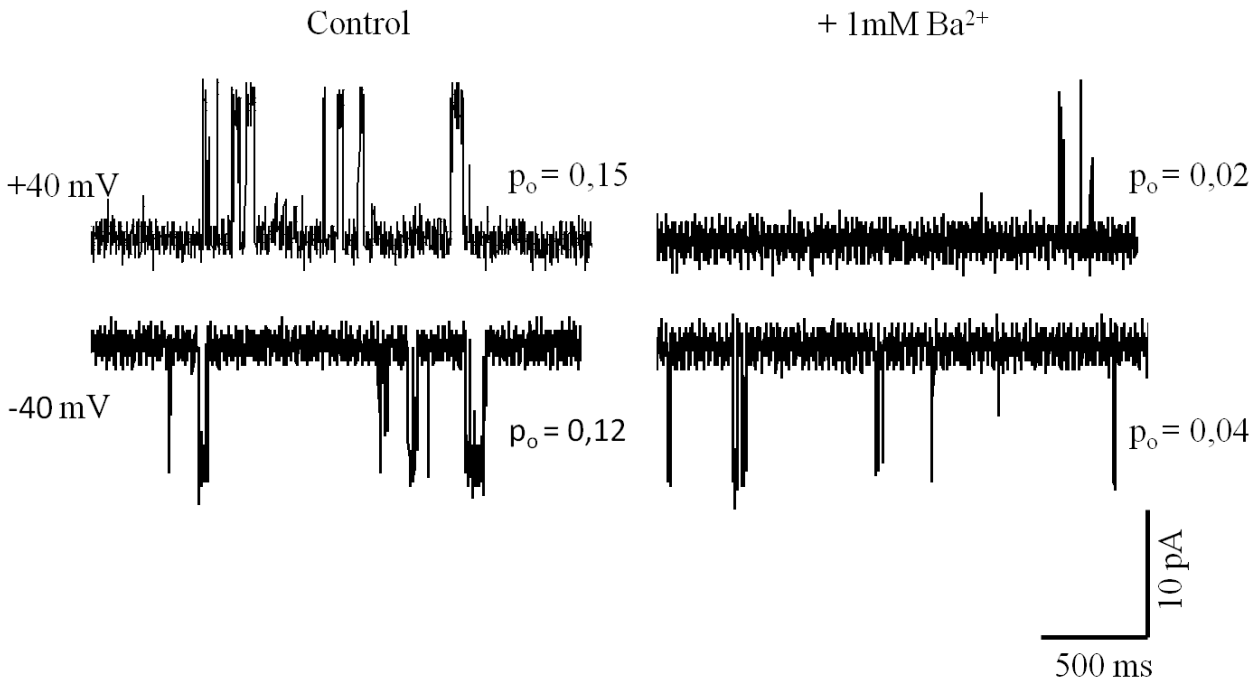

Fig. 2.10. Exemplary currents registered at +/-40 mV of MA-1D Kcv wt, without (control) and with 1 mM $BaCl_2$. The indicated p_o values were obtained by longer time series.

Similarly to what already demonstrated for PBCV-1 Kcv, addition of 1 mM $BaCl_2$ to MA-1D Kcv strongly decreases the p_o (as indicated by the values reported on the figure 2.10), while the current level seems not to be affected.

To further confirm this observation I have tested several other concentrations of barium from 10 µM to 20 mM and, as for PBCV-1 Kcv, what is evident is that the block has no influence on the conductance of the channel. In fact, as can be seen by the I/V curves plotted together (fig. 2.11) where the I/V curve of the wt channel measured in control solution without barium is superimposed to the I/V curves obtained with the measurement of the protein after addition of the blocker, the six curves perfectly match confirming that there's no difference in the maximal conductances.

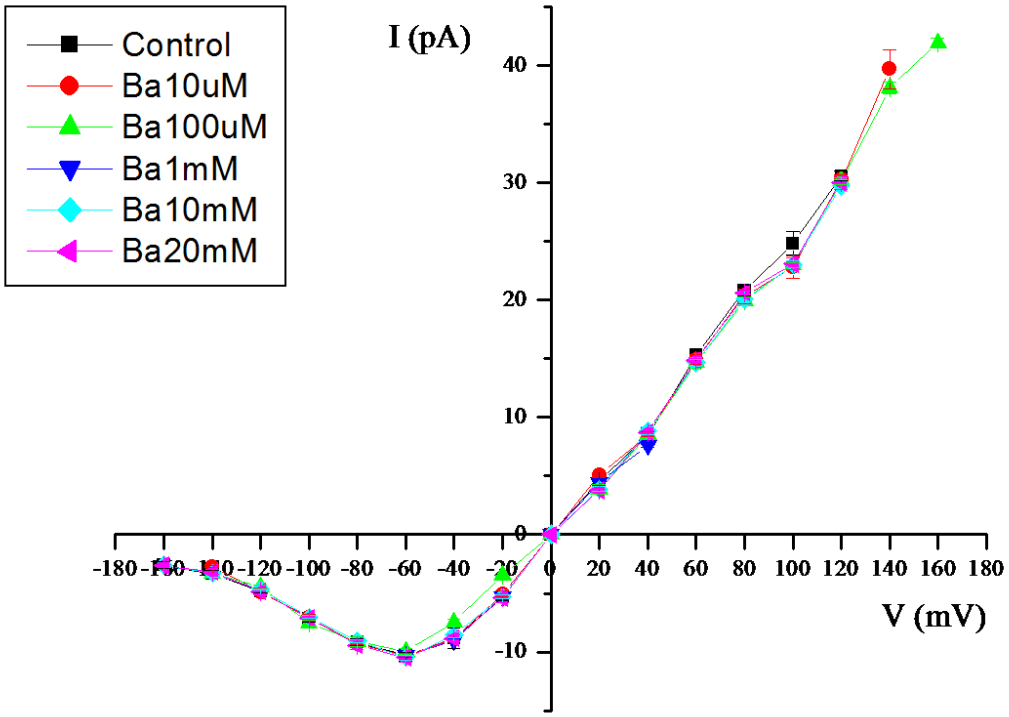

Fig. 2.11. I/V curve of the maximal single channel conductance of MA-1D Kcv wt in presence of different concentrations of $BaCl_2$. Data are means of experiments in 500 mM KCl symmetrical solution.

The mutation T63S was introduced in the gene of MA-1D Kcv and the protein was produced and purified in the presence of L-DAO detergent, as reported for the wt.

Preliminary analysis of the fluctuations (fig. 2.12) showed that the channel is functional and that it has a behavior similar but not identical to the T63S mutant of PBCV-1 Kcv. Similarly to PBCV-1 Kcv mutant, it shows substates that are not observed in wt channel, but differently from PBCV-1 mutant, there's only one prevailing substate.

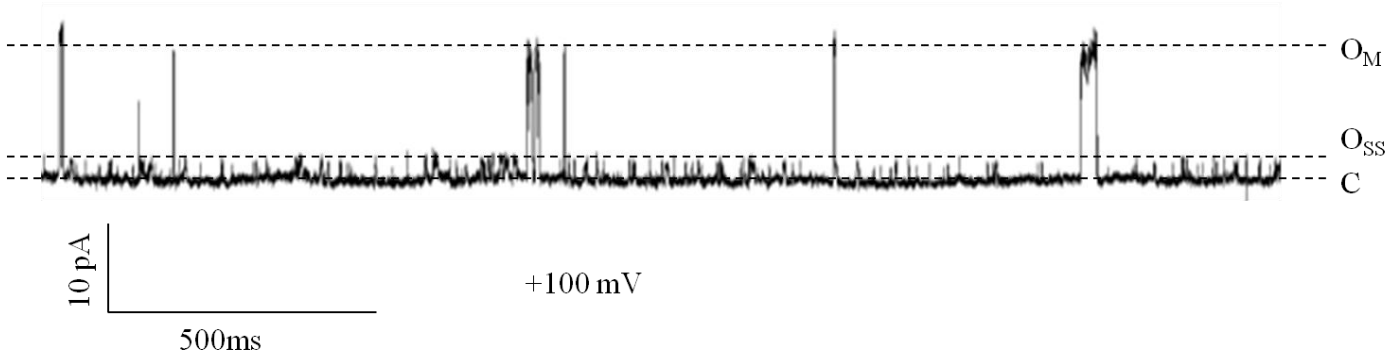

Fig. 2.12. Exemplary current registered at +100 mV of MA-1D Kcv T63S. O_{SS} indicates the level of substates and O_M the maximal opening.

The open probabilities of the maximal conductance level and the substate have been plotted towards the voltage, and a high voltage dependency of the open probability of the subconductance level is showed.

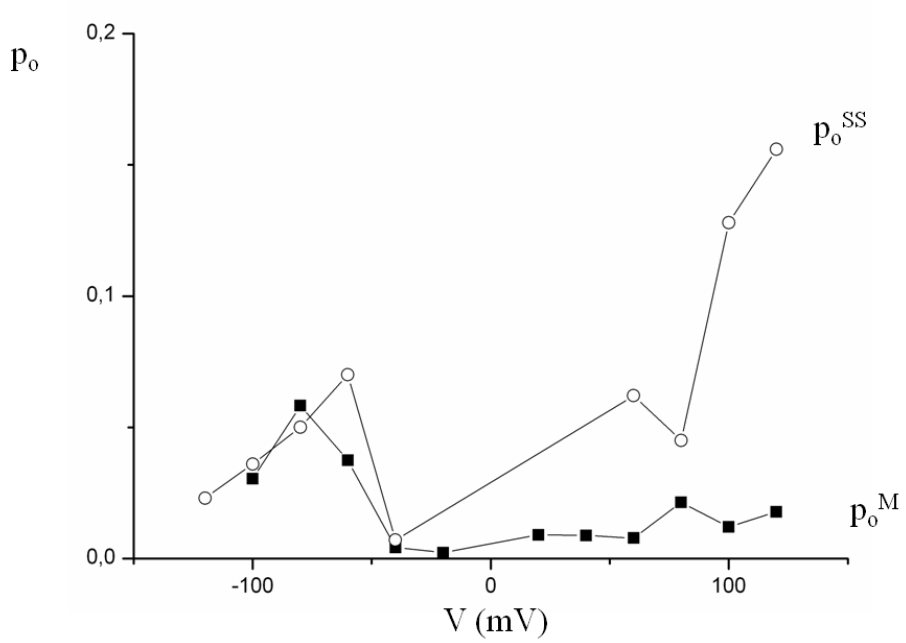

Fig. 2.13. Open probabilities as functions of voltage for MA-1D Kcv T63S. Black squares indicate the open probability for the maximal conductance and white circles represents the probability for the subconductance levels (Graph done by Dr. Braun).

As can be seen in figure 2.12 the mutant channel also reaches the maximal conductance levels from which the I/V curve in figure 2.14 is obtained.

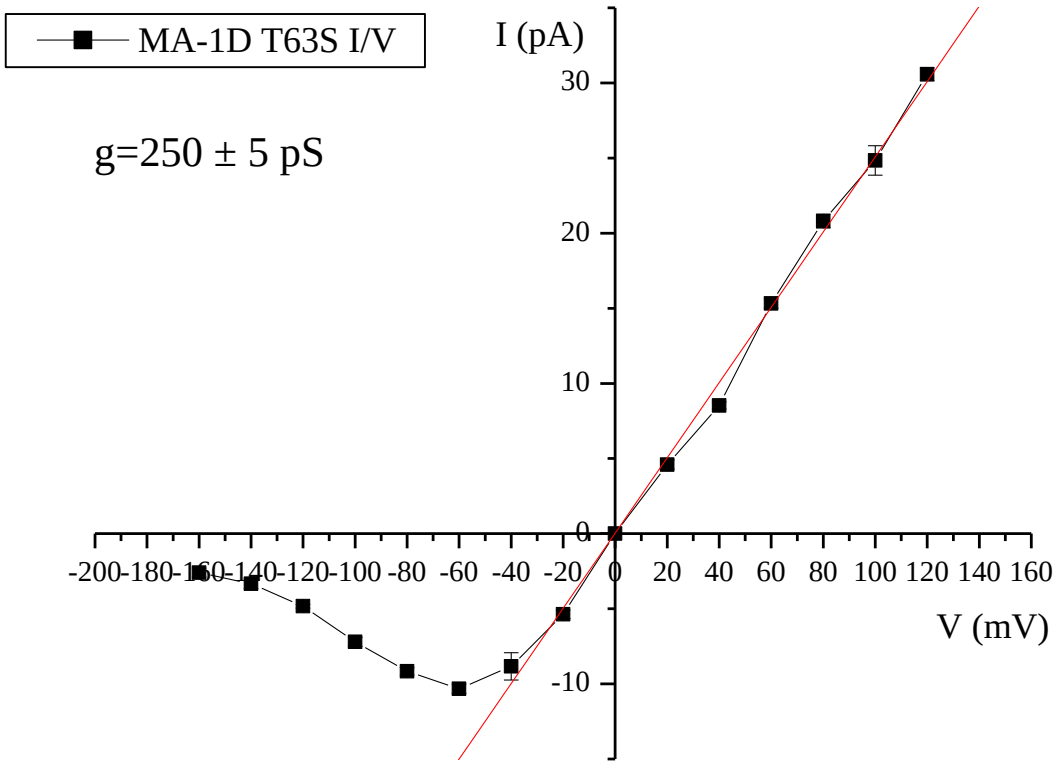

Fig. 2.14. I/V curve of the maximal single channel conductance of MA-1D Kcv T63S. Data are mean of experiments in 500 mM KCl symmetrical solution.

The curve has the same shape of the wt one, displaying a negative slope conductance for potentials more negative than -60 mV.

The effect of barium has to be analyzed yet.

Discussion part 2

In this part of my PhD thesis I have studied the barium block in Kcv at the single channel level. Previous analysis of the macrocurrents showed that PBCV-1 Kcv is blocked by Ba^{2+} ions, and that the mutant T63S is insensitive to the blocker [Chatelain et al., 2009]. We had previously attempted to measure the single channel of T63S mutant directly from *Xenopus* oocytes. Even though we could easily measure the wt single channel, it was impossible to detect single channel fluctuations from oocytes injected with the T63S mutant. It seemed as if the channel was always open. Reconsidering these results at the light of the extremely high open probability that characterizes this mutant in lipid bilayer, it seems plausible that we were indeed looking at the same phenomenon. Since the T63S mutant was first selected for its insensitivity to barium block, I will first discuss this feature.

First evidence emerging from the analysis of the wt channel in the presence of barium is that it is blocked but barium has no influence on the value of conductance, but decreases the probability of the channel to open both as number and length of opening events. The single mutant T63S by the contrary is insensitive to barium, because its open probability is not affected by the blocker, or maybe the reduction is so small that it is not possible to detect it in the bilayer system. Finally, the double mutant re-establishes the behavior of the wt, since its open probability sensitively decreases.

This experiments confirm the importance of the mutation T63S and its involvement in the barium block mechanism. From structural studies based on the homology of Kcv with the crystal structure of KirBac1.1 we can assume that the position 63 corresponds to the 4^{th} binding site for K^+ in the selectivity filter, which is also the binding site for Ba^{2+} [Jiang & MacKinnon, 2000]. Mutations in this position alter the affinity for barium and therefore the block of the currents. In the wt channel the barium, which has a high affinity, interacts with the 4^{th} site and closes the channel, while in the mutant the affinity is so low that there are no closure of the channel. The higher affinity of the wt for Ba^{2+} compared to the T63S mutant is consistent with other experimental data on stability in SDS-PAGE gel in presence of these ions, that for the mutant should be in higher concentration to keep the tetramer stable [Chatelain et al., 2009]. The only difference between the wt and the mutant T63S is the additional methyl group of the threonine that is supposed to be involved in the affinity mechanism, idea supported by the fact the re-introduction of a methyl group in position 62, where a serine is present, makes the K_d decrease of 10 times and recover the wt behavior in lipid bilayer. So probably the barium block is due to a steric modulation of the 4^{th} site of the selectivity filter.

An interesting information that came out from these experiments is that the mutation does not influence only the barium block but also the gating behavior of the mutant channel that presents

several substates. As previously mentioned, T63 contributes to form the 4th binding site for potassium ions and coordinates K^+ ions during their transition through the selectivity filter. Due to this mutation, not only the affinity for barium but also for K^+ ions is reduced (Arrigoni, personal communication). The dramatic change in open probability introduced by the T63 mutation, is important because it connects permeability and gating within the filter of K^+ channels.
Assuming that the selectivity filter contributes to gating [Cordero-Morales et al., 2006; Abenavoli et al., 2009], the shift from high to low affinity has an influence on this channel property. If the site responsible of the affinity is altered the stability of the filter is affected and results in increase in open probability. This can be explained according to the model proposed by VanDongen [VanDongen, 2004] in which gating is described as the transition of the binding sites between a high and a low affinity state. This model therefore links permeability to gating and, according to our results, this can be extended to the behavior observed in Kcv too.

These data are consistent with recent experiments on KcsA and mutants that also shown the coupling of selectivity filter and gating [Cordero-Morales et al., 2006] and confirm the role of the selectivity filter in channel gating.

It is worth noting that introducing the same mutation in other Kcv-like channels, was producing the same effects on barium block, appearance of substates and increased open probability.

Results and Discussion

Part 3.

Kesv, a mitochondrial potassium channel: expression and electrophysiological characterization

Aim of part 3

In order to study different channels for crystallization, Kesv seemed to be an interesting candidate. The ORF, coding for a 124 amino acids protein, was found in the genome of *Ectocarpus siliculosus* virus-1 (EsV-1) [Chen et al., 2005], infecting a filamentous marine brown alga [Van Etten et al., 2002] (see Introduction).

Kesv is 29% homologue to PBCV-1 Kcv but presents. GYG instead of GFG in its signature sequence in the selectivity filter (as most prokaryotic or eukaryotic potassium channels).

Despite their similarity, Kcv and Kesv in heterologous expression systems are sorted to different cellular compartments: Kcv reaches the plasma membrane, while Kesv is sorted to the mitochondria [Balss et al., 2008]. Although some measurement of Kesv activity in *Xenopus* oocytes have been published [Chen et al., 2005], in our lab we were not able to express the protein in oocyte or HEK239 cells. This is consistent with the fact that intracellular localization of Kesv is not in the plasma membranes and so it has been argued that the published data are endogenous currents from the oocytes and not related to Kesv activity [Balss et al., 2008]. This interpretation is also confirmed by yeast complementation of mutants lacking the K^+ endogenous uptake systems [Balss et al., 2008].

Because of the mitochondrial sorting and the similarity to the Kcv channel the Kesv protein is really an interesting target for the analysis of structure/function correlates.

In order to characterize the Kesv channel, I have therefore decided to produce and purify the protein in *Pichia pastoris*. The resulting protein was to be used for crystallization screenings and for a functional analysis of the channel in planar lipid bilayers.

Results

Expression of Kesv in *Pichia pastoris*

The gene, which codes for the 124 amino acid long Kesv protein was first cloned in the *Pichia pastoris* expression vector pPIC3.5K with a tag of 7 histidines fused at the N terminus. The plasmid was amplified in *E. coli* and after purification and sequencing it was used for yeast transformation (see M&M).

The first selective step was performed by growing the cells on a medium (RDB) without histidine since the pPIC3.5K plasmid comprises the HIS4 gene coding for histidine dehydrogenase. In this first selection step I have obtained a normal number of colonies (about 50col/plates that I normally obtain with Kcv channels). The colonies were than subjected to a second round of selection on geneticin because the plasmid also brings the resistance gene to this antibiotic. In this case I recovered only 3 colonies (fig. 3.1).

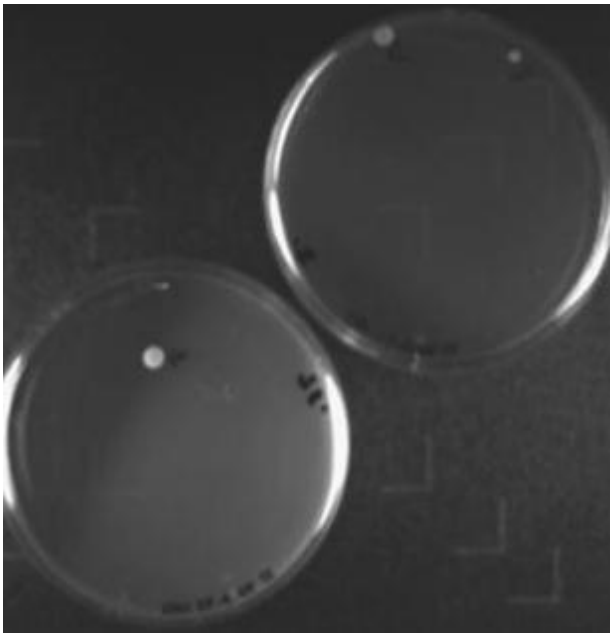

Fig. 3.1. Photo of the YNB + Geneticin plates with the 3 colonies of transformed *Pichia pastoris*.

These three colonies were tested by PCR and they were all positive for the presence of the insert in the genome (lane 2-4 in fig. 3.2); they were used for subsequent liquid growth and protein expression.

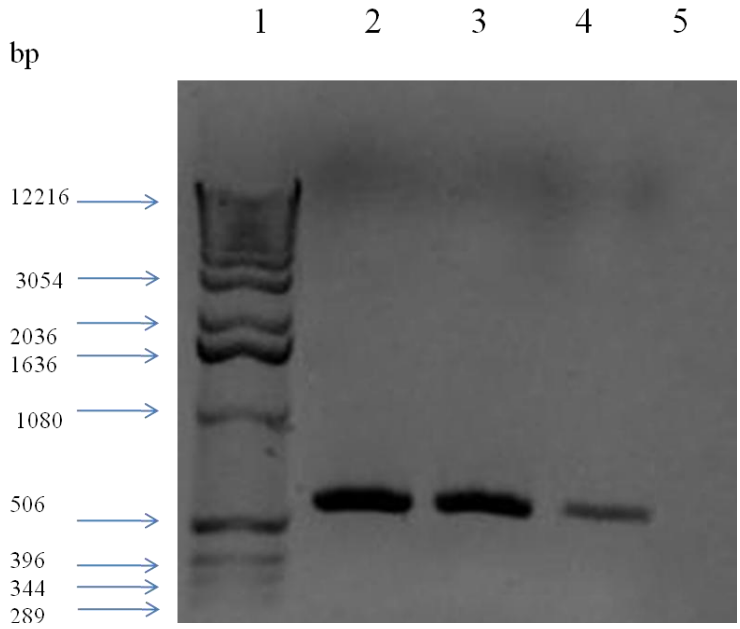

Fig. 3.2 Colony PCR of the 3 colonies: Lane 1: 12 marker 1 kb; lane 2-4: 10 µl of the PCR reaction; lane 5: 10 µl of negative PCR control obtained without the template. The expected length of the band is 592 bp (399 of Kesv 7His $^{+}$ 193 bp of the sequence of the plasmid between the AOX primers). 1% agarose gel.

The three colonies were grown in MGY medium (see M&M) but they were growing much slower than the reference *P. pastoris* cells containing the Kcv gene. In fact the desired optical density for induction (OD_{600} 6) was never reached. In spite of the low cell number the yeasts were nevertheless induced for protein expression with methanol. After 24 h of induction, the cells were collected and the protein expression was tested by western blot on purified microsomes.

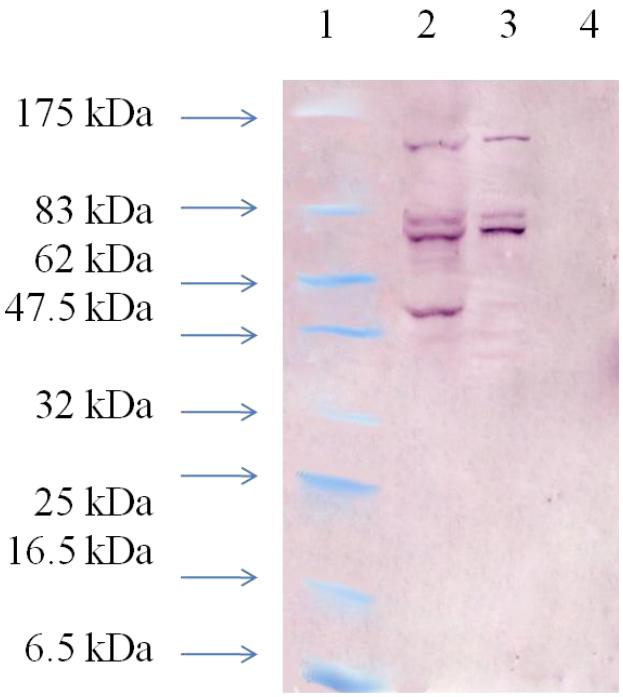

Fig. 3.3. Expression of Kesv. Lane 1: marker 5 µl; lane 2-4: 15 µl of microsomes of Kesv of the three induced colonies. Western blot of the SDS-PAGE 4%-20% gel.

The western blot of the microsomal fractions of the three colonies shows in 2 lanes several bands, which are recognized by the anti-polyHis antibody. The four prominent bands in lane 2 and three in lane 3 are however not at the expected molecular weight of the Kcv tetramer (43 kDa). The results of these experiments imply that the bands are due to aspecific interaction of the anti-polyHis antibody with proteins other than Kesv. It is however also possible that the bands at high molecular weight represent aggregated forms of the Kesv protein itself. For this reason I decided to proceed with the purification protocol. Membrane proteins were solubilized by means of DDM detergent and the supernatant was further purified by affinity chromatography on a Co^{2+}-NTA column. The eluted fractions were separated on SDS-PAGE gel and the blot immunodecorated with the anti-polyHis antibody.

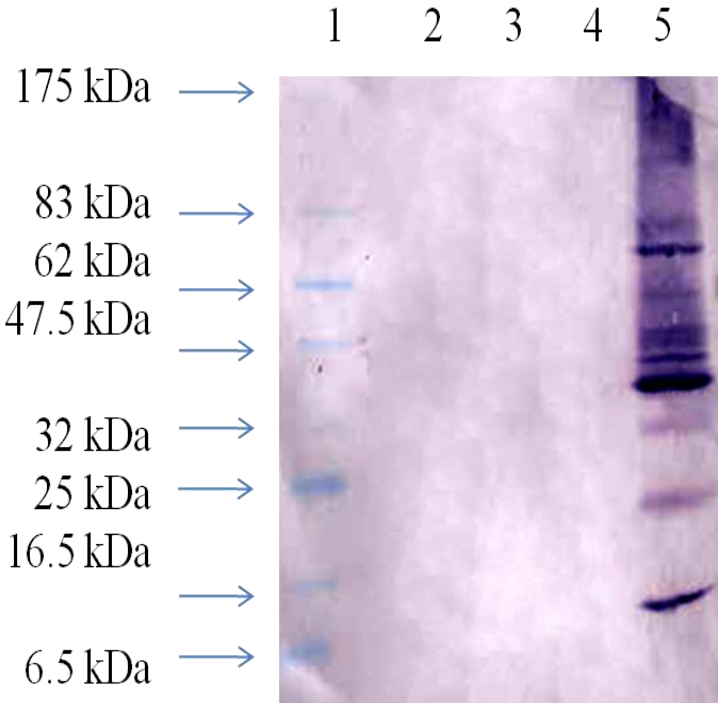

Fig. 3.4. Kesv purification. Lane 1: marker 5 µl; lane 2-4: 22.5 µl of purified protein from Co^{2+}-NTA column. In each lane purified protein of one of the three colonies was loaded. Lane 5: 100 ng of purified MA-1D Kcv as control. Western blot of the SDS-PAGE 4%-20% gel.

Figure 3.4 shows that even after long exposure, that led to the overexposition of the MA-1D Kcv protein as control, no bands are visible in lanes 2-4 where the elution of the purification of the proteins from the three colonies have been loaded. The experiment was repeated under the same condition and gave the same negative result. The results of these experiments imply that the bands which are visible in the western blots of the microsomes are only unspecific interactions of the antibody. Even though this interpretation still needs a confirmation by a negative control, nevertheless the negative result suggests that Kesv is not expressed in the cells that survive the induction. The very low rate of cells growth and the high percentage of cell death after the methanol induction, furthermore, suggests that the Kesv channel may be expressed and targeted to the mitochondria as demonstrated by previous experiments [Balss et al., 2008]; a channel which might short circuits the membrane voltage of the mitochondria could be toxic for *Pichia*.

Cell-free expression (P-CF, Precipitate Cell Free) of Kesv

To bypass the problem of cytotoxicity we used a cell-free expression in collaboration with the group of Dr F. Bernhard (Institute of Biophysical Chemistry, Centre of Biomolecular Magnetic Resonance, Goethe-University, Frankfurt).

Cell-free expression is a technique which combines in vitro transcription and translation allowing over expression of proteins in *E. coli* or wheat germ extracts. In this cell-free system even proteins which would be normally toxic for the heterologous cell, can be produced in large amounts.

In Prof. Bernhard's lab, the cell-free (CF) expression system has been optimized for the production of large amounts of membrane proteins suitable for structural studies [Klammt et al., 2006; Klammt et al., 2007; Schwarz et al., 2007; Schwarz et al., 2008] (see Introduction). Tuning up of the system included manipulation of the reaction condition, a constant supply of cofactors and inhibitors that can positively contribute to protein synthesis. Also chaperons, detergent (D-CF) and lipids (L-CF) for the correct folding of the recombinant protein [Junge et al., 2010] can be constantly added during protein synthesis. Of the three possible protocols, P-CF, L-CF and D-CF, the P-CF (Precipitate CF) approach was first used to synthesize Kesv.

The P-CF reaction, where P means precipitate, produces protein as a precipitate pellet without any addition of detergents or lipids. Among the three protocols this is the most efficient reaction in terms of yield because there is not interference with components which could inhibit the reaction.

The gene of Kesv was cloned in the vector PET21cHx (Novagen) provided by the group in Frankfurt. It was fused to a N terminus T7 tag and a C terminus 5 histidines tag between the restriction sites of BamHI and XhoI, after removing with a point mutation the XhoI site at the end of the gene.

After *E. coli* (DH5α strain) transformation, I obtained a regular number of transformants but when the single colonies were grown in liquid culture and the cell growth rate was increased, the bacterial cells were dying.

We followed the hypothesis that because of a "leaky" expression system, some protein was produced that was toxic also for *E. coli* cells.

As an alternative, the *E. coli*, BL21 pLysS strain was used. This strain contains the plasmid pLysS, which carries the gene encoding T7 lysozyme. T7 lysozyme lowers the background expression level

of genes under the control of the T7 promoter. Unfortunately also with this strain it was not possible to grow the transformed cells in liquid medium.

Other conditions, such as the addition of glucose to the liquid culture to repress the lac operon, or the use of lower temperature (20°C), did not improve bacterial survival. Also the use of another antibiotic, carbenicillin did not change the situation. Carbenicillin is usually preferred as a selecting agent because its breakdown generates byproducts with a lower toxicity than ampicillin.

It was therefore decided to change the plasmid and Kesv was inserted into pSGEM, a vector which is usually used to express proteins in *Xenopus laevis.* This vector contains the T7 promoter for Eukaryotes and it is not an expression vector for *E. coli*.

The gene sequence fused to the two tags was amplified and cloned in the pSGEM vector and the plasmid subsequently grown for amplification in *E. coli* with no problems. The plasmid was sent for cell-free protein production, to the lab of Dr. Bernhard.

The first attempts of cell free production gave very low protein yield. According to the lab's experience, this could depend on the initial sequence of the gene that can form secondary structure at the beginning of the m-RNA transcript. These secondary structures could arise from an unfavorable match of the T7 tag sequence with that of the gene. It was therefore decided to remove the N-terminal tag.

The gene was therefore sub-cloned into another vector, pIVEX2.3 (Roche), with a 10 histidine tag fused at the C terminus of the gene, after removal of the stop codon. The gene was cloned between NdeI and XhoI restriction sites.

The construct was used as template for the in-vitro reaction and this time the protein was expressed with an appreciable yield (fig. 3.5).

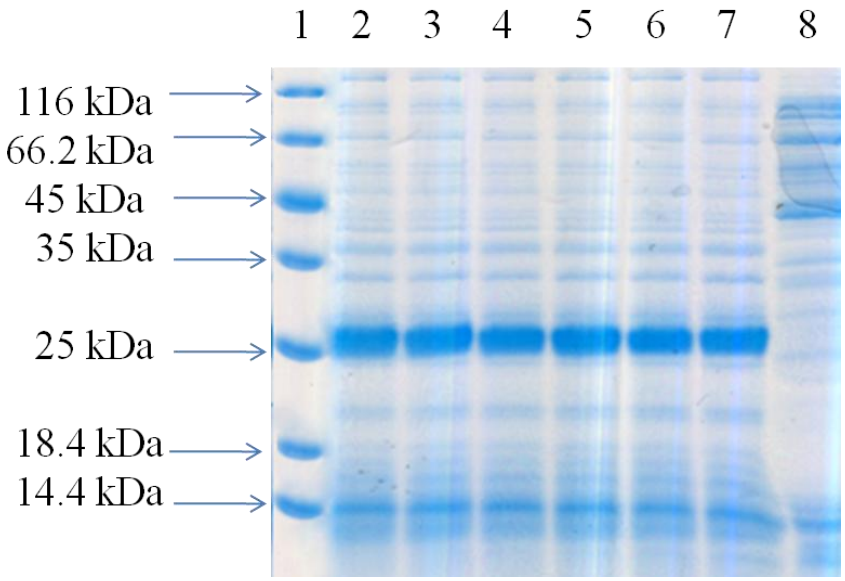

Fig. 3.5. Optimization of the in-vitro expression with different Mg^{2+} concentration. Lane 1: marker 10 µl; lane 2-7: 10 µl of reaction with Mg^{2+} 18-23 mM; lane 8: 10 µl of negative control without DNA. Coomassie staining of SDS-PAGE 16% glycine gel.

From the coomassie staining of the SDS-PAGE gel in figure 3.5 a prevalent band that runs at 25 kDa can be seen in each lane of the reactions (lane 2-7). This band is absent from the negative control implying that the protein band is due to the synthesis of the Kesv channel (lane 8). A protein with a molecular weight of 25 kDa would be consistent with the dimer of the channel protein. The lower band at 14.4 kDa could be the monomer. Since the blot was done with a denaturing gel it is possible that the tetrameric complex, which is expected for a K^+ channel protein, was not stable in SDS. To further characterize the molecular identity of the purified protein it was necessary to examine whether it forms functional channels in planar lipid bilayer.

Kesv in planar lipid bilayer

The protein was solubilized in DDM and used to prepare proteoliposomes by adding L-α-phosphatidilcholine according to a previously optimized protocol (see M&M). The proteoliposomes were used in planar lipid bilayer experiments which I performed in the laboratory of Prof. Gerhard Thiel in Darmstadt, Germany. The experimental procedure is the same that was reported previously for the functional expression of the other viral K^+ channel Kcv [Pagliuca et al., 2007]. The proteoliposomes were added to the trans chamber of the bilayer setup. Both trans and cis chambers contained a buffered solution with 500 mM KCl. The channel activity was recorded at test voltages between -100 mV to +100 mV. Figure 3.6 shows traces of single channel fluctuations between a closed and an open state. Channel activity occurred after reconstitution of the Kesv protein in lipid bilayer and was recorded at +80 and -80 mV.

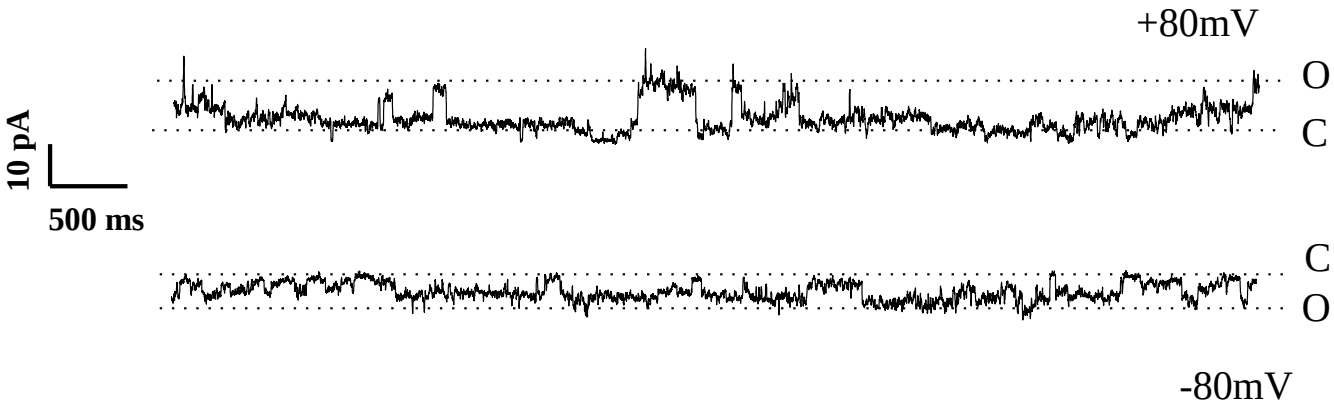

Fig. 3.6. Putative Kesv single channel fluctuations recorded at +80 and -80 mV. Closed and open levels are indicated by dashed lines.

The channel shows a fluctuation typical of a potassium channel, between closed and open states although the baseline of the close state is a little bit noisy. The lower conductance at -80 mV can be due to the rectification phenomenon.

The mean current was plotted against the voltage in an I/V curve (fig. 3.7).

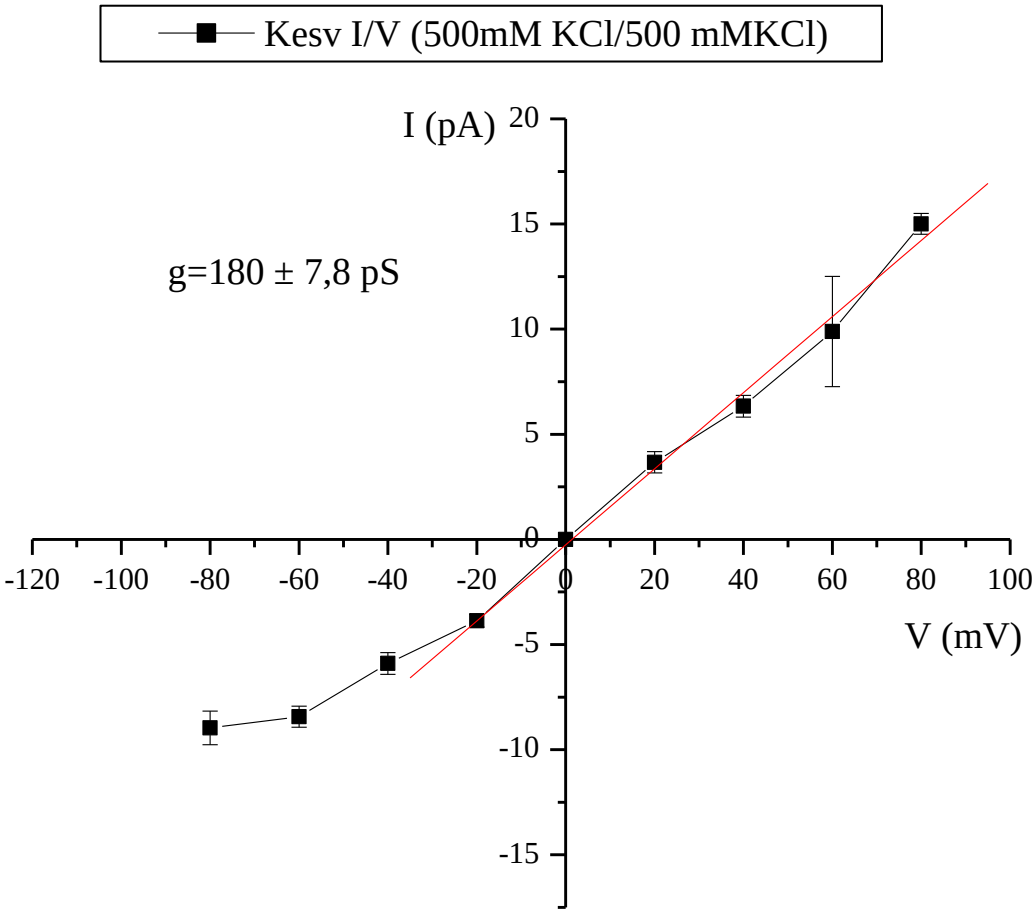

Fig. 3.7. I/V curve of the Kesv channel activity in symmetrical 500 mM KCl solution.

The I/V curve in figure 3.7 has a behavior similar to other Kcv channels, with a similar conductance of 180 pS calculated from the slope in the linear range of the curve. After -60 mV the curve starts to rectify.

The experiment was not easily reproducible and it was not possible to analyze selectivity, block or other properties. Following preparations of proteoliposomes that were obtained from new protein preparations were contaminated with larger conductances that interfered with the measurements.

To avoid contamination of the protein, purification on Ni-NTA column was performed to remove impurities that had prevented before the measurement. The proteoliposomes were made following the usual protocol (see M&M) and were measured in symmetric 100 mM KCl (fig. 3.8). The 100 mM KCl concentration was chosen as start concentration to analyze the permeability to potassium, increasing it in one of the chambers of the bilayer. Contamination is still present, with high conductances especially at positive voltages (fig. 3.9).

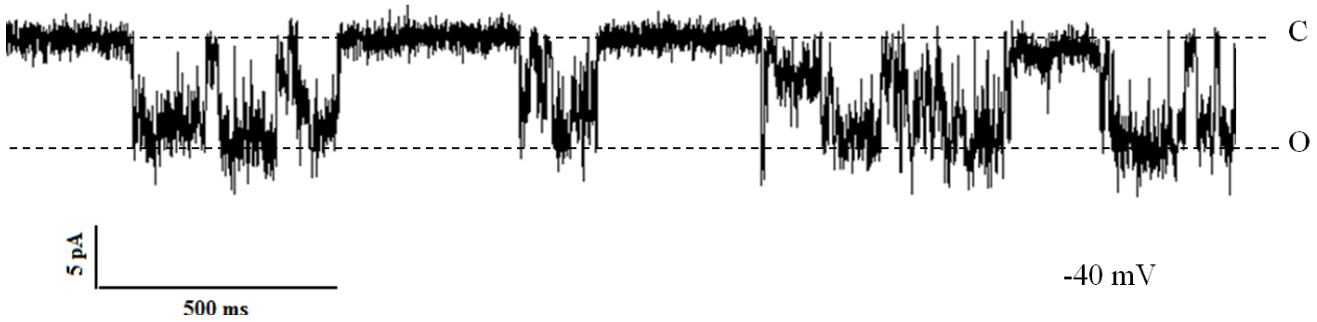

Fig. 3.8. Kesv single channel fluctuations recorded at -40 mV. Closed and open levels are indicated by dashed lines

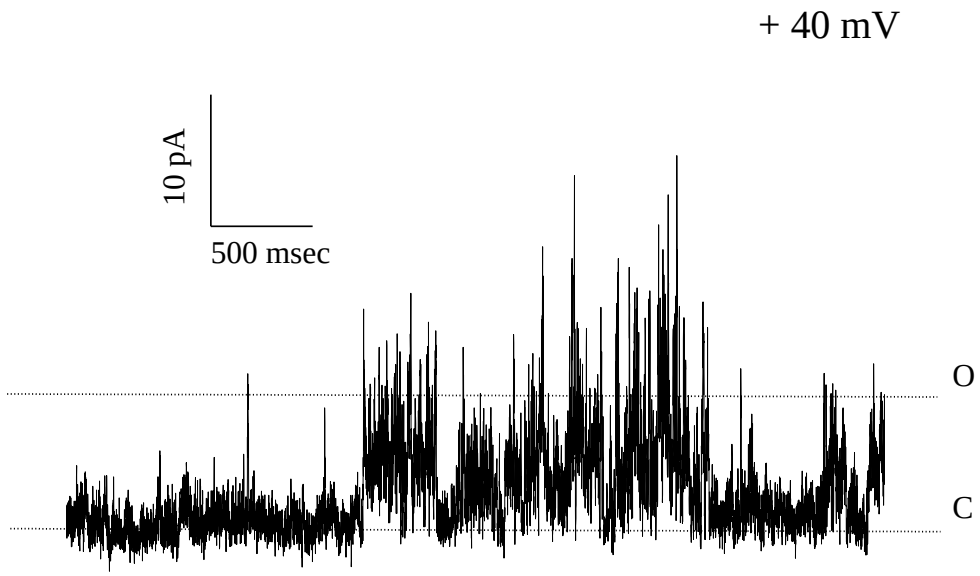

Fig. 3.9. Contaminants recorded at +40 mV. Closed and open levels are indicated by dashed lines.

I/V curve of the measurement with the purified protein of which there is an exemplary current in figure 3.8 is showed in figure 3.10.

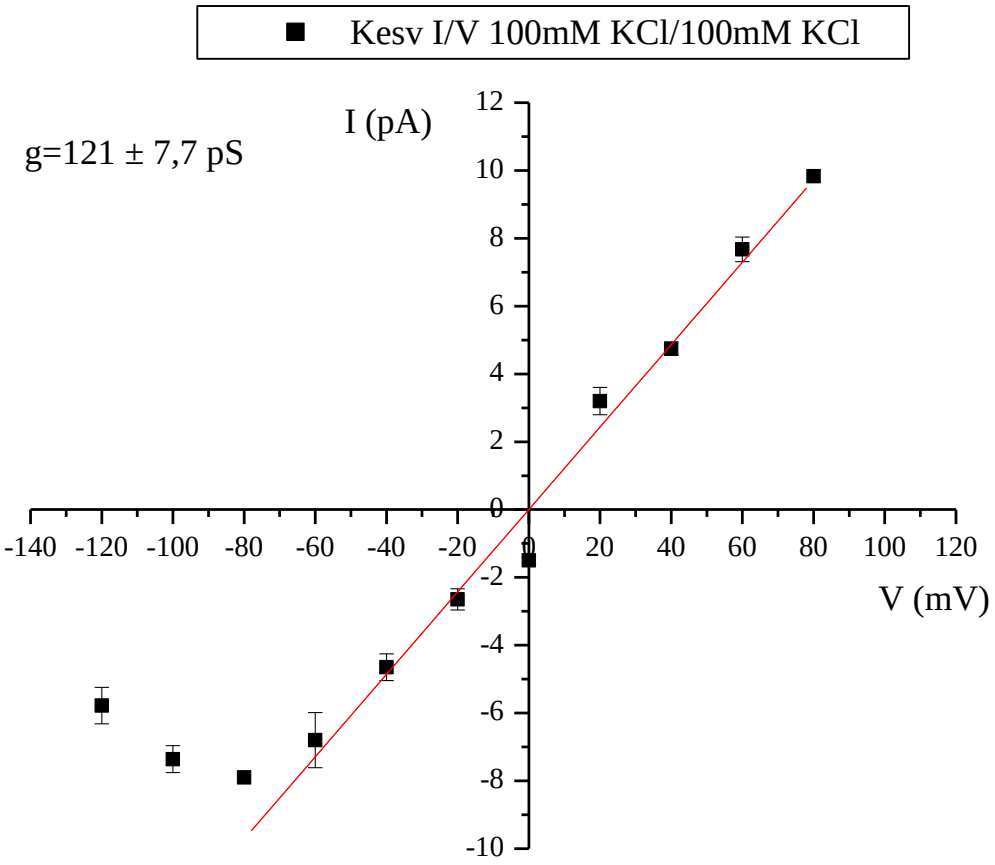

Fig. 3.10. I/V curve of Kesv 10His in symmetrical solution 100 mM solution.

The I/V curve, from an experiment in symmetrical 100 mM KCl, shows a conductance similar to the previous measurement in figure 3.7 and rectification after -80 mV, a behavior typical of Kcv channels. Also with this sample was not possible to investigate for different properties due to contamination that made the measurement difficult. So, I have to conclude that the purification of the protein on the on Ni-NTA column was not sufficient to remove the contaminant proteins from the sample.

Further protein preparation with *E. coli* extract previously purified by ultracentrifugation led too to a more pure protein easier to measure. Selectivity to potassium and barium block were finally tested too (measurements done by Dr. Braun) (fig. 3.11, 3.12).

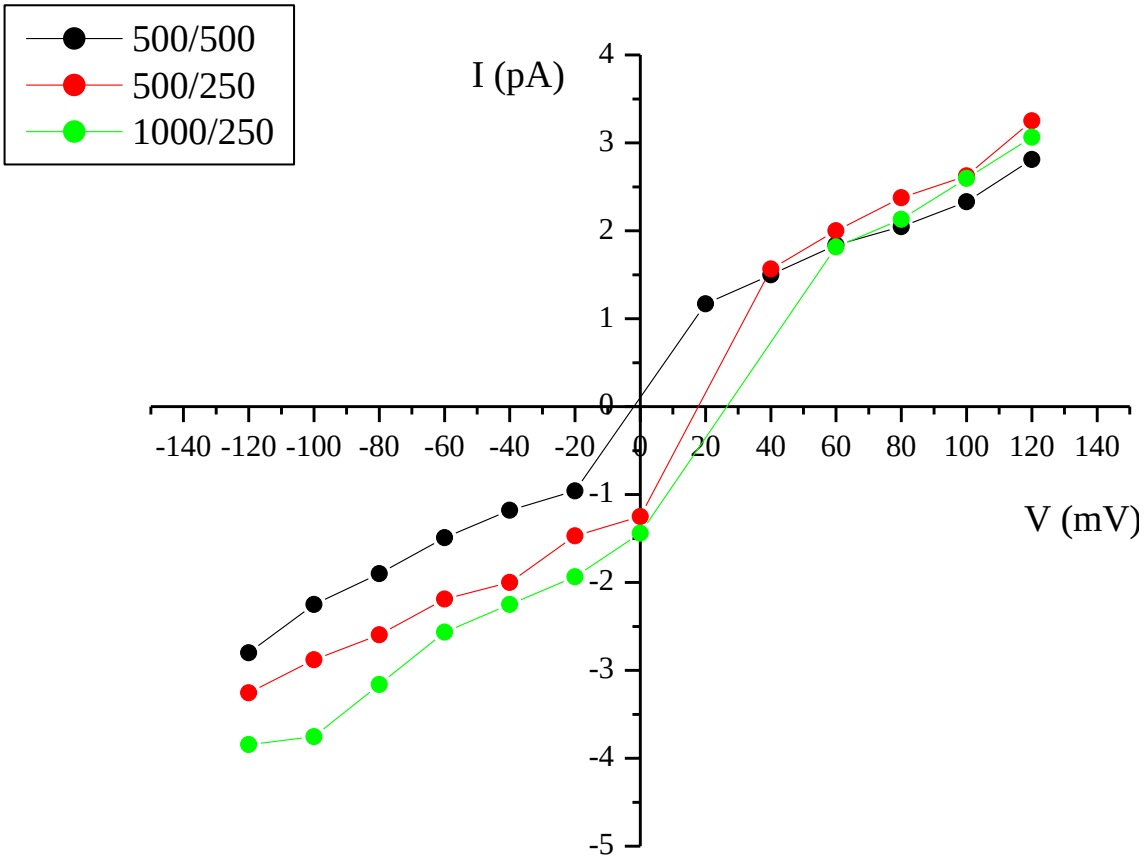

Fig. 3.11. I/V curve of the Kesv tag-less channel activity in asymmetrical KCl solution.

As showed by the I/V curve where three I/V curves are plotted together, there's a shift in the reversal potential when the solution are not symmetrical. The calculated reversal potential is 17.5 for the 500/250 mM KCl solutions and 35 for the 1000/250 mM KCl solutions. The measured values are consistent with the calculated theoretical and it is that a revealing that the channel is selective for potassium.

Permeability to sodium was tested and resulted that the channel does not let the Na^+ ions to pass through the filter (data not showed).

Barium block was also analyzed by adding increasing concentration of $BaCl_2$ to both chambers.

Current traces are showed in figure 3.12.

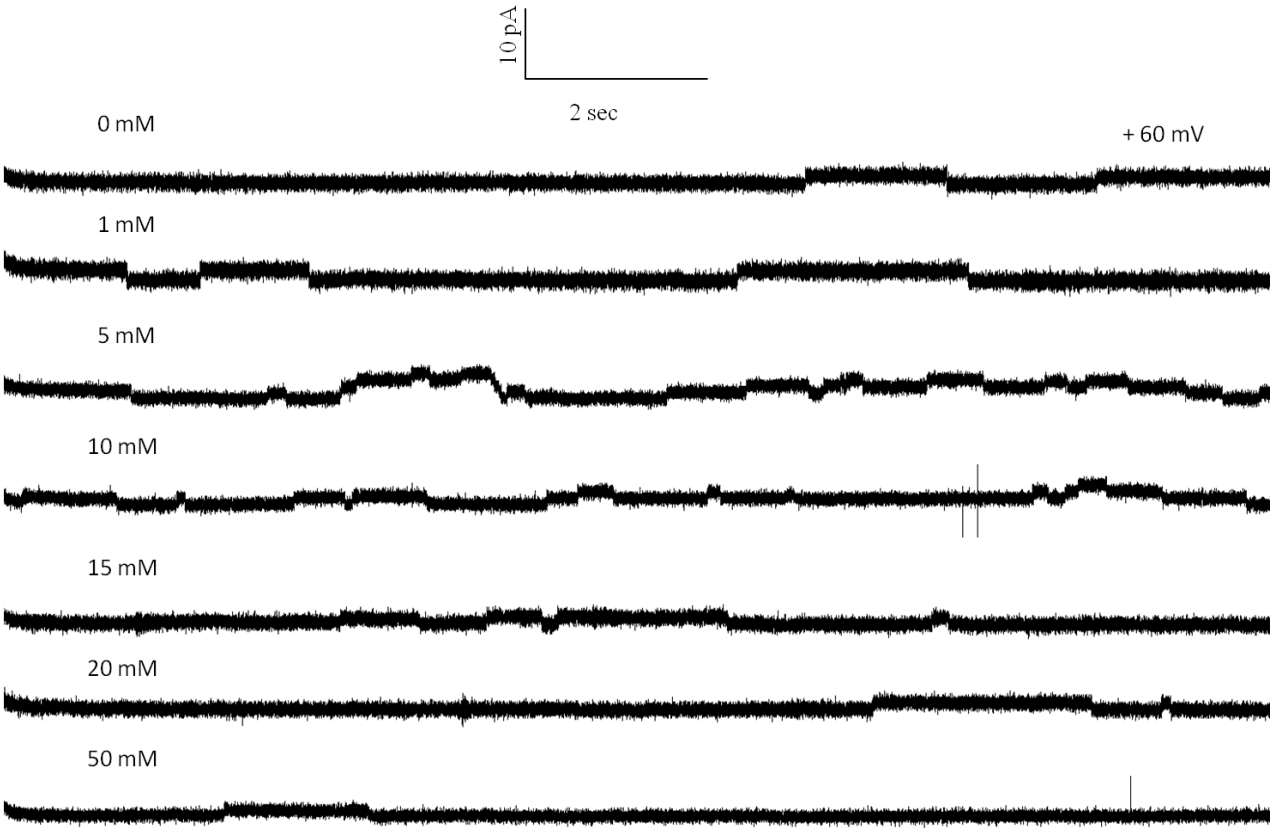

Fig. 3.12. Kesv single channel fluctuations with barium increasing concentration addition recorded at +60 mV.

The addition of increasing concentration of barium slightly blocks the channel. This can be due to the fact that the channel is only moderately sensitive to Barium. In Kcv channels, barium block is known to be controlled by the couple of aa in position 62 and 63. A combination of SS in these two positions tends to remove completely barium sensitivity. In the equivalent positions Kesv shows also SS. It has a serine instead of a threonine in the site where the barium ion binds in the selectivity filter and this led to loss of barium capacity to block channel current.

Since the measurement were difficult due to contamination, it is necessary to exclude that the currents measured are not generated by contaminant protein but by our Kesv channel. Although the E. *coli* extract is purified by several centrifugation steps residual amount of lipids can be left and these lipids can also contain *E. coli* membrane protein. A putative potassium channel has been found in *E. coli* genome [Milkman, 1994], Kch, homologue to eukaryotic channels, that in-vivo forms a functional K^+ conduit [Munsey et al., 2002; Kuo et al., 2003]. To confirm that what I measure is really Kesv and not a contaminant, further experiments has still to be done.

As said before the threonine in the selectivity filter is responsible for barium block of potassium channel. The point mutation of the SS in ST in the selectivity filter of Kesv will be introduced to check whether the barium block is restored.

Kesv protein analysis and large scale purification for crystallization trials

The measurement in planar lipid bilayer demonstrated that the Kesv protein reconstituted in the liposomes forms a functional channel that should be tetrameric for sure. As the goal is make crystallization trials with Kesv it was necessary to get enough protein in tetrameric conformation pure and homogeneous. Since the protein is produced as a pellet in a precipitated form, and in SDS-PAGE gel it runs as a dimer (fig. 3.5), a protocol for tetramer reconstitution has to be introduced to get enough protein in its tetrameric native conformation for crystallization screenings.

The pellet of the protein produced by 1 ml of reaction, that should be around 1 mg, was then sent to us to Milano.

First point of protein reconstitution is the solubilization from the pellet and so the best detergent for solubilization has to be found. I have started with a detergent screening with LPPG (1-palmitoyl-2-hydroxy-sn-glycero-3-[phospho-rac-(1-glycerol)]), LMPG (1-myristoyl-2-hydroxy-sn-glycero-3-[phospho-rac-(1-glycerol)]), SDS (Sodium-n-dodecylsulfate) and β-OG (*n*-octyl-β-D-glucopyranoside) and the results are showed in figure 3.13.

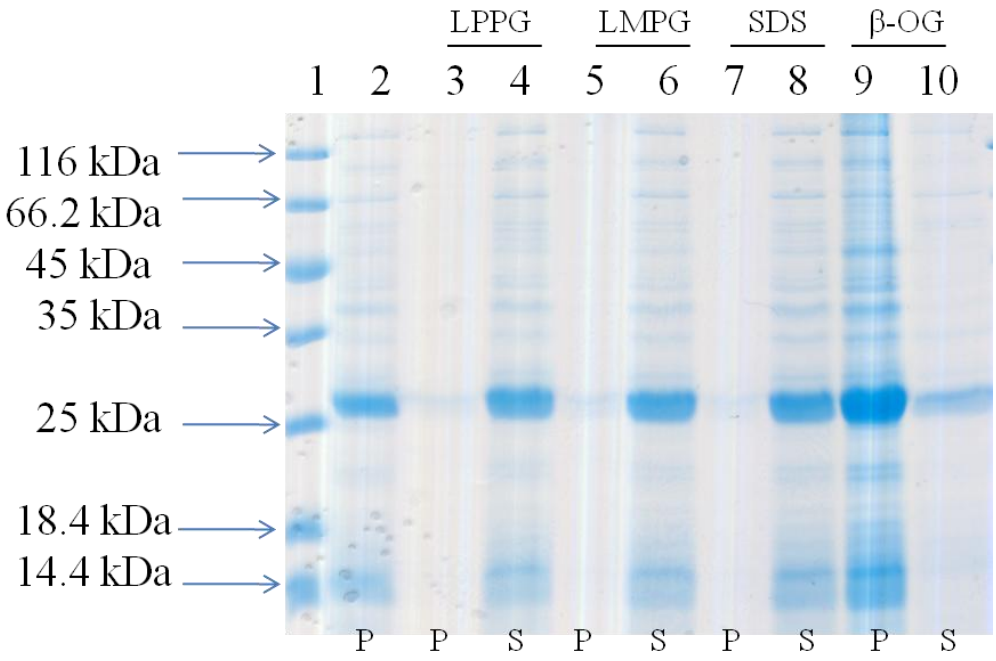

Fig. 3.13. Solubilization screening of Kesv protein. Lane 1: marker 10 µl; lane 2: 1 µl of pellet of the reaction; lane 3: 10 µl of pellet dissolved in water after solubilization with LPPG; lane 4: 10 µl of LPPG solubilized protein; lane 5: 10 µl of pellet dissolved in water after solubilization with LMPG; lane 6: 10 µl of LMPG solubilized protein; lane 7: 10 µl of pellet dissolved in water after solubilization with SDS; lane 8: 10 µl of SDS solubilized protein; lane 9: 10 µl of pellet dissolved in water after solubilization with β-OG; lane 10: 10 µl of β-OG solubilized protein. Coomassie staining of SDS-PAGE 16% glycine gel.

The SDS-PAGE gel in figure 3.13 shows the solubilization with the four tested detergents. In the gel were loaded sample of solubilized protein and their correspondent remained unsolubilized pellet that was solved in water to be loaded on the gel to check the efficiency of the solubilization. In lane 2 is loaded the whole pellet of the reaction and the band at 25 kDa, probably corresponding to dimers of Kesv is visible. In lane 3 and 4 are loaded the pellet solubilized in water of the solubilization with LPPG, in lane 5 and 6 the protein solubilized with LMPG, in lane 7 and 8 the protein solubilized in SDS and in lane 9 and 10 the solubilization with β-OG. What can be concluded from this first experiment is that LPPG, LMPG and SDS are able to solubilized the protein since it is almost all in the samples after the solubilization (lane 4, 6 and 8) and there's a really small amount in the remained pellet after the solubilization (lane 3,5 and 7). The opposite happened for the β-OG solubilized sample in which the protein is all in the pellet (lane 9) and only a small amount was solubilized (lane 10) leading to the conclusion that it is not a good detergent for solubilization.

DM (n-decyl-β-D-maltoside), DDM (n-dodecyl-β-d-maltoside), Triton (polyethylene glycol P-1,1,3,3-tetramethyl-butylphenyl ether) and L-Dao (Lauryldimethylamine-N-oxide) were tested too

and DM, DDM and Triton revealed to be good detergents for Kesv solubilization, while L-Dao was not able to solubilized the protein from the pellet.

Although SDS gave positive results it was discarded because it precipitates at 4°C and was not suitable for some of our screenings, while Triton was discarded too because it is not a good detergent for crystallization.

Since the SDS-PAGE is in denaturing condition, to check the quality of the sample it is necessary to work in non-denaturing condition, so to perform native gel and size exclusion chromatography (Gel Filtration). A GF was performed with all solubilized sample to check the quality of the protein (fig. 3.14).

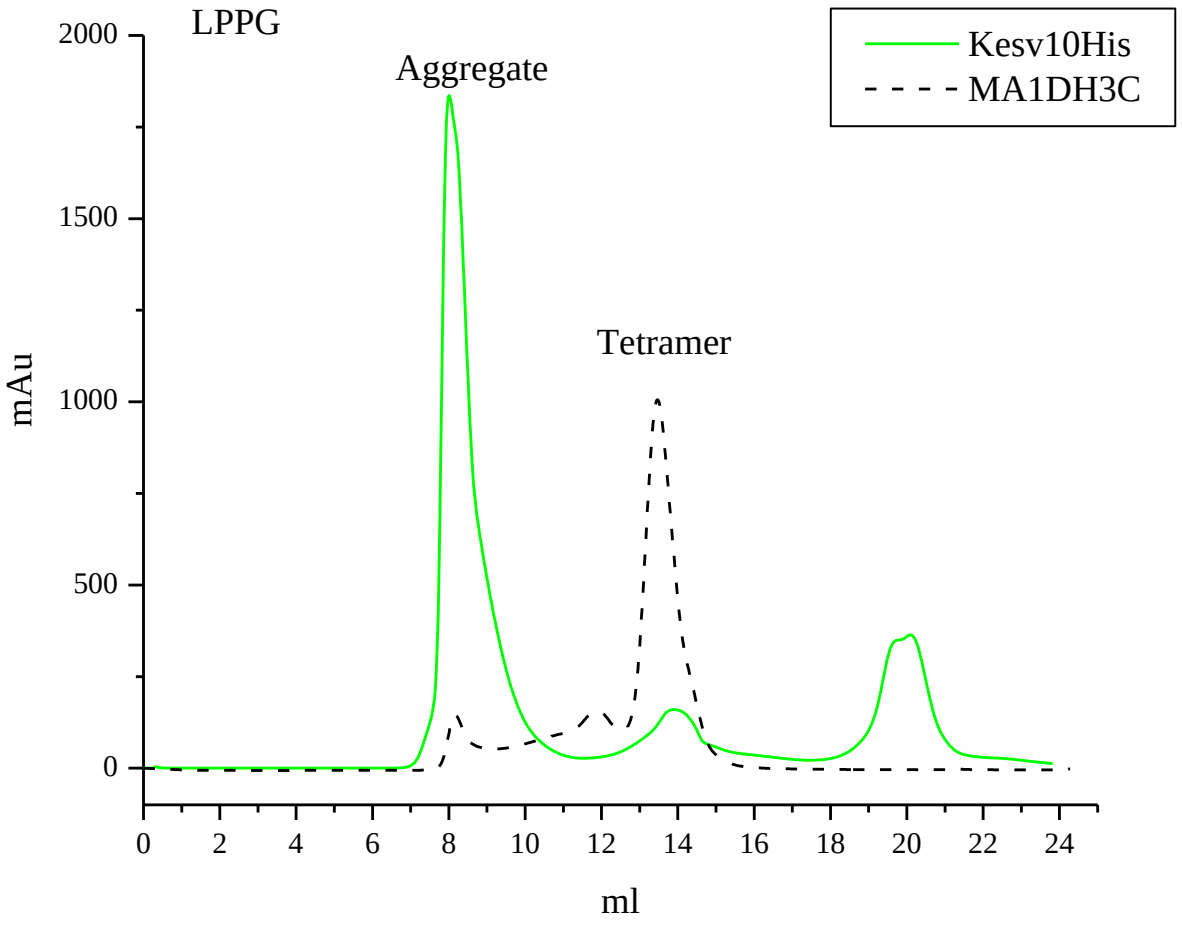

Fig. 3.14. Chromatogram of the gel filtration of Kesv protein solubilized in LPPG (in green) compared with MA-1D Kcv chromatogram (in black).

The gel filtration in figure 3.14 shows that the protein solubilized in LPPG (green chromatogram) is almost all aggregate because the higher peak indicates that the protein elutes at high molecular

weight (between 7 and 10 ml) the same of MA-1D Kcv aggregate peak, that in the black chromatogram is a very low. There's only a small peak corresponding to the tetramer eluting between 13 and 15 ml as indicated by the gel filtration of the MA-1D Kcv protein. The smaller peak that elutes between 19 and 21 ml is probably due to detergent, because loaded on SDS-PAGE gel had no protein inside (data not showed).

The same profile was also found for the other samples with the other detergents (data not showed). So the protein in this condition was not suitable for crystallization screening and further improvement of the protein quality was necessary.

Some solubilization parameters were changed to try to increase the quality and the yield of the tetrameric protein. First of all the solubilization was performed at 4°C that is the solubilization temperature used during Kcv protein solubilization, and for 16 hours. Also a double volume of solubilization buffer was used but this led not to any improvement. Since some ions are able to stabilize the filter [Krishnan et al., 2005; Pagliuca et al., 2007], the samples for SDS-PAGE gel were also prepared in presence of Ba^{2+} and K^{+}. In some of these samples DTT was also added to reduce hypothetical disulfide bond, but all the samples showed in the western blot revealed the same pattern (data not showed).

The aggregation of the protein during gel filtration can be explained by the presence of a long sequence of histidines in the tag that, in our experience, promote the formation of aggregates.

To solve the problem and obtain tetrameric protein for the crystallization, a construct with the protein without any tag and a construct with the H3C recognition site for tag removal were designed. The constructs have been cloned in the plasmid pIVEX2.3 for transcription and translation, between NdeI and XhoI restriction sites.

The solubilization of the tag-less protein was done at 4°C for 16 hours in 3 LPPG solubilization buffers that contained different salts composition. The solubilization buffer of usual protocol contained NaCl and it was substituted or supplemented with KCl because it is known that potassium can increase the stability of the filter and of the whole channel [Krishnan et al., 2005; Pagliuca et al., 2007]. The only noticeable results is that in the buffer with only KCl salts there is a little bit more tetramer, but the protein is still almost all aggregate. This buffer with KCl has been used from this point on for solubilization buffers preparation.

Another parameter that can influence the aggregation could be the low temperature (4°C) at which the GF was performed. Solubilization and the relative gel filtrations at room temperature and at 4°C were performed and the two chromatograms were compared (data not showed). Although there was still a low amount of the tetramer, the aggregate form was sensitively reduced working at room temperature, and this seemed a good condition to be developed.

The three constructs, the tag-less, the 10His and the H3C-10His have been solubilized in parallel were performed at 27°C for 16 hours with DDM as detergent and a step of TFE (2,2,2 Trifluoethanol) denaturation was done before the solubilization. In literature was found that TFE destabilized the tetramer of the potassium channel KcsA reducing it to monomers in a reversible way [Barrera et al., 2005]. 33% TFE was used to denature the protein pellet before solubilization with detergent that also dilutes TFE concentration to a 16% non-denaturing concentration. This step was done with the purpose of reducing all the protein to monomer to facilitate the reconstitution into tetramer. DDM was used as detergent because from our experience is one of the most suitable for Kcv protein solubilization.

The three solubilizations were compared with a gel filtration (fig. 3.15).

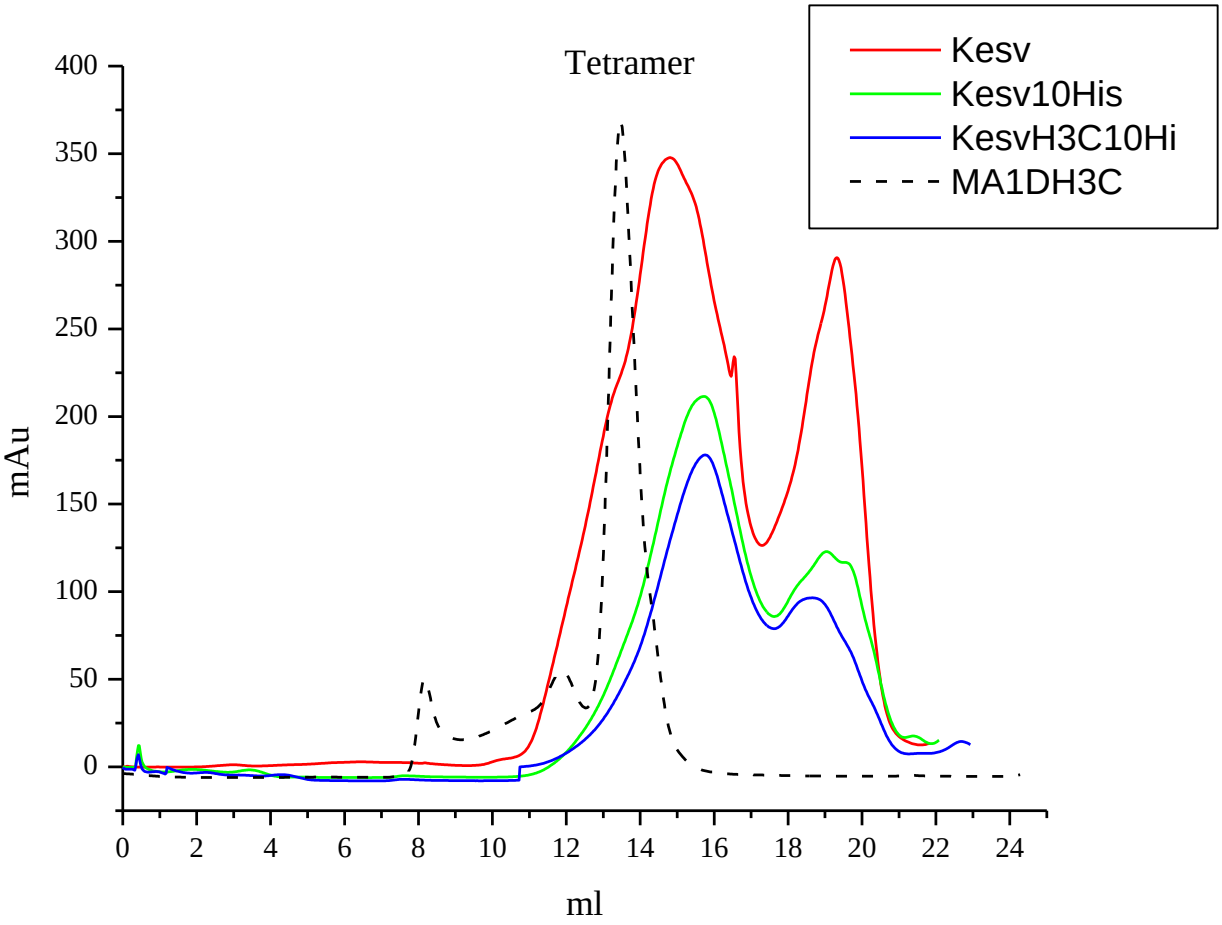

Fig. 3.15. Chromatogram of the gel filtration of Kesv solubilized in DDM at 27°C after TFE denaturation ON. In red the protein Kesv tag-less, in green the Kesv 10His and in blue the Kesv H3C-10His. In black the MA-1D Kcv gel filtration as reference.

From the superimposition of the chromatograms of the solubilization of the three channel can be seen that the aggregate for completely disappeared and also the amount of tetramer is increased.

These experiments confirmed that the temperature is critical and that the treatment with TFE is really enhancing the quality of reconstitution. The fractions containing the tetramer of Kesv tag-less (13-15 ml) were loaded on a Native-PAGE gel (fig. 3.16).

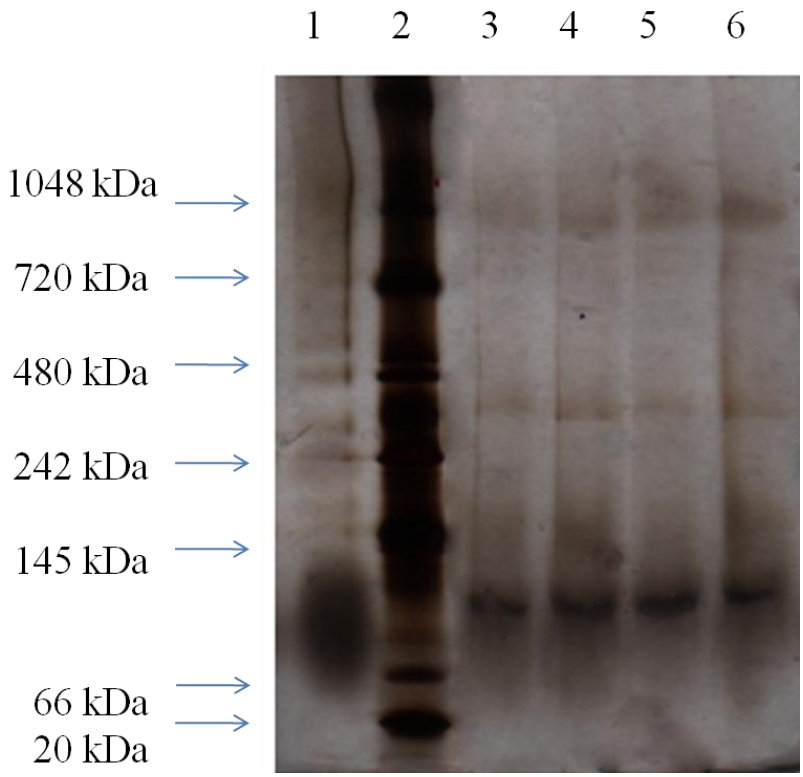

Fig. 3.16. Gel filtration fractions. Lane 1: 10 µl of purified MA-1D Kcv; lane 2: marker 10 µl; lane 3-6: 10 µl of 12-15 ml fraction of the GF. Silver staining of Native-PAGE 4-16% Bis-Tris gel.

As showed by Native-PAGE gel in all fraction of the tetramer peak loaded (lane 3-6) there's a clear band at the molecular weight of MA-1D Kcv as reference in lane 1 (the band is so stretched maybe because the protein sample was old). The same bands but of lower intensity were found also for the other two constructs in the fraction 13-16 ml (data not showed).

The solubilization with these condition: TFE denaturing, and solubilization with DDM for 16 hours at 27°C will be scaled-up and the tetrameric protein will be used in the near future for crystallization screenings.

D-CF (Detergent Cell-Free) and L-CF (Lipid Cell-Free) of Kesv

The in-vitro cell free transcription and translation system for membrane protein expression also allows the addition in the reaction mixture of detergents (D-CF) or lipids (L-CF).

In parallel with our tetramerization screenings of the protein produced with P-CF, D-CF and L-CF have been performed in Frankfurt in Prof. F. Bernhard lab by Dr. Roos to check if the use of detergents or lipids to the reaction mixture can increase the quality of the protein, allowing it to assembling itself into tetramers.

First preliminary screenings have been done with D-CF expression of Kesv tag-less in presence of hemi-fluorinated surfactant (F_6TAC n=8,5) in the concentration of 1, 2 or 5 mM was performed. Fluorinate surfactants are components that resemble detergents but their hydrophobic tails contains fluorine atoms. Since they are not detergent but interfere less than detergents to stabilize protein/protein and protein/lipid interactions, they can be suitable for in-vitro synthesis of protein.
L-CF expression in presence of 2 mg/ml of DMPC (1,2-Dimyristoyl-sn-glycero-3-phosphocholine) that forms liposomes that in CF system act as chaperons for the nascent peptide chain [Kalmbach et al., 2007], was also performed but none of the two methods gave better results.

These experiments were only two preliminary tests of the D-CF and L-CF. As for the P-CF a lot of trials are necessary to optimize the reaction and after it, to find the best condition to solubilized and fold the protein, also for these two techniques it is required to improve the quality of the products finding the best reagents.

Discussion part 3

Due to the already mentioned localization of Kesv in mitochondria, it was not possible to measure currents in oocytes and HEK cells transfected with Kesv. We decided to express the Kesv protein in *Pichia pastoris* in order to produce and purify enough protein for both structural and functional studies [Balss et al., 2008].
Fist attempts to express the protein in *Pichia* failed, probably due to the localization of the protein in the mitochondria that can disturb the cells growth.

Thus we decided to produce the protein with the cell-free system optimized for membrane proteins by Dr. Bernhard (University of Frankfurt). The protein was first expressed with the P-CF method that produces the protein as a precipitate. Therefore my first goal was to try to get from the precipitate the tetrameric protein to test the functionality in planar lipid bilayer and then to try get enough pure protein to make crystallization screenings.

After improving the protocol in order to remove contaminants, I was successfully measuring functional Kesv channels. These channels have a conductance of 180 pS (in 500 mM K^+) and are therefore comparable to the Kcv channels (conductance 250 in 500 mM K^+). Permeability to sodium was tested and resulted that the channel does not pass Na^+ ions to. The selectivity for K^+ was confirmed in experiments with asymmetric solution in which the measured reversal potential is compatible with the theoretical. In conclusion, I was able to reconstitute the tetramer from the precipitate and to show that the reconstituted channel is functional and selective. A great achievement was also that Kesv has been the first potassium channel expressed with P-CF technique.

The effect of barium was tested too and reveals a weak influence of the blocking ion on the single-channel currents. This is consistent with the presence in the selectivity filter of Kesv of a serine in position 86, corresponding to 63 in Kcv. Similarly to the Kcv mutant T63S that is insensitive to barium, also Kesv seems insensitive [Chatelain et al., 2009]. To prove this, we have planned to mutate Kesv, S86T, and test its barium sensitivity.

Another aim of this part of my PhD project concerning Kesv was to produce the protein in large quantities for structural studies. After several attempts, I was able to find the best conditions for solubilization and reconstitution of the tetrameric protein, starting from the in vitro produced precipitate. This protein will be used in the near future for structural analysis as an alternative to

Kcv channels. The advantage over Kcv is that, being 23 amino acids longer at the soluble N terminus, Kesv might provide more surfaces for protein-protein interaction.

Bibliography

1. Abenavoli A., DiFrancesco M.L., Schroeder I., Epimashko S., Gazzarrini S., Hansen U.P., Thiel G., Moroni A.: Fast and slow gating are inherent properties of the pore module of the K^+ channel Kcv. *J. Gen. Physiol*. 2009 Sep;134(3):219-29.
2. Armstrong C.M., Taylor S.R.: Interaction of barium ions with potassium channels in squid giant axons. *Biophys. J*. 1980 Jun; 30(3): 473-88.
3. Armstrong C.M., Swenson R.P. Jr., Taylor S.R.: Block of squid axon K channels by internally and externally applied barium ions. *J. Gen. Physiol*. 1982 Nov; 80(5): 663-82.
4. Ashcroft F. M.: Ion channels and disease. 2nd edition, Academic Press San Diego, CA. 2000.
5. Balss J., Papatheodorou P., Mehmel M., Baumeister D., Hertel B., Delaroque N., Chatelain F.C., Minor D.L. Jr., Van Etten J.L., Rassow J., Moroni A., Thiel G.: Transmembrane domain length of viral K^+ channels is a signal for mitochondria targeting. *Proc. Natl. Acad. Sci. U S A.* 2008 Aug 26; 105(34): 12313-8.
6. Baneyx F.: Recombinant protein expression in *Escherichia coli*. *Curr. Opin. Biotechnol.* 1999 Oct; 10(5): 411-21. Review.
7. Bannwarth M., Schulz G.E.: The expression of outer membrane proteins for crystallization. *Biochim. Biophys. Acta*. 2003 Feb 17; 1610(1): 37-45.
8. Barhanin J., Lesage F., Guillemare E., Fink M., Lazdunski M., Romey G.: K(V)LQT1 and lsK (minK) proteins associate to form the I(Ks) cardiac potassium current. *Nature.* 1996 Nov 7; 384(6604): 78-80.
9. Barrera F.N., Renart M.L., Molina M.L., Poveda J.A., Encinar J.A., Fernández A.M., Neira J.L., González-Ros J.M.: Unfolding and refolding in vitro of a tetrameric, alpha-helical membrane protein: the prokaryotic potassium channel KcsA. *Biochemistry*. 2005 Nov 1; 44(43): 14344-52.
10. Baumann A., Grupe A., Ackermann A., Pongs O.: Structure of the voltage-dependent potassium channel is highly conserved from Drosophila to vertebrate central nervous systems. *EMBO J.* 1988 Aug; 7(8): 2457-63.
11. Becker D., Dreyer I., Hoth S., Reid J.D., Busch H., Lehnen M., Palme K., Hedrich R.: Changes in voltage activation, Cs+ sensitivity, and ion permeability in H5 mutants of the plant K^+ channel KAT1. *Proc. Natl. Acad. Sci. U S A.* 1996 Jul 23; 93(15): 8123-8.
12. Benham C.D., Bolton T.B., Lang R.J,. Takewaki T.: The mechanism of action of Ba^{2+} and TEA on single Ca^{2+}-activated K^+-channels in arterial and intestinal smooth muscle cell membranes. *Pflugers Arch*. 1985 Feb; 403(2): 120-7.

13. Brüggemann A., Farre C., Haarmann C., Haythornthwaite A., Kreir M., Stoelzle S., George M., Fertig N.: Planar patch clamp: advances in electrophysiology. *Methods Mol. Biol.* 2008;491:165-76.

14. Buckholz R.G., Gleeson M.A.: Yeast systems for the commercial production of heterologous proteins. *Biotechnology (N Y).* 1991 Nov; 9(11): 1067-72.

15. Burmester J. and Pluckthun A.: Construction of svFc fragments from hybridoma or spleen cells by PCR assembly. In antibody engineering. Springer-Verlag New York, Inc. 2001; 19-40.

16. Carrasco L.: Modification of membrane permeability by animal viruses. *Adv. Virus Res.* 1995; 45: 61-112.

17. Chase T.E., Nelson J.A., Burbank D.E., Van Etten J.L.: Mutual exclusion occurs in a Chlorella-like green alga inoculated with two viruses. *J. Gen. Virol*. 1989 Jul; 70 (Pt 7): 1829-36.

18. Chatelain F.C., Alagem N., Xu Q., Pancaroglu R., Reuveny E., Minor D.L. Jr.: The pore helix dipole has a minor role in inward rectifier channel function. *Neuron.* 2005 Sep 15;47(6): 833-43.

19. Chatelain F.C., Gazzarrini S., Fujiwara Y., Arrigoni C., Domigan C., Ferrara G., Pantoja C., Thiel G., Moroni A., Minor D.L. Jr.: Selection of inhibitor-resistant viral potassium channels identifies a selectivity filter site that affects barium and amantadine block. *PLoS One*. 2009 Oct 16; 4(10): e7496.

20. Chen J., Cassar S.C., Zhang D., Gopalakrishnan M.: A novel potassium channel encoded by Ectocarpus siliculosus virus. *Biochem. Biophys. Res. Commun*. 2005 Jan 28; 326(4): 887-93.

21. Christie M.J., Adelman J.P., Douglass J., North R.A.: Expression of a cloned rat brain potassium channel in Xenopus oocytes. *Science*. 1989 Apr 14; 244(4901): 221-4.

22. Ciampor F., Cmarko D., Cmarková J., Závodská E.: Influenza virus M2 protein and haemagglutinin conformation changes during intracellular transport. *Acta Virol*. 1995 Jun; 39(3): 171-81. Review.

23. Coady M.J., Daniel N.G., Tiganos E., Allain B., Friborg J., Lapointe J.Y., Cohen E.A. : Effects of Vpu expression on *Xenopus* oocyte membrane conductance. *Virology*. 1998 Apr 25; 244(1): 39-49.

24. Coetzee W.A., Amarillo Y., Chiu J., Chow A., Lau D., McCormack T., Moreno H., Nadal M.S., Ozaita A., Pountney D., Saganich M., Vega-Saenz de Miera E., Rudy B.: Molecular diversity of K^+ channels. *Ann. N. Y. Acad. Sci*. 1999 Apr 30;868: 233-85. Review.

25. Cohen A., Ben-Abu Y., Zilberberg N.: Gating the pore of potassium leak channels. *Eur. Biophys. J.* 2009 Dec; 39(1): 61-73. Review.

26. Cordero-Morales J.F., Cuello L.G., Zhao Y., Jogini V., Cortes D.M., Roux B., Perozo E.: Molecular determinants of gating at the potassium-channel selectivity filter. *Nat. Struct. Mol. Biol.* 2006 Apr; 13(4): 311-8.

27. Cortes D.M, Perozo E.: Structural dynamics of the Streptomyces lividans K+ channel (SKC1): oligomeric stoichiometry and stability. *Biochemistry*. 1997 Aug 19; 36(33): 10343-52.

28. Covarrubias M., Wei A.A., Salkoff L.: Shaker, Shal, Shab, and Shaw express independent K^+ current systems. *Neuron*. 1991 Nov; 7(5): 763-73.

29. de Hoop M.J., Cregg J., Keizer-Gunnink I., Sjollema K., Veenhuis M., Ab G.: Overexpression of alcohol oxidase in *Pichia pastoris*. *FEBS Lett*. 1991 Oct 21; 291(2): 299-302.

30. Dornmair K., Kiefer H., Jähnig F.: Refolding of an integral membrane protein. OmpA of Escherichia coli. J Biol Chem. 1990 Nov 5;265(31):18907-11.

31. Doyle D.A., Morais Cabral J., Pfuetzner R.A., Kuo A., Gulbis J.M., Cohen S.L., Chait B.T., MacKinnon R.: The structure of the potassium channel: molecular basis of K^+ conduction and selectivity. *Science*. 1998 Apr 3; 280(5360): 69-77.

32. Drenth J.: Principles of Protein X-ray Crystallography. Springer-Verlag New York, Inc., 1999.

33. Durell S.R. and Guy H.R.: A family of putative Kir potassium channels in prokaryotes. *BMC Evol Biol*. 2001; 1:14.

34. Dutzler R., Campbell E.B., Cadene M., Chait B.T., MacKinnon R.: X-ray structure of a ClC chloride channel at 3.0 A reveals the molecular basis of anion selectivity. *Nature*. 2002 Jan 17;415(6869):287-94.

35. Eaton D.C., Brodwick M.S.: Effects of barium on the potassium conductance of squid axon. *J. Gen. Physiol*. 1980 Jun; 75(6): 727-50.

36. Elbaz Y., Steiner-Mordoch S., Danieli T., Schuldiner S.: In vitro synthesis of fully functional EmrE, a multidrug transporter, and study of its oligomeric state. *Proc. Natl. Acad. Sci. U S A.* 2004 Feb 10; 101(6): 1519-24.

37. Fitzgerald L.A., Graves M.V., Li X., Hartigan J., Pfitzner A.J., Hoffart E., Van Etten J.L.: Sequence and annotation of the 288-kb ATCV-1 virus that infects an endosymbiotic

chlorella strain of the heliozoon Acanthocystis turfacea. *Virology*. 2007 Jun 5; 362(2): 350-61.

38. Gambale F. and Uozumi N.: Properties of shaker-type potassium channels in higher plants. J Membr Biol. 2006 Mar; 210(1):1-19.
39. Garavito R.M. and Ferguson-Miller S.: Detergents as Tools in Membrane Biochemistry. *J. Biol. Chem.* 2001 Aug 31; 276(35): 32403-6.
40. Garofoli S., Jordan P.C.: Modeling permeation energetics in the KcsA potassium channel. *Biophys. J.* 2003 May; 84(5): 2814-30.
41. Gazzarrini S., Severino M., Lombardi M., Morandi M., DiFrancesco D., Van Etten J.L., Thiel G., Moroni A.: The viral potassium channel Kcv: structural and functional features. *FEBS Lett*. 2003 Sep 18; 552(1): 12-6. Review.
42. Gazzarrini S., Kang M., Van Etten J.L., Tayefeh S., Kast S.M., DiFrancesco D., Thiel G., Moroni A.: Long distance interactions within the potassium channel pore are revealed by molecular diversity of viral proteins. *J. Biol. Chem*. 2004 Jul 2; 279(27): 28443-9.
43. Gazzarrini S., Kang M., Epimashko S., Van Etten J.L., Dainty J, Thiel G., Moroni A.: *Chlorella* virus MT325 encodes water and potassium channels that interact synergistically. *Proc. Natl. Acad. Sci. U S A.* 2006 Apr 4; 103(14): 5355-60.
44. Gazzarrini S., Kang M., Abenavoli A., Romani G., Olivari C, Gaslini D., Ferrara G., van Etten J.L., Kreim M., Kast S.M., Thiel G., Moroni A.: *Chlorella* virus ATCV-1 encodes a functional potassium channel of 82 amino acids. *Biochem . J.* 2009 May 13; 420(2): 295-303.
45. Greiner T., Frohns F., Kang M., Van Etten J.L., Käsmann A., Moroni A., Hertel B., Thiel G.: *Chlorella* viruses prevent multiple infections by depolarizing the host membrane. *J.Gen. Virol*. 2009 Aug; 90(Pt 8): 2033-9.
46. Harris R.E., Larsson H.P., Isacoff E.Y.: A permanent ion binding site located between two gates of the Shaker K^+ channel. *Biophys J*. 1998 Apr; 74(4): 1808-20.
47. Heginbotham L., Abramson T., MacKinnon R.: A functional connection between the pores of distantly related ion channels as revealed by mutant K+ channels. *Science*. 1992 Nov 13; 258(5085): 1152-5.
48. Heginbotham L., Lu Z., Abramson T., MacKinnon R.: Mutations in the K^+ channel signature sequence. *Biophys. J*. 1994 Apr; 66(4): 1061-7.
49. Heginbotham L., Odessey E., Miller C.: Tetrameric stoichiometry of a prokaryotic K+ channel. *Biochemistry*. 1997 Aug 19; 36(33): 10335-42.

50. Heginbotham L., Kolmakova-Partensky L., Miller C.: Functional reconstitution of a prokaryotic K^+ channel. *J. Gen. Physiol*. 1998 Jun;111(6):741-9.
51. Hertel B., Tayefeh S., Mehmel M., Kast S.M., Van Etten J.L., Moroni A., Thiel G.: Elongation of outer transmembrane domain alters function of miniature K^+ channel Kcv. J. *Membr. Biol.* 2006 Mar; 210(1): 21-9.
52. Hilf R.J., Dutzler R.: X-ray structure of a prokaryotic pentameric ligand-gated ion channel. *Nature*. 2008 Mar 20; 452(7185): 375-9
53. Hille B.: Ionic Channels of Excitable Membranes. Hardcover, Subsequent Edition. 1992.
54. Hille B.: Ionic Channels of Excitable Membranes. 3rd Edition Sinuaer Ass. 2001.
55. Ichida A.M., Schroeder J.I.: Increased resistance to extracellular cation block by mutation of the pore domain of the Arabidopsis inward-rectifying K+ channel KAT1. J. *Membr. Biol*. 1996 May;151(1):53-62.
56. Iverson L.E., Tanouye M.A., Lester H.A., Davidson N., Rudy B.: A-type potassium channels expressed from Shaker locus cDNA. *Proc. Natl. Acad. Sci. U S A*. 1988 Aug; 85(15): 5723-7.
57. Jan L.Y. and Jan Y.N.: A superfamily of ion channels. *Nature*. 1990 Jun 21; 345(6277): 672
58. Jiang Y., MacKinnon R.: The barium site in a potassium channel by x-ray crystallography. *J. Gen. Physiol*. 2000 Mar; 115(3): 269-72.
59. Jenkinson D.H.: Potassium channels--multiplicity and challenges. *Br J. Pharmacol*. 2006 Jan;147 Suppl 1: S63-71. Review.
60. Junge F., Schneider B., Reckel S., Schwarz D., Dötsch V., Bernhard F.: Large-scale production of functional membrane proteins. *Cell. Mol. Life Sci*. 2008 Jun;65(11):1729-55. Review.
61. Kalmbach R., Chizhov I., Schumacher M.C., Friedrich T., Bamberg E., Engelhard M.: Functional cell-free synthesis of a seven helix membrane protein: in situ insertion of bacteriorhodopsin into liposomes. *J. Mol. Biol*. 2007 Aug 17;371(3):639-48.
62. Kamb A., Iverson L.E., Tanouye M.A.: Molecular characterization of Shaker, a Drosophila gene that encodes a potassium channel. *Cell*. 1987 Jul 31; 50(3): 405-13.
63. Kang M., Moroni A., Gazzarrini S., Van Etten J.L.: Are *chlorella* viruses a rich source of ion channel genes?. *FEBS Lett*. 2003 Sep 18; 552(1): 2-6.
64. Kang M., Moroni A., Gazzarrini S., DiFrancesco D., Thiel G., Severino M., Van Etten J.L.: Small potassium ion channel proteins encoded by *chlorella* viruses. *Proc. Natl. Acad. Sci. U S A*. 2004 Apr 13; 101(15): 5318-24.

65. Kapust R.B., Waugh D.S.: *Escherichia coli* maltose-binding protein is uncommonly effective at promoting the solubility of polypeptides to which it is fused. *Protein Sci*. 1999 Aug; 8(8) :1668-74.
66. Karniely S., Pines O.: Single translation--dual destination: mechanisms of dual protein targeting in eukaryotes. EMBO Rep. 2005 May;6(5):420-5. Review.
67. Katz, B.: The electric membrane constants of muscle. *Arch. Sci. Physiol*. 1949; 3: 285-300.
68. Kim D.: Physiology and pharmacology of two-pore domain potassium channels. *Curr. Pharm. Des*. 2005; 11(21): 2717-36. Review.
69. Klammt C., Schwarz D., Löhr F., Schneider B., Dötsch V., Bernhard F. : Cell-free expression as an emerging technique for the large scale production of integral membrane protein. *FEBS J.* 2006 Sep; 273(18): 4141-53.
70. Klammt C., Schwarz D., Eifler N., Engel A., Piehler J., Haase W., Hahn S., Dötsch V., Bernhard F.: Cell-free production of G protein-coupled receptors for functional and structural studies. *J. Struct. Biol.* 2007 Jun; 158(3): 482-93..
71. Kleymann G., Ostermeier C., Ludwig B., Skerra A., Michel H.: Engineered Fv fragments as a tool for the one-step purification of integral multisubunit membrane protein complexes. *Biotechnology* (N Y). 1995 Feb;13(2): 155-60.
72. Köhler G., Milstein C.: Continuous cultures of fused cells secreting antibody of predefined specificity. *Nature.* 1975 Aug 7;256(5517):495-7.
73. Krishnan M.N., Bingham J.P., Lee S.H., Trombley P., Moczydlowski E.: Functional role and affinity of inorganic cations in stabilizing the tetrameric structure of the KcsA K+ channel. *J. Gen. Physiol*. 2005 Sep;126(3):271-83.
74. Krishnan M.N., Trombley P., Moczydlowski E.G.: Thermal stability of the K+ channel tetramer: cation interactions and the conserved threonine residue at the innermost site (S4) of the KcsA selectivity filter. *Biochemistry*. 2008 May 13; 47(19): 5354-67.
75. Kubo Y., Reuveny E., Slesinger P.A., Jan Y.N., Jan L.Y.: Primary structure and functional expression of a rat G-protein-coupled muscarinic potassium channel. *Nature*. 1993 Aug 26; 364(6440): 802-6.
76. Kuo M.M., Saimi Y., Kung C.: Gain-of-function mutations indicate that Escherichia coli Kch forms a functional K+ conduit in vivo. *EMBO J.* 2003 Aug 15;22(16):4049-58.
77. Kuo A., Gulbis J.M., Antcliff J.F., Rahman T., Lowe E.D., Zimmer J., Cuthbertson J., Ashcroft F.M., Ezaki T., Doyle DA.: Crystal structure of the potassium channel KirBac1.1 in the closed state. *Science*. 2003 Jun 20; 300(5627): 1922-6.

78. Landau E.M. and Rosenbusch J.P.: Lipidic cubic phases: a novel concept for the crystallization of membrane proteins. *Proc. Natl. Acad. Sci. U S A*. 1996 Dec 10; 93(25): 14532-5.
79. Latorre R., Muñoz F., González C., Cosmelli D.: Structure and function of potassium channels in plants: some inferences about the molecular origin of inward rectification in KAT1 channels (Review). *Mol. Membr. Biol*. 2003 Jan-Mar; 20(1): 19-25. Review.
80. Li Z., Leung W., Yon A., Nguyen J., Perez V.C., Vu J., Giang W., Luong L.T., Phan T., Salazar K.A., Gomez S.R., Au C., Xiang F., Thomas D.W., Franz A.H., Lin-Cereghino J., Lin-Cereghino G.P.: Secretion and proteolysis of heterologous proteins fused to the *Escherichia coli* maltose binding protein in *Pichia pastoris*. *Protein Expr. Purif*. 2010 Jul;72(1):113-24.
81. Long S.B., Campbell E.B., Mackinnon R.: Crystal structure of a mammalian voltage-dependent Shaker family K+ channel. *Science*. 2005 Aug 5; 309(5736): 897-903.
82. Lu Z., Li Y., Que Q., Kutish G.F., Rock D.L., Van Etten J.L.: Analysis of 94 kb of the chlorella virus PBCV-1 330-kb genome: map positions 88 to 182. *Virology*. 1996 Feb 1; 216(1): 102-23.
83. Lu, Z.: Mechanism of rectification in inward-rectifier K^+ channels. *Annu. Rev. Physiol*. 2004; 66: 103-29.
84. Lu Z., Klem A.M., Ramu Y.: Ion conduction pore is conserved among potassium channels. *Nature*. 2001 Oct 25; 413(6858): 809-13.
85. Macauley-Patrick S., Fazenda M.L., McNeil B., Harvey L.M.: Heterologous protein production using the *Pichia pastoris* expression system. *Yeast.* 2005 Mar; 22(4) :249-70.
86. MacKinnon R.: Potassium channels. *FEBS Lett*. 2003 Nov 27; 555(1): 62-5.
87. Makrides S.C.: Strategies for achieving high-level expression of genes in *Escherichia coli*. *Microbiol. Rev*. 1996 Sep;60(3):512-38. Review.
88. Martin K., Helenius A.: Nuclear transport of influenza virus ribonucleoproteins: the viral matrix protein (M1) promotes export and inhibits import. *Cell*. 1991 Oct 4; 67(1): 117-30.
89. McRee D. E.: Practical Protein Crystallography. San Diego: Academic Press, 1993 (pp. 1-23).
90. Mehmel M., Rothermel M., Meckel T., Van Etten J.L., Moroni A., Thiel G.: Possible function for virus encoded K^+ channel Kcv in the replication of chlorella virus PBCV-1. *FEBS Lett.* 2003 Sep 18; 552(1): 7-11. Review.
91. Michel H.: Crystallization of membrane proteins. *Trends Biochem .Sci* . 1983; 8:56-59.

92. Milkman R.: An Escherichia coli homologue of eukaryotic potassium channel proteins. *Proc. Natl. Acad. Sci. U S A.* 1994 Apr 26; 91(9): 3510-4.
93. Miller, C.: Trapping single ions inside single ion channels. *Biophys. J.* 1987; 52:123–126.
94. Minor D.L. Jr, Masseling S.J., Jan Y.N., Jan L.Y.: Transmembrane structure of an inwardly rectifying potassium channel. *Cell.* 1999 Mar 19;96(6):879-91.
95. Miyazaki E., Kida Y., Mihara K., Sakaguchi M.: Switching the sorting mode of membrane proteins from cotranslational endoplasmic reticulum targeting to posttranslational mitochondrial import. *Mol. Biol. Cell*. 2005 Apr; 16(4): 1788-99.
96. Montal M., Müeller P.: Formation of bimolecular membranes from lipid monolayers and a study of their electrical properties. *Proc. Natl. Acad. Sci. U S A.* 1972 Dec; 69(12): 3561-6.
97. Moroni A., Viscomi C., Sangiorgio V., Pagliuca C., Meckel T., Horvath F., Gazzarrini S., Valbuzzi P., Van Etten J.L., DiFrancesco D., Thiel G.: The short N-terminus is required for functional expression of the virus-encoded miniature $K(^{+})$ channel Kcv. *FEBS Lett*. 2002 Oct 23; 530(1-3): 65-9.
98. Munsey T.S., Mohindra A., Yusaf S.P., Grainge A., Wang M.H., Wray D., Sivaprasadarao A.: Functional properties of Kch, a prokaryotic homologue of eukaryotic potassium channels. *Biochem. Biophys. Res. Commun*. 2002 Sep 13; 297(1): 10-6.
99. Neupärtl M., Meyer C., Woll I., Frohns F., Kang M., Van Etten J.L., Kramer D., Hertel B., Moroni A., Thiel G.: *Chlorella* viruses evoke a rapid release of K^{+} from host cells during the early phase of infection. *Virology*. 2008 Mar 15; 372(2): 340-8.
100. Neyton J., Miller C.: Potassium blocks barium permeation through a calcium-activated potassium channel. *J. Gen. Physiol*. 1988 Nov;92(5):549-67 (a)
101. Neyton J., Miller C.: Discrete Ba^{2+} block as a probe of ion occupancy and pore structure in the high-conductance Ca^{2+} -activated K+ channel. *J. Gen. Physiol*. 1988 Nov; 92(5): 569-86. (b).
102. Nimigean C.M.: A radioactive uptake assay to measure ion transport across ion channel-containing liposomes. *Nat. Protoc*. 2006; 1(3): 1207-12.
103. Nishida M., Cadene M., Chait B.T., MacKinnon R.: Crystal structure of a Kir3.1-prokaryotic Kir channel chimera. *EMBO J*. 2007 Sep 5; 26(17): 4005-15.
104. Ostermeier C., Iwata S., Ludwig B., Michel H.: Fv fragment-mediated crystallization of the membrane protein bacterial cytochrome c oxidase. *Nat. Struct. Biol*. 1995 Oct; 2(10): 842-6.
105. Ostermeier C. and Michel H.: Crystallization of membrane proteins. *Curr. Opin. Struct. Biol.* 1997 Oct; 7(5): 697-701. Review.

106. Pagliuca C., Goetze T.A., Wagner R., Thiel G., Moroni A., Parcej D.: Molecular properties of Kcv, a virus encoded K^+ channel. *Biochemistry*. 2007 Jan 30;46(4):1079-90.
107. Papazian D.M., Schwarz T.L., Tempel B.L., Timpe L.C., Jan L.Y.: Ion channels in Drosophila. *Annu. Rev. Physiol*. 1988; 50: 379-94. Review.
108. Patel A.J., Honoré E.: Properties and modulation of mammalian 2P domain K+ channels. *Trends Neurosci.* 2001 Jun; 24(6): 339-46. Review
109. Petersen K.R., Nerbonne J.M.: Expression environment determines K^+ current properties: Kv1 and Kv4 alpha-subunit-induced K+ currents in mammalian cell lines and cardiac myocytes. *Pflugers Arch*. 1999 Feb; 437(3): 381-92.
110. Plückthun A.: Antibody engineering: advances from the use of Escherichia coli expression systems. *Biotechnology* (N Y). 1991 Jun; 9(6): 545-51. Review.
111. Plugge B., Gazzarrini S., Nelson M., Cerana R., Van Etten J.L., Derst C., DiFrancesco D., Moroni A., Thiel G.: A potassium channel protein encoded by chlorella virus PBCV-1. *Science*. 2000 Mar 3; 287(5458): 1641-4.
112. Porath J., Carlsson J., Olsson I., Belfrage G.: Metal chelate affinity chromatography, a new approach to protein fractionation. *Nature*. 1975 Dec 18; 258(5536): 598-9.
113. Rath A., Glibowicka M., Nadeau V.G., Chen G., Deber C.M.: Detergent binding explains anomalous SDS-PAGE migration of membrane proteins. *Proc. Natl. Acad. Sci*. U S A. 2009 Feb 10; 106(6): 1760-5
114. Regueiro P., Monreal J., Díaz R.S., Sierra F.: Preparation of giant myelin vesicles and proteoliposomes to register ionic channels. *J. Neurochem*. 1996 Nov; 67(5): 2146-54.
115. Rhodes G.: Crystallography Made Crystal Clear. San Diego: Academic Press, 1993 (pp. 8-10, 29-38).
116. Romanos M.A., Scorer C.A., Clare J.J.: Foreign gene expression in yeast: a review. *Yeast*. 1992 Jun;8(6):423-88.
117. Saiki R.K., Gelfand D.H., Stoffel S., Scharf S.J., Higuchi R., Horn G.T., Mullis K.B., Erlich H.A.: Primer-Directed Enzymatic Amplification of DNA with a Thermostable DNA Polymerase. *Science.* 1988 239: 487 - 491.
118. Sambrook, J., Fritsch E. F., Maniatis T.: Molecular Cloning: A Laboratory Manual. New York: Cold Spring Harbor. Laboratory Press, 1989.
119. Sansuk K.., Balog C. I., van der Does A. M., Booth R.: GPCR proteomics: Mass spectrometric and functional analysis of histamine H1 receptor after baculovirus-driven and *invitro* cell free expression. *J. Proteome Res.* 2008; *7*, 621–629.

120. Schrempf H., Schmidt O., Kümmerlen R., Hinnah S., Müller D., Betzler M., Steinkamp T., Wagner R.: A prokaryotic potassium ion channel with two predicted transmembrane segments from Streptomyces lividans. *EMBO J.* 1995 Nov 1; 14(21): 5170-8.
121. Schroeder J. I., Ward J. M., Gassmann W.: Perspectives on the physiology and structure of inward rectifying K+ channels in higher plants: Biophysical implications for K+ uptake. *Ann. Rev. Biophys. Biomol. Struct*. 1994; 23: 441-71.
122. Scorer C.A., Buckholz R.G., Clare J.J,. Romanos MA.: The intracellular production and secretion of HIV-1 envelope protein in the methylotrophic yeast *Pichia pastoris*. *Gene.* 1993 Dec 22; 136(1-2): 111-9.
123. Sørensen H.P., Mortensen K.K.: Advanced genetic strategies for recombinant protein expression in *Escherichia coli*. *J. Biotechnol*. 2005 Jan 26; 115(2): 113-28. Review.
124. Stühmer W., Stocker M., Sakmann B., Seeburg P., Baumann A., Grupe A., Pongs O.: Potassium channels expressed from rat brain cDNA have delayed rectifier properties. *FEBS Lett*. 1988 Dec 19; 242(1): 199-206.
125. Schwarz D., Junge F., Durst F., Frölich N., Schneider B., Reckel S., Sobhanifar S., Dötsch V., Bernhard F.: Preparative scale expression of membrane proteins in Escherichia coli-based continuous exchange cell-free systems. *Nat. Protoc*. 2007; 2(11): 2945-57.
126. Schwarz D., Dötsch V., Bernhard F.: Production of membrane proteins using cell-free expression systems. *Proteomics.* 2008 Oct; 8(19): 3933-46.
127. Sreekrishna K., Brankamp R.G., Kropp K.E., Blankenship D.T., Tsay J.T., Smith P.L., Wierschke J.D., Subramaniam A., Birkenberger L.A.: Strategies for optimal synthesis and secretion of heterologous proteins in the methylotrophic yeast *Pichia pastoris*. *Gene*. 1997 Apr 29; 190(1): 55-62
128. Swenson R.P. Jr., Armstrong C.M.: K^+ channels close more slowly in the presence of external K^+ and Rb^+. *Nature*. 1981 Jun 4; 291(5814): 427-9.
129. Tao X., Avalos J.L., Chen J., MacKinnon R.: Crystal structure of the eukaryotic strong inward-rectifier K+ channel Kir2.2 at 3.1 A resolution. *Science*. 2009 Dec 18; 326(5960): 1668-74.
130. Tayefeh S., Kloss T., Thiel G., Hertel B., Moroni A., Kast S.M.: Molecular dynamics simulation of the cytosolic mouth in Kcv-type potassium channels. *Biochemistry.* 2007 Apr 24; 46(16): 4826-39.
131. Tucker J., Grisshammer R: Purification of a rat neurotensin receptor expressed in *Escherichia coli*. *Biochem J.* 1996 Aug 1; 317 (Pt 3): 891-9.

132. Uysal S., Vásquez V., Tereshko V., Esaki K., Fellouse F.A., Sidhu S.S, Koide S., Perozo E. Kossiakoff A.: Crystal structure of full-length KcsA in its closed conformation. *Proc. Natl. Acad. Sci. U S A*. 2009 Apr 21;106(16):6644-9.

133. VanDongen A.M.: K channel gating by an affinity-switching selectivity filter. *Proc. Natl. Acad. Sci. U S A*. 2004 Mar 2;101(9):3248-52.

134. Van Etten J.L., Meints R.H.: Giant viruses infecting algae. *Annu. Rev. Microbiol*. 1999; 53: 447-94.

135. Van Etten J.L. Graves M.V., Müller D.G., Boland W., Delaroque N.: Phycodnaviridae--large DNA algal viruses. *Arch. Virol*. 2002 Aug; 147(8): 1479-516. Review.

136. Vergara C., Latorre R.: Kinetics of Ca^{2+}-activated K+ channels from rabbit muscle incorporated into planar bilayers. Evidence for a Ca^{2+} and Ba^{2+} blockade. *J. Gen. Physiol.* 1983 Oct; 82(4): 543-68.

137. Vergara C., Alvarez O., Latorre R.: Localization of the K^+ lock-In and the Ba^{2+} binding sites in a voltage-gated calcium-modulated channel. Implications for survival of K+ permeability. *J. Gen. Physiol*. 1999 Sep;114(3): 365-76.

138. Varnier A., Kermarrec F., Blesneac I., Moreau C., Liguori L., Lenormand J.L., Picollet-D'hahan N.: A simple method for the reconstitution of membrane proteins into giant unilamellar vesicles. *J. Membr. Biol*. 2010 Feb; 233(1-3): 85-92.

139.

140. Wallin E. and von Heijne G.: Genome-wide analysis of integral membrane proteins from eubacterial, archaean, and eukaryotic organism. *Protein sci*. 1998 Apr.; 7(4):1029-38.

141. Wang Q.M., Johnson R.B.: Activation of human rhinovirus-14 3C protease. *Virology*. 2001 Feb 1; 280(1): 80-6.

142. Yan X., Olson N.H., Van Etten J.L., Bergoin M., Rossmann M.G., Baker T.S.: Structure and assembly of large lipid-containing dsDNA viruses. *Nat Struct Biol*. 2000 Feb; 7(2): 101-3.

143. Yang J., Jan Y.N., Jan L.Y.: Determination of the subunit stoichiometry of an inwardly rectifying potassium channel. *Neuron.* 1995 Dec; 15(6): 1441-7.

144. Ye S., Li Y., Jiang Y.: Novel insights into K^+ selectivity from high-resolution structures of an open K^+ channel pore. *Nat. Struct. Mol. Biol*. 2010 Aug; 17(8): 1019-23.

145. Zhou H., Chepilko S., Schütt W., Choe H., Palmer L.G., Sackin H.: Mutations in the pore region of ROMK enhance Ba^{2+} block. *Am. J. Physiol*. 1996 Dec; 271(6 Pt 1): C1949-56.

146. Zhou Y., Morais-Cabral J.H., Kaufman A., MacKinnon R.: Chemistry of ion coordination and hydration revealed by a K+ channel-Fab complex at 2.0 Å resolution. *Nature*. 2001 Nov 1; 414(6859): 43-8.

147. Zhou Y., MacKinnon R.: Ion binding affinity in the cavity of the KcsA potassium channel. *Biochemistry*. 2004 May 4;43(17): 4978-82.

148. Zhou M., MacKinnon R.: A mutant KcsA K(+) channel with altered conduction properties and selectivity filter ion distribution. *J. Mol. Biol*. 2004 May 7; 338(4): 839-46.

149. Zulauf M.: Detergent phenomena in membrane protein crystallization. In Crystallization membrane proteins. CRC Press, Inc. 1991; 54-71.

Acknowledgments

I want to thank Prof. Anna Moroni and Gerhard Thiel for being part of their lab groups for all these years.

Thanks to my colleagues and friends Giulia, Cristina, Marco, Sabrina and Andrea for the support, help and exchange of ideas during my PhD.

Thanks to Mattia, Michael Henkel, Christian Roos and Christian Braun for the collaboration in my PhD projects.

And thanks to my family and Giuseppe for supporting and understanding.